

The influence of spatial aggregation of wind data in modeling of energy systems

Department of
Wind Energy
Master Report

Toke Tobiasen

DTU Wind Energy-M-0103

June 2016

DTU Wind Energy
Department of Wind Energy



Authors: Toke Tobiasen

Title: The influence of spatial aggregation of wind data in modeling of energy systems

DTU Wind Energy-M-0103

June 2016

Project Period: January – June 2016

ECTS: 30

Education:

Master of Science in Engineering

Field: Sustainable Energy

Supervisors:

Niels-Erik Clausen

Neil Davis

DTU Wind Energy

Olexander Balyk

DTU Management

Bjarne Bach

Ea Energianalyse A/S

Remarks:

This report is submitted as partial fulfillment of the requirements for graduation in the above education at the Technical University of Denmark.

Technical University of Denmark

Department of Wind Energy

Frederiksborgvej 399

4000 Roskilde

Denmark

www.vindenergi.dtu.dk

Abstract

Wind power has become a much larger part of the Danish energy system in recent years. Being a non-dispatchable power source, much more planning of the energy system is required in order to utilize the wind resource optimally. The Danish energy system was modeled using the mathematical modeling tool Balmorel. The focus of this thesis was to optimize the method for modeling wind power in relation to the remaining energy system. The optimization primarily looked into the effects of spatial aggregation of wind power, but also briefly investigated the effects of temporal aggregation.

An investigation into usable wind data sets showed that CFSR wind data made by the NCEP, generally has low wind speeds compared to observed production. Therefore, a method was implemented such that the hourly variations from a reanalysis data set is scaled to distributions of the GWA, using the Weibull distribution parameters from both datasets. The GWA was used to correct the CFSR data, set, as this wind distribution corresponded better with observed production data.

A method was developed for the creation of aggregated power curves for a modeled wind area. These were created using a reference power curve, a representative wind time series as well as observed wind turbine heights, installed capacities and yearly production for the chosen site. The method fits the power curves to observed production and therefore corrects the corresponding wind time series to produce power equivalent to observed values. A single representative time series was used for each area. The site of the time series is based on the site where most wind turbines currently exist.

Five cases were created, dividing Denmark into 1, 2, 5, 10 and 20 areas respectively, to investigate the impact of spatial aggregation on the results based on total wind power production, curtailment and power prices. Above two areas, the effects of implementing more areas were seen to be miniscule. Two areas are seen to be enough to model Denmark, although adding more areas will increase the accuracy slightly.

Investigations of the temporal resolution shows that when modeling Denmark as an island, the time aggregation does not yield the same results as hourly resolution. This is due primarily to hours with very high power prices that are extrapolated when using the time aggregation.

Finally, it was found that the distance from a site, where wind speeds are no longer representative, is ≈ 250 km. Therefore, the modeled wind areas should have a radius no longer than 250 km. This distance will be shorter if the terrain becomes more complex, i.e. mountains or similar. Furthermore the area size needs to consider the wind turbine capacities, as an area with almost no installed wind capacity will not change anything, if combined with an area with much larger existing capacity.

Resume

Vindenergi er blevet en meget større del af det danske energisystem i de seneste år. Idet vinden ikke kan kontrolleres, kræver denne udvikling en større grad af planlægning for at kunne udnytte vinden optimalt.

Det matematiske modelleringsværktøj Balmorel blev i denne afhandling benyttet til at modellere det danske energisystem. Afhandlingens fokus var at optimere metoden hvormed vindenergi bliver modelleret i relation til resten af energisystemet. Denne optimering fokuserer primært på effekten af at ændre den rumlige sammenlæggelse af områder, men en mindre undersøgelse af tidsmæssig sammenlæggelse blev også foretaget.

En undersøgelse af forskellige vinddatasæt viste at CFSR datasættet, lavet af NCEP, havde lave vindhastigheder sammenlignet med observeret elproduktion. En metode til at kombinere udsvingene fra et datasæt med fordelingen af et andet datasæt, ved at benytte Weibullfordelingsparametrene, blev derfor benyttet. Datasættet hvor fordelingen blev fundet fra, var GWA. Det kombinerede datasæt viste at være tættere på observeret elproduktionsdata.

En metode til at lave aggregerede effektkurver, for et større modelleret vindområde, blev udviklet. Denne metode kræver en reference effektkurve for området, samt en vind tidsserie og data for de vindmøller der allerede er installeret i området. Metoden tilpasser effektkurverne til observeret elproduktion. En repræsentativ vind tidsserie for området udvælges, baseret på hvor flest vindmøller allerede findes i det givne område.

Fem forskellige inddelinger af Danmark, i henholdsvis 1, 2, 5, 10 og 20 områder blev testet i modellen. Disse blev evalueret på basis af den totale elproduktion, indskrænkning af vindproduktionen samt elpriserne. Det blev fundet at effekten, af at modellere Danmark i mere end to vindområder, ikke gav en stor forskel.

Undersøgelser af den tidsmæssige opløsning viste at hvis man modellerer Danmark som en \emptyset , uden mulighed for at transmittere strøm til udlandet, giver denne tidsopløsning ikke de samme resultater, som hvis man lod modellen køre med timeopløsning. Dette skyldes, at meget høje elpriser i højere grad blev fundet på grund af tidsopløsningen.

Til sidst blev det fundet at afstanden, hvormed vind tidsserien ikke længere er repræsentativ, er omkring 250 km. Derfor bør man ikke modellere vindområder større end 250 km. Denne afstand bliver dog mindre, hvis terrænet bliver mere komplekst som ved for eksempel bjerge. Udover dette kommer områdestørrelsen også an på den kapacitet, der er installeret i området. Et område kan derfor sagtens være større, hvis den ekstra kapacitet der kommer med udvidelsen, er meget lille i forhold til den kapacitet, der allerede var installeret i området inden for en 250 km radius.

Preface

This master thesis was carried out as the final project of Toke Tobiasen for the master program Sustainable Energy at the Technical University of Denmark (DTU). The thesis corresponds to 30 ECTS points and was carried out at DTU Wind Energy with cooperation from DTU Management Engineering and the consultant firm Ea Energy Analyses A/S.

Toke Tobiasen

Toke Tobiasen

Acknowledgements

Supervisors

Bjarne Bach - Ea Energy Analyses A/S

For helping me understand the Balmorel model and interpreting the results.

Olexandr Balyk - DTU Management Engineering

For helping me with energy systems analysis and modeling.

Niels-Erik Clausen - DTU Wind energy

For helping me with the structure of the project and the wind data study.

Neil Davis - DTU Wind energy

For helping me with the structure of the project and the wind data study.

Others

Katja Jensen - Ea Energy Analyses A/S

For helping me with Balmorel-related challenges.

Hanne Lauridsen

For proofreading

Dávid í Lág - Ea Energy Analyses A/S

For developing the program to extract CFSR data.

Casper Lundbak - Ea Energy Analyses A/S

For helping me gain access to the CFSR data.

Marie Münster - DTU Management Engineering

For helping me shape the project in the beginning.

Per Nørgaard - DTU Electrical Engineering

For discussions and help in the method for creating aggregated power curves.

Michael Nørskov - Netcompany

For proofreading and feedback of the thesis.

Alberto Riva - Ea Energy Analyses A/S

For discussions on how to develop the aggregated power curve method.

Poul Sørensen - DTU Wind Energy

For discussions and help in the method for creating aggregated power curves.

Nicky Torstensson - Netcompany

For proofreading and feedback of the thesis.

Finally, a huge thanks to the rest of Ea Energy Analyses A/S for a place to write my thesis, kind and helpful people and the opportunity to work on this thesis.

Abbreviation and symbols list

Symbols used in calculations

A	Weibull scale parameter
A_{CFSR}	Weibull scale parameter from the CFSR data
A_{GWA}	Weibull scale parameter from the GWA data
A_{rotor}	Rotor area [m ²]
α	Shear factor
C_b	Technology parameter
CC	Correlation coefficient [%]
CF	Capacity factor [%]
COP	Coefficient of performance
C_p	Power coefficient
C_v	Technology parameter
f_U	Probability density function
F_U	Cumulative density function
GR	Growth rate
Γ	Gamma function
HF	Height factor
k	Weibull shape parameter
k_{CFSR}	Weibull shape parameter from the CFSR data
k_{GWA}	Weibull shape parameter from the GWA data
κ	Von Kármán constant (≈ 0.41)
MG	Maximum growth [m/s]
MP	Maximum production [p.u]
μ_U	Mean wind speed [m/s]
N	Length of vector
p	Pressure [Pa]
Pm_j	Discrete multi turbine power production [kW]
Ps_i	Discrete probability of element i in the spatial distribution
Ps_{j+i}	Discrete power production of production element j and distribution element i
P_{cap}	Capacity [kW]
P	Power production [kWh]
$P_{\text{tot,y}}$	Total yearly production [kWh]
R_{specific}	Specific gas constant $\approx 8.31 \text{ J mol}^{-1}\text{K}^{-1}$
ρ_{air}	Air density [kgm ⁻³]
σ_U^2	Variance [m ² /s ²]
T	Temperature [K]
U	Wind speed [m/s]

U_{CFSR}	Wind speed from the CFSR used in the CDF [m/s]
U_{GWA}	Wind speed from the GWA used in the CDF [m/s]
U_{mast}	Wind speed at measurement height [m]
U_*	Friction velocity [m/s]
$V1$	Vector of length N
$V2$	Vector of length N
z	Height [m]
z_0	Roughness length [m]

Symbols used in mathematical modeling

Sets

a	Area
f	Fuel type
e	Emission type (CO ₂ , SO ₂ and NO _x)
g	Generation technologies
t	Time (Given in either years, seasons or time steps)
r	Region
r_x	Region where power is exported to
c	Country
\mathbb{A}_r	Subset of all areas a in a region r
\mathbb{A}_c	Subset of all areas a in a country c
\mathbb{R}_x	Subset of all regions r_x where power is exported to

Parameters

$C_{a,f}^{\text{fuel}}$	Fuel costs for fuel type f in area a [DKK/MWh]
$C_{a,g}^{\text{O\&M}}$	Operation and maintenance costs for technology type g in area a [DKK/MWh]
C_{r,r_x}^{trans}	Electricity transmission costs between regions [DKK/MWh]
$C_{c,e}^{\text{emis}}$	Cost of emission e in country c [DKK/kg]
$D_{r,t}^{\text{el}}$	Demand for electricity in a region r at time t [MWh]
$E_{g,e}^{\text{gen.tech}}$	Emission of type e for generation technology g [kg/MWh]
$E_{c,e}^{\text{emis.lim}}$	Limit for emission of type e in country c [kg/GJ]
$\eta_{g,a}$	Efficiency of technology g in area a [-]

Variables

$V_{a,g,t}^{\text{fuel.cons}}$	Fuel consumption for area a and technology type g at time t [MWh]
--------------------------------	---

$V_{a,g,t}^{\text{el.gen}}$	Electricity generation for area a and technology type g at time t [MWh]
$V_{r,r_x,t}^{\text{trans}}$	Transmission of power from one region to another at time t [MWh]

Abbreviations

a.g.l	Above ground level
Avg	Average
bb1	Run option for Balmorel with yearly optimization
bb3	Run option for Balmorel with weekly optimization
CDF	Cumulative density function
CF	Capacity factor
CFSR	Climate Forecast System Reanalysis
DK_E	Denmark East power market
DK_W	Denmark West power market
Ea	Ea Energy Analyses A/S
GRG	Generalized Reduced Gradient Algorithm
GWA	Global wind atlas
MERRA	Modern-Era Retrospective analysis for Research Applications
NCEP	National center for environmental prediction
PC	Power curve
PDF	Probability density function
p.u.	Per unit
SSM/I	Special Sensor Microwave Imager
TS	Time series
VSWT	Variable speed wind turbine
WRF	Weather Research and Forecast model

Subscripts

air	Air
cap	Capacity
dec	Decline
i	Discrete element
inc	Incline
j	Discrete element
mast	Measurement height
P	Power
rotor	Rotor
specific	Specific
tot	Total
U	Wind speed
y	Year

0 Roughness length
* Friction velocity

Contents

1	Background	2
2	Motivation	5
2.1	Thesis structure	6
3	Vertical extrapolation	7
3.1	Log-law	7
3.2	Power-law	7
4	Wind turbine power curves	10
I	Wind study	13
5	Introduction to wind datasets	14
5.1	Validation basis of wind time series	14
5.2	Wind direction	15
5.3	Temporal modeling	15
6	Description of used datasets	16
6.1	CFSR data	16
6.2	Global Wind Atlas	17
6.3	Mesoscale data	22
6.4	Wind data summary	23

7	Reference year	24
8	Comparing mesoscale and CFSR data	27
9	Validation of the Global wind atlas	29
10	Combining datasets	33
10.1	Sensitivity of GWA Weibull parameters	34
10.2	Comparing mesoscale to combined dataset	35
10.3	Using combined time series in Balmorel	39
11	Aggregated power curves	41
	Choosing a reference power curve	42
	Creating smoothed power curve	42
	Fitting logistic function	44
	Fitting to capacity factor	46
	Sensitivy of power curve fitting	48
12	Discussion of wind study	50
12.1	Discussion of wind datasets	50
12.2	Discussion of aggregated power curves	51
II	Modeling of energy systems	53
13	Introduction to modeling of wind power in energy systems	54
14	Balmorel	55
14.1	Introduction to Balmorel	55
14.2	Geography	55
14.3	Time structure	56
14.4	Generation technologies	56

14.5 Fuel	57
14.6 Demand	57
14.7 Transmission	57
14.8 Objective function and constraints	57
Sets	60
Parameters	60
Variables	60
Objective function	61
Balmorel constraints	61
14.9 Strengths and weaknesses	62
Other modeling tools	62
15 Creation of aggregated cases	63
15.1 Spatial aggregation	63
Case 1 - 1 area	64
Case 2 - 2 areas	65
Case 3 - 5 areas	66
Case 4 - 10 Areas	67
Case 5 - 20 areas	68
15.2 Temporal aggregation	70
16 Results	71
16.1 Validation of results	71
16.2 Spatial aggregation	71
16.3 Temporal aggregation	73
16.4 Model run times	74
16.5 Choice of reference year	75
16.6 Power curve swapping	76

17 Discussion on energy systems modeling	78
III Correlations in wind power production	81
18 Correlations in wind time series	82
18.1 Mesoscale data	82
18.2 CFSR combined with GWA data	83
18.3 Hourly wind speeds	84
18.4 Weighted wind speeds	86
19 Correlations in power production	88
20 Correlations in power production after Balmorel implementation	90
20.1 Comparison of power production before and after Balmorel implementation	92
20.2 Wind areas in Denmark	92
21 Correlations in wind speeds for longer distances	94
22 Area size	96
IV Discussion and conclusion	99
23 Discussion	100
24 Conclusion	102
25 Future work	104
25.1 Capacity weighting	104
25.2 Transmission to neighbouring countries	104
25.3 Time aggregation	104
25.4 Investment runs	104

Bibliography	105
A Coordinates of extracted CFSR data	108
B Matlab script to combine CFSR and GWA data	110
C Power curve implementation in Balmorel	114
D Wind turbine costs from Ea	116

List of Figures

1.1	Wind power in Denmark	2
1.2	Danish power system	3
3.1	Roughness length Denmark	8
3.2	Sensitivity of log- and power-law	9
4.1	Power curve example	11
6.1	CFSR resolution	17
6.2	Seasonal cycle CFSR	18
6.3	GWA methodology	19
6.4	Weibull distribution	19
6.5	GWA A -parameter	20
6.6	GWA k -parameter	21
6.7	Mesoscale points	22
7.1	Wind index comparison	25
7.2	Storms in Denmark	25
8.1	PDF comparison of CFSR and mesoscale	28
9.1	Validation of GWA	30
9.2	Weibull parameter contour plots	31

10.1 CDF comparion	34
10.2 Combined dataset compared to CFSR	35
10.3 Weibull parameter sensitivity	36
10.4 Weibull parameter sensitivity time series	37
10.5 PDF comparison of mesoscale and combined dataset	38
10.6 Reference case with new TS	39
11.1 Reference wind turbine models	43
11.2 Reference power curves	44
11.3 Smoothed power curve fit	45
11.4 Logistic PC fit	46
11.5 CF PC fit	47
11.6 PC sensitivity	48
14.1 Feasible regions for energy technologies	58
14.2 Transmission grid in northern Europe	59
15.1 Case 1	64
15.2 Case 2	65
15.3 Case 3	66
15.4 GWA mean wind speeds	67
15.5 Case 4	68
15.6 Case 5	69
16.1 Spatial aggregation residual duration curve	72
16.2 Power price duration curve for temporal aggregation	74
16.3 Reference year sensitivity results	75
16.4 PC swap sensitivity	76
17.1 Residual duration curve zoom	79

18.1 Mesoscale wind time series	83
18.2 Time series CFSR dataset	84
18.3 Hourly median wind speeds	85
18.4 Normalized hourly median wind speeds	85
18.5 Weighted wind speeds	87
19.1 Calculated power production	89
20.1 Hourly power production after Balmorel	91
20.2 Zoom of Balmorel power production	91
20.3 Power production before and after Balmorel	93
21.1 Northern Europe wind sites	95
21.2 Correlation coefficients plotted against distance	95
23.1 Wind speeds with weighted capacities	101
A.1 Map showing the extracted CFSR coordinates.	109

List of Tables

6.1	Wind data summary	23
8.1	CF CFSR data	27
9.1	CF calculated from GWA	32
10.1	Weibull parameter comparison	34
10.2	CF comparison for mesoscale and combined dataset	38
10.3	Balmorel results with new TS	40
11.1	Reference wind turbines	42
11.2	PC parameter constraints	45
15.1	Case 1	64
15.2	Case 2	65
15.3	Case 3	66
15.4	Case 4	67
15.5	Case 5	69
16.1	Spatial aggregation modeling results	72
16.2	Temporal and spatial aggregation modeling results	73
16.3	Reference year sensitivity results	75
16.4	PC swap sensitivity	77

18.1	Correlation coefficient mesoscale	83
18.2	Correlation coefficient CFSR	84
18.3	Correlation coefficient for weighted wind speeds	86
19.1	Correlation coefficients for hourly power production	88
19.2	Total power production before Balmorel	89
20.1	Correlation coefficient of power production after Balmorel	90
22.1	Corner point correlation coefficients and distances	96
A.1	Coordinates of extracted CFSR data, shown in Fig. A.1.	108
D.1	Approximate default costs for wind turbines.	116



Introduction

CHAPTER 1

Background

Wind power generation has become a much larger part of energy systems in the world. For Denmark, the percentage of power coming from wind has increased from $\approx 18\%$ to 42% over the last ten years, as seen in Fig. 1.1.

Wind, being a non-dispatchable and fluctuating resource, requires more planning in order to ensure security of supply. At times with low wind power production, other technologies will have to cover the remaining production in order to meet the demand. This can be an expensive affair since the different technologies have different running costs as well as differing start-up times. For this, mathematical modeling of the energy system can be used to minimize the costs of the system, as well as identifying which plants to turn on and off for different time periods [10]. Furthermore, modeling is used to predict the future power prices along with predicting how investments into new technologies should be done in future years.

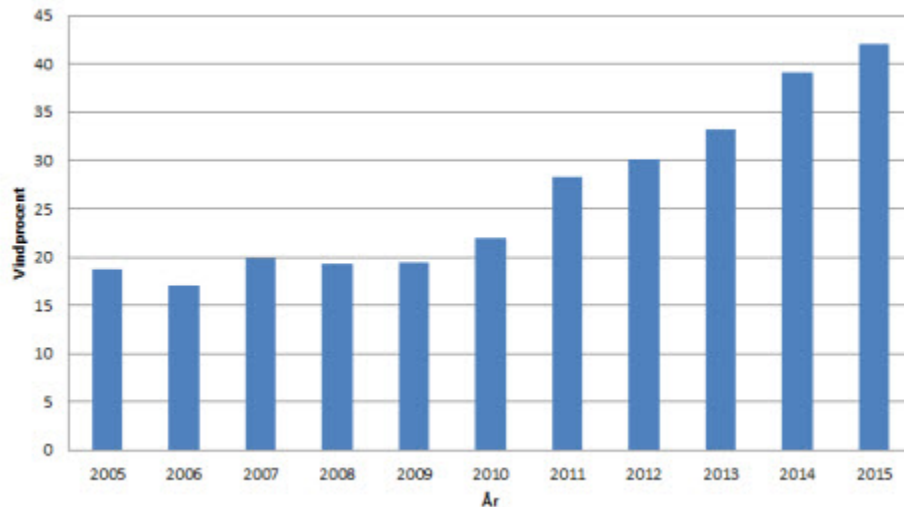


Figure 1.1: Figure showing the percentage of power production in Denmark coming from wind turbines for the last ten years [13].

The Balmorel model [36] is an excellent tool for this type of problem. It is a mathematical modeling tool that minimizes the total energy system costs. Fully explaining Balmorel is somewhat beyond the scope of this thesis. The focus of this thesis will mainly be the parts of the model concerning wind power generation, which will be explained further in Part II.

Ea Energy Analyses A/S (Ea) is one of the companies who uses the Balmorel model. As Balmorel is open-source, it can be altered in great detail by the user. The version described in this thesis is the Balmorel model currently used by Ea. Here, wind modeling is currently done by separating Denmark into two regions mirroring the two power markets in Denmark: Denmark East (DK_E) and Denmark West (DK_W). These regions are sub-divided into smaller areas in the model, by the capacities installed at different sites.

Western Denmark is modeled as one onshore area with a reference wind time series (TS) found for Herning and two offshore sites representing the larger offshore wind farms Anholt and Horns rev¹ respectively[14]. Eastern Denmark is represented by an onshore area represented with a wind time series for Holbæk and an offshore area represented by Rødsand². The different areas, with corresponding points where the representative wind time series are found, are seen in Fig. 1.2.

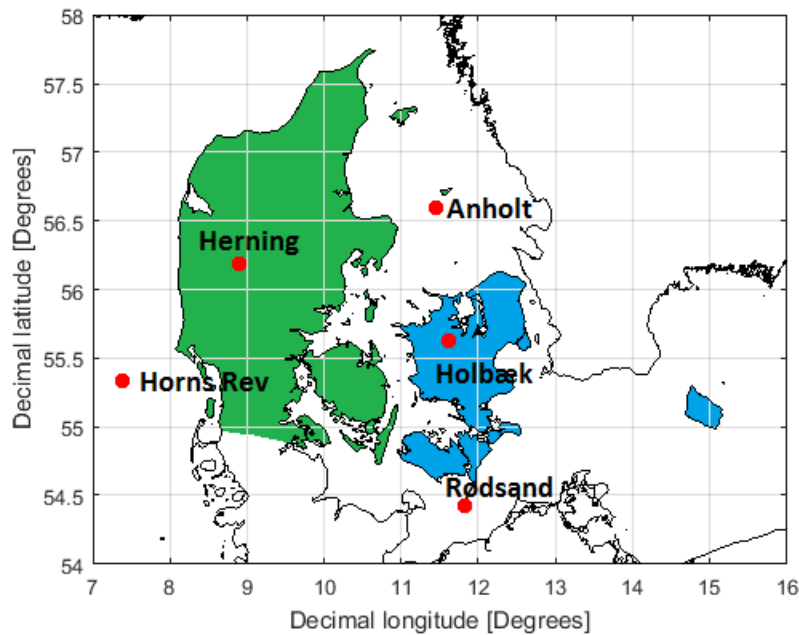


Figure 1.2: Sketch of the current way to model wind power in Balmorel for Denmark. Western Denmark is shown in green and eastern Denmark is shown in blue. Coastline data for Denmark is supplied by [34].

Whereas in real life, every turbine installed would see a different wind climate and have a power curve pertaining only to that single wind turbine, Balmorel models larger areas. Therefore it is necessary to find wind speeds and power curves representative for larger areas. These area-representative entities are known as aggregated entities.

¹Horns Rev referring to both wind farms Horns Rev I and Horns Rev II.

²Rødsand referring to both Rødsand I and Rødsand II (Also known as Nysted)

A method for creating a representative wind speed that is spatially altered is seen in Nørgaard et. al [32]. This method creates a rolling average for the wind speeds instead of finding a single representative wind speed for an area. For this thesis, a representative wind speed for every area is however used. This is used such that a wind dataset can be used without having to alter it. Furthermore, the addition of more areas should converge towards the same effect when implementing more areas. This approach will also ease the implementation of more wind power production areas and make the model more accepting to using different wind time series data sets.

CHAPTER 2

Motivation

Due to the fluctuations in wind speeds, there will be times where no wind power production is available. Denmark, although being a small country, will have spatial variations in the wind speeds due to atmospheric and terrain effects. This will lead to times where production is high in one part of the country and low in other parts.

From these effects, one could be lead to believe that too few representative wind speeds for a country, will lead to a more extreme power production going between high and low production levels. By extreme power production is meant that the wind power production depends only on the fluctuations in very few wind time series and will therefore often either be very high or very low across the country.

The hypothesis of this thesis is that, with a larger degree of spatial disaggregation, a smoothing of the wind power production will be seen, as more spatial variations will be taken into account. The power production is believed to become less extreme, as large wind speeds in a single area will affect the overall power production much less if the area, where the wind is present, is small compared to the other areas.

Capturing more spatial variations in wind speeds are believed to result in a better utilization and representation of the wind resource as it does not only depend on a single, somewhat arbitrarily chosen, wind speed.

Large amounts of data is required in order to investigate the spatial aggregation, and for this thesis the focus will be on Denmark as an isolated country. This will have an effect on the overall energy system as wind turbines sometimes will have to be curtailed, meaning a decrease in production or full stop of production, whereas in reality the power might have been exported to another country. This means that the power prices and total curtailment will not be directly comparable to real life cases. The effect of changing the aggregation will in exchange be more distinguishable and pronounced.

2.1 Thesis structure

The thesis is divided into four parts.

Part I - Wind study

An investigation into three different wind time series. These datasets are evaluated on the basis of different criteria and how it fits into modeling of energy systems. A method for combining datasets is explained and a validation of the datasets has been performed. Lastly a method for creating aggregated power curves for an area is discussed.

Part II - Modeling of energy systems

General description of the Balmorel model, focusing on the parts related to wind power production. The basis for validating the modeling results and creation of the spatial aggregation are explained. Furthermore, a study of temporal aggregation of the wind power modeling was carried out.

Part III - Correlations in wind power production

An investigation into the temporal correlation coefficients of the wind speeds for varying degrees of spatial aggregation for different datasets. The change in correlation coefficients before and after modeling of the wind power production is explained, and a study is made for correlations in wind for longer distances. Finally a maximum size of the wind area for modeling wind power is suggested.

Part IV - Discussion and conclusion

A discussion of the results and the most critical assumptions is made. Finally, a conclusion is made based on the results and an outlook into further work is described.

CHAPTER 3

Vertical extrapolation

Optimal comparison of wind time series requires the datasets to be measured at the same height. This is however rarely the case when comparing different datasets. Friction from the orography and terrain will affect the wind speeds in the surface layer. The change in wind speed with height can be calculated in different ways.

3.1 Log-law

One way is to use the roughness of the surrounding area using the log-law [28] seen in Eq. (3.1) [6].

$$U(z) = \frac{U_*}{\kappa} \ln \left(\frac{z}{z_0} \right) \quad (3.1)$$

This method requires the friction velocity U_* and the surface roughness z_0 with κ being the Von Kármán constant and z being the height [28]. With changes in wind direction, the roughness used for the calculation has to be changed according to the terrain the wind passes over from the given direction. This makes modeling complicated, as the directions and all of the roughness data needs to be used. Fig. 3.1 shows the surface roughness used in the Global wind atlas (GWA). From here it is seen that the roughness varies greatly across Denmark.

3.2 Power-law

Another method has been found empirically and is known as the power-law [28]. This method relates the wind speeds at different heights to an empirically found shear factor α . Eq. (3.2) shows the relationship between wind speeds and height.

$$U = U_{\text{mast}} \left(\frac{z}{z_{\text{mast}}} \right)^\alpha \quad (3.2)$$

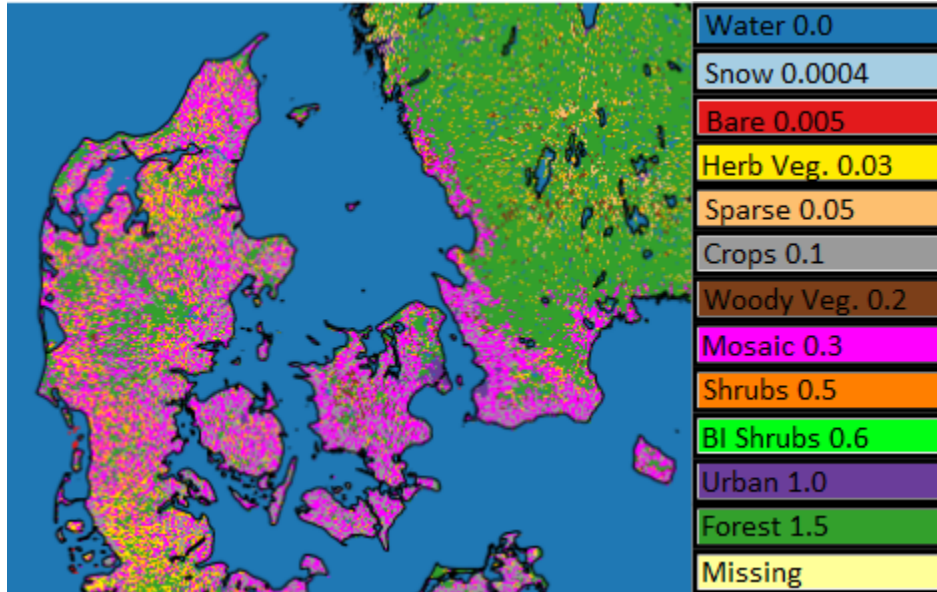


Figure 3.1: Surface roughness values for Denmark used in the Global wind atlas [16].

The shear value varies depending on the terrain and roughness, but will usually be around $1/7 \approx 0.14$. The shear values used in this thesis are from a confidential source and will not be shown.

Both the log-law and power-law are viable as a method as seen in Kubik et. al[25]. Here it is concluded that the wind speeds are more sensitive to changes in the power-law when changing the shear factor, than the log-law when changing the roughness length. This is also seen in Fig. 3.2. Although this is an issue, the distance between the turbine height and the data measurements are most commonly less than 10 m. Due to this the choice of method does not matter that much. For this thesis, the aim is to investigate the effects on spatial aggregation in modeling which should be possible with either vertical extrapolation method. Therefore using the power-law was chosen due to easier implementation.

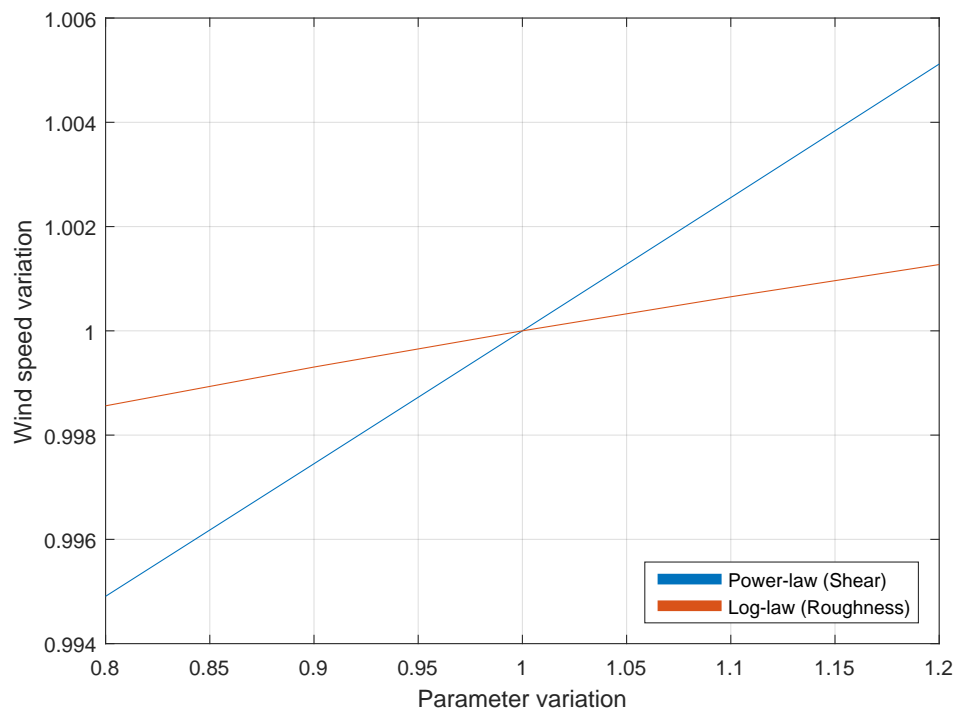


Figure 3.2: Sensitivity of the power-law and log-law when changing either the surface roughness or the shear factor by different percentages. For this figure the height has been altered from 50 m above ground level (a.g.l) to 60 m a.g.l.

CHAPTER 4

Wind turbine power curves

Wind power production is calculated as a function of the wind speed seen in Eq. (4.1) [28].

$$P = \frac{1}{2} \rho_{\text{air}} A_{\text{rotor}} C_P U^3 \quad (4.1)$$

The power production P for a pitch-regulated wind turbine is calculated from the air density ρ_{air} , the cross-sectional area A_{rotor} , the power coefficient C_P and the wind speed U . The power coefficient C_P changes for different wind speeds and pitch to obtain a power curve as seen in Fig. 4.1. This power curve shows the power produced at different wind speeds. For a pitch-regulated turbine like this, the power production will start at a certain wind speed known as the cut-in wind speed, seen in Fig. 4.1 around 3 m/s. The power will then increase with wind speed until rated power is reached at around 14 m/s, where it will stay constant until cut-out wind speeds at 25 m/s.

An important aspect of these power curves are that they are created by the manufacturer for specific conditions, so that the power curves will often not produce exactly the same amount as specified by the manufacturer. Furthermore, it is important to note that the power curves stop producing power above the cut-out wind speed in an effort to keep the turbines from getting damaged. This effect is known as curtailment due to high wind speeds. Another type of curtailment arises when the turbines produce more power than can be used or exported. Both of these effects contribute to the turbines not producing for a period of time. It is however important to distinguish between whether the curtailment comes from high wind speeds or from the energy system.

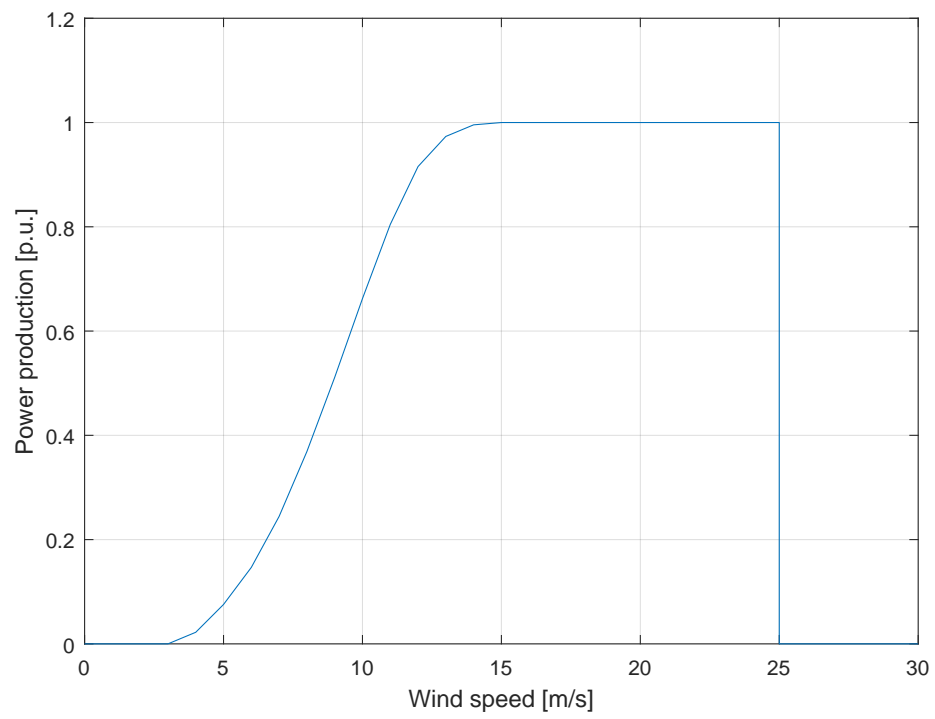


Figure 4.1: Example of a power curve for wind turbine power production.

Part I

Wind study

CHAPTER 5

Introduction to wind datasets

For the use of energy systems modeling, the input wind time series are an important factor for the realism of the model. Many different datasets exist and the difference between how the data is created varies greatly. Resolution of these wind datasets is an important parameter as a higher resolution will make the use of the dataset more flexible for different analyses. Actual measurements of wind speeds and direction at a high resolution, requires many resources to erect meteorological masts, which is undesirable. Furthermore, some sites are not suited for the erection of masts and the local population might oppose the idea of masts being placed everywhere.

Therefore several atmospheric models to describe the wind speeds are made, with varying degrees of approximations, such that a general wind pattern can be described. The different models all have their strengths and weaknesses and the usage very much depends on the study being conducted using the time series. For energy systems modeling purposes, a time series describing the fluctuations in the wind is needed. As modeling is often used to describe future energy systems, the wind dataset has to be representative for the wind that will be experienced in the future.

5.1 Validation basis of wind time series

In this thesis, different wind datasets will be described and compared. Different parameters are inspected in order to evaluate which dataset makes the most sense to use for Balmorel modeling. Test of spatial aggregation requires plenty of datasets, such that every modeled area will have at least one designated time series. Therefore a certain spatial resolution of data is desired.

Temporal resolution of data plays a role in modeling as well. Wind speeds are often averaged over a chosen time period, as every single fluctuation in wind speed will require a huge dataset. For modeling in Balmorel the shortest time period, without extra add ons, is hourly. This temporal resolution is desired for the wind datasets to be able to run Balmorel without time aggregation. The years, where data is available, is an important parameter as well. Comparison between different datasets will have to be from the same time period in order to conclude anything accurately.

5.2 Wind direction

Along with wind speeds, the direction of the wind will also change in time. In the datasets, the wind speed will take the direction change into account and often give both a direction as well as a wind speed. Wind turbines produce the most power when facing the wind head on, at a perpendicular angle and therefore the wind direction will have an effect on the power production. Wind turbines can however be turned to face the wind at all directions. Due to this, it the direction of the wind speeds are not necessary to model as it is expected that the wind turbines will be regulated to face the wind direction for all times when no yaw is necessary.

As the terrain around the wind turbine site is rarely uniform, the terrain will affect the power curves used to calculate the production. These effects will be further explained in Chapter 11.

5.3 Temporal modeling

Modeling in Balmorel, which will be further explained in Part II, does not model time to be exactly as in reality. In Balmorel, a year consists of 52 seasons, with 168 hours in each season. This means that a Balmorel year consists of 8736 hours, whereas a normal real year consists of 8760 hours¹. Therefore, roughly 1.5 days are left out during modeling. As the Balmorel year starts on the 1st of January, the last days of December are thus left out. This does have a small effect on the generation, on a yearly basis, especially since the generation during winter months on average is higher than during summer months [12].

¹Normal year meaning a year with 24 hours a day and 365 days a year.

CHAPTER 6

Description of used datasets

6.1 CFSR data

The Climate Forecast System Reanalysis (CFSR) wind data set is created by the National Center of Environmental Prediction (NCEP). The dataset was created over a period from 1979-2009 and extended further to 2011 [37]. CFSR includes much more data than just wind speeds. These however will not be described in this thesis. A global model of the wind speeds is created attempting to predict global wind speeds at different pressure levels as well as heights. This is then calibrated using mast data at several locations across the world, and ocean wind speed observations are calibrated using a Special Sensor Microwave Imager (SSM/I) mounted on several satellites [33].

The wind speed data is given for different heights with the dataset available to Ea at 10 m a.g.l. Data is found from [31]. Different resolutions exist, with the best having a spatial data resolution of $0.3^\circ \times 0.3^\circ$ longitude and latitude. This corresponds to a distance of 20-30 km between each point in Denmark, depending on the geographical location. A plot of the points where data is available is seen in Fig. 6.1 marked by red dots.

Temporal resolution of the dataset is hourly, meaning that an average wind speed for every hour at every location is found. A plot of the CFSR time series for Fyn, 2009 in Western Denmark is seen in Fig. 6.2. In order to investigate the seasonal cycle of the dataset, a smoothing filter has been applied to the time series taking the average of a four week period. As described in Chapter 5.3, four weeks is the Balmorel equivalent of modeling a month. Hour 1 corresponds to the first hour in January 2009. Inspection of the figure shows higher average wind speeds for the winter months compared to the summer months. This is in correspondence with what can actually be observed from real measurement [12].

No validation has been found for Denmark, although Sharp et. al [39] showed that for the UK, the CFSR wind estimates are well correlated to real measurements. Some differences was however found depending on the site.

Sites where data has been extracted with coordinates are seen in Appendix A.

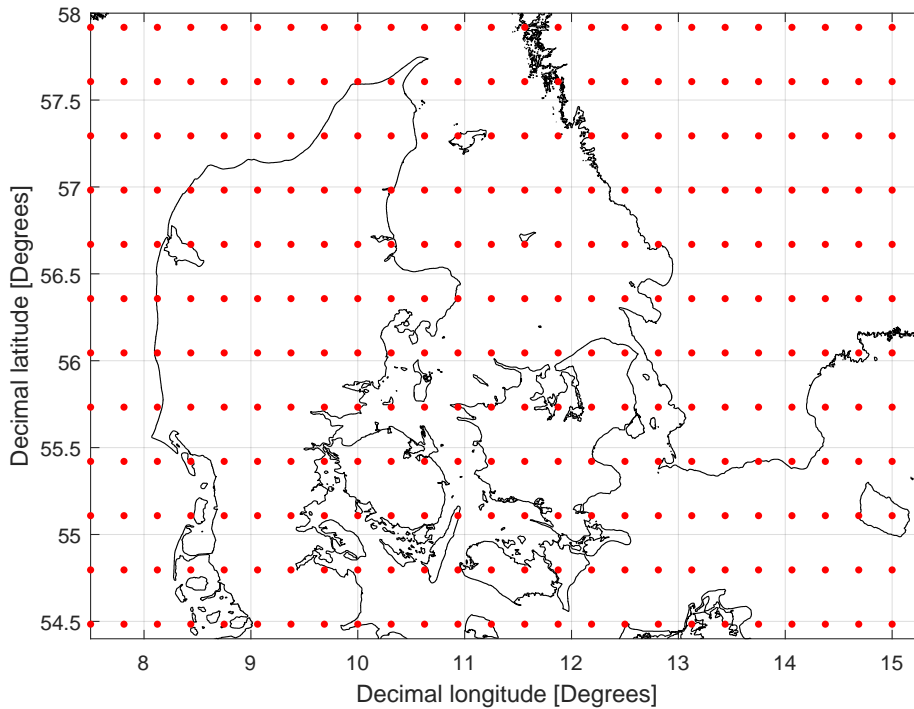


Figure 6.1: Figure showing the points where CFSR data is found, shown as red dots.

6.2 Global Wind Atlas

The Global wind atlas dataset is created from a reanalysis dataset [4]. This reanalysis data set is called Modern-Era Retrospective analysis for Research Applications (MERRA) [30], and is created much in the same manner as the CFSR dataset. In the GWA, high resolution topography is applied in order to do microscale modeling and estimate the wind resource. Finally the wind resource is verified. This process is seen in Fig. 6.3. The methodology is based on the older European wind atlas [42].

The data is found as an average over the years 1979-2013.

The GWA has a resolution in Denmark of $250 \text{ m} \times 250 \text{ m}$ in three different heights: 50 m, 100 m and 250 m a.g.l. This is by far the finest resolution of the datasets used in this thesis, meaning that the other datasets will be the limiting factor. The GWA dataset does not consist of time series, but rather Weibull distribution parameters [26]. These are known as the scale parameter A and the shape parameter k and the probability density function (PDF) of the distribution is given as seen in Eq. (6.1). Fig. 6.4 shows the Weibull distribution for different values of A and k .

$$f(x) = \begin{cases} \frac{k}{A} \left(\frac{U}{A}\right)^{k-1} e^{-(U/A)^k} & U \geq 0 \\ 0 & U < 0 \end{cases} \quad (6.1)$$

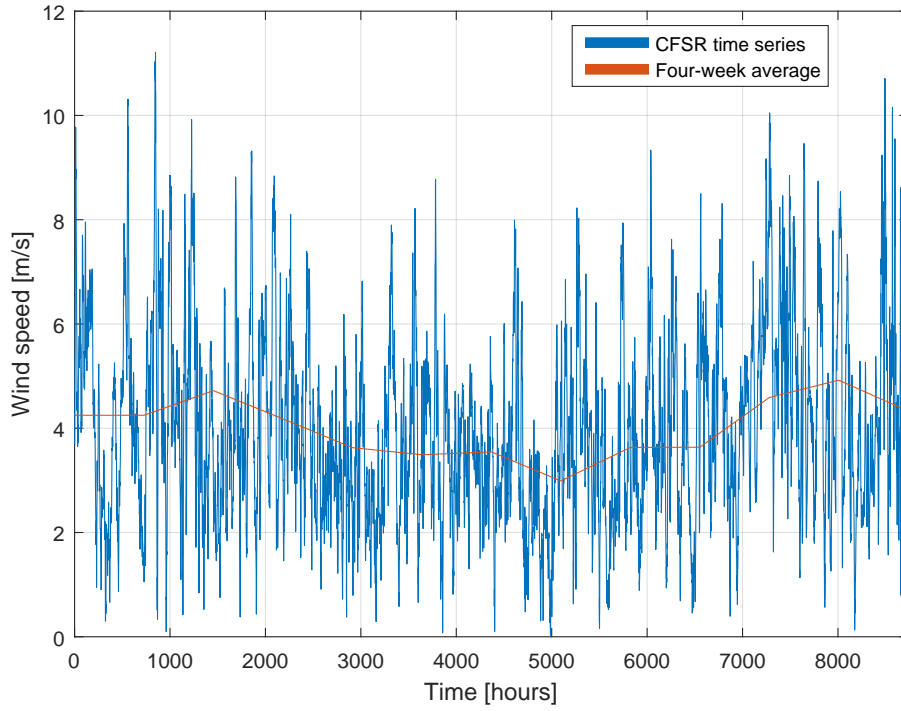


Figure 6.2: Figure showing the hourly time series values for Fyn (blue) plotted together with a four weekly average (red). Wind speeds are found for 2009 at 10 m a.g.l.

These parameters are related to the mean wind speed μ and the variance σ^2 by Eq. (6.2) and (6.3) as seen in [5].

$$\mu_U = A\Gamma(1 + 1/k) \quad (6.2)$$

$$\sigma_U^2 = A^2 (\Gamma(1 + 1/k) - \Gamma^2(1 + 1/k)) \quad (6.3)$$

Here, Γ is known as the Gamma function [5]. From Eq. (6.2), it is seen that the A parameter is closely related to the mean wind speed. For Denmark, it can roughly be said that with $k \approx 2$, the relationship between the scale parameter and the mean wind speed $\mu_U \approx 0.9A$.

In the GWA, the Weibull parameters are separated into 12 directions for every point. As explained in Section 5.2, the specific directions are not used. For the use in this thesis, the directions are therefore aggregated into a single set of Weibull parameters using a weighted average.

Contour plots of the Weibull parameters are seen in Fig. 6.5 and Fig. 6.6. In areas with no data available $A = 0$ m/s and $k = 2$ to ensure better interpretation of the color scales of the plot.

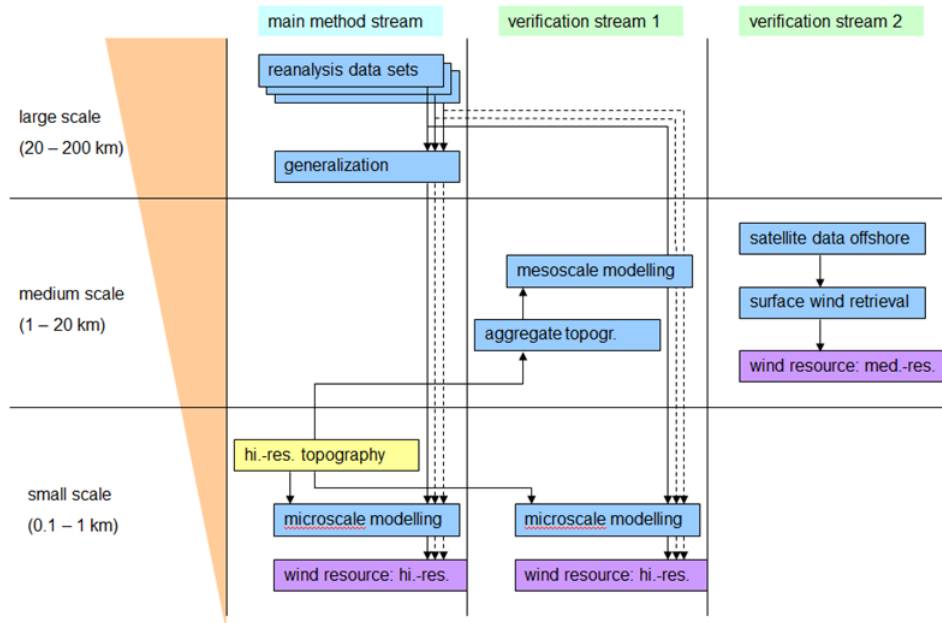
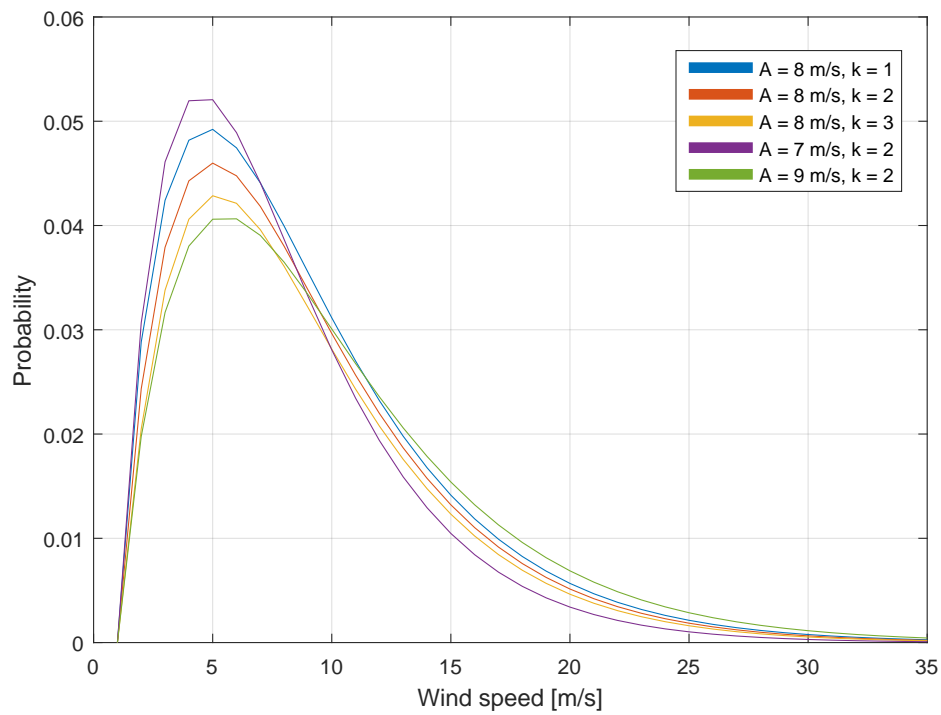


Figure 6.3: Method for the creation of the GWA dataset. Figure from [4].

Figure 6.4: Weibull distributions for different values of A and k .

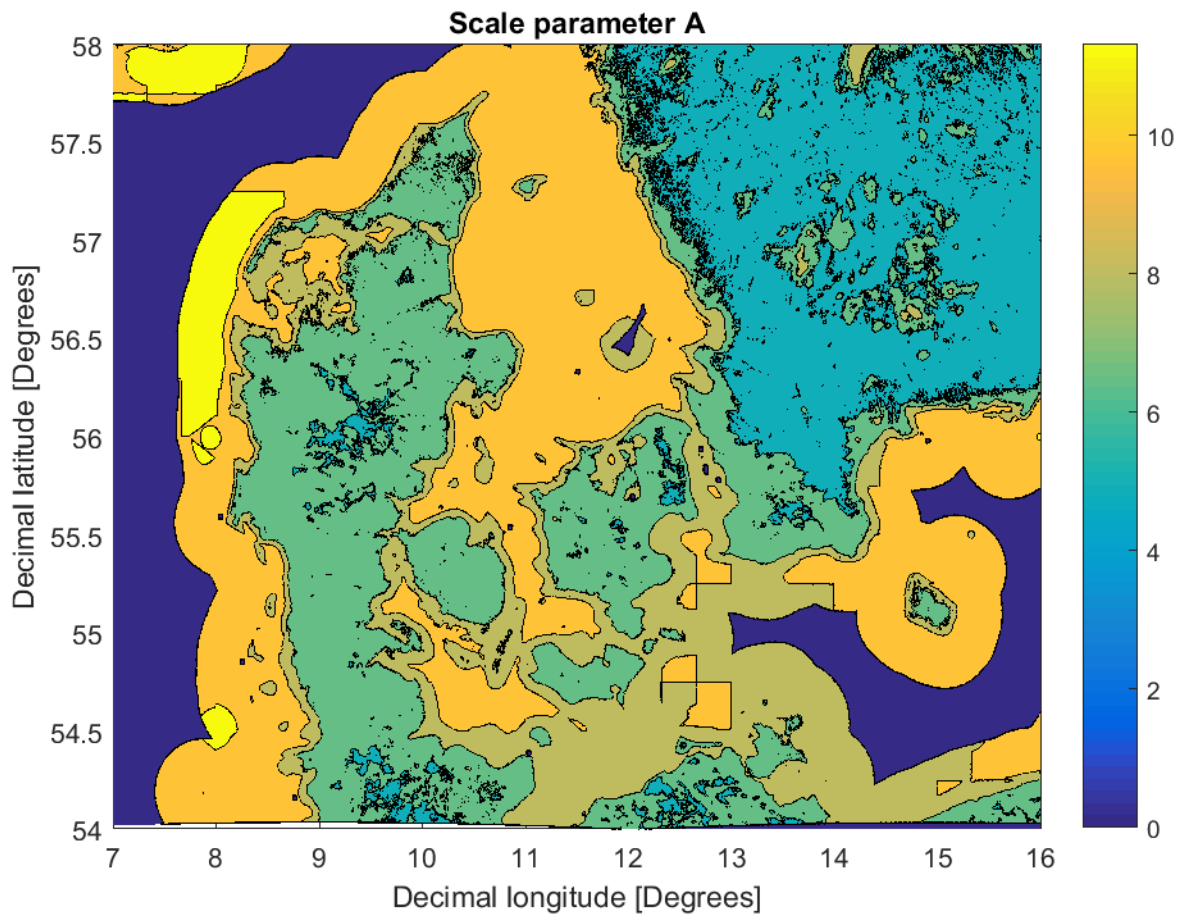


Figure 6.5: Contour plot showing the value of the scale parameter A in the GWA for Denmark.

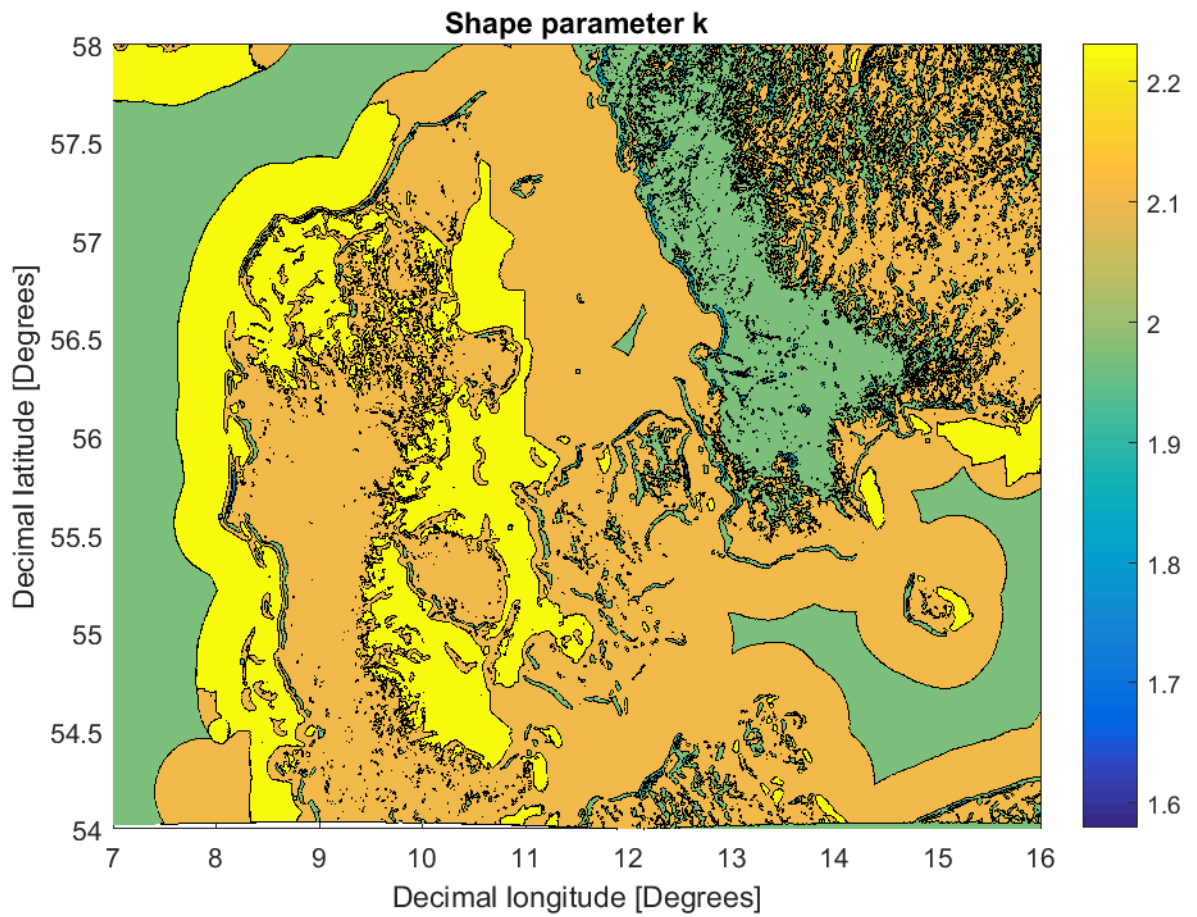


Figure 6.6: Contour plot showing the value of the shape parameter k in the GWA for Denmark.

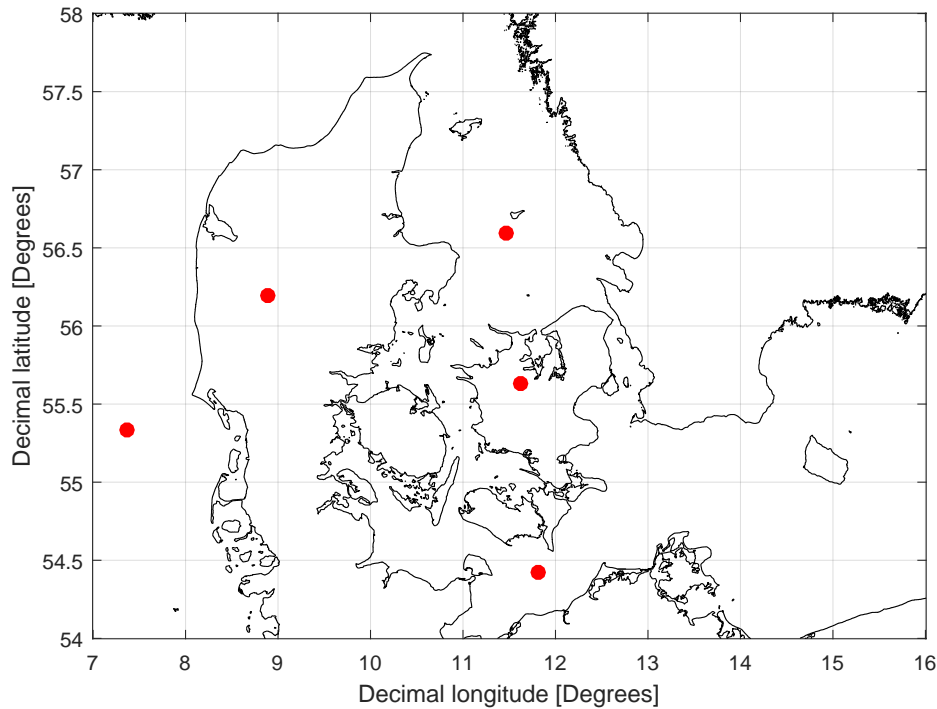


Figure 6.7: Points where datasets can be found in the mesoscale data.

6.3 Mesoscale data

This dataset is the data currently used in wind modeling by Ea, and has been supplied by Vestas. The dataset consists of mesoscale time series at heights of 10 m and 100 m a.g.l. Mesoscale meaning that the model has finer resolution and is only created for a limited area. The data is available for the years 2001-2010. The data is prepared specifically with modeling in Balmorel in mind and is made using the Weather Research and Forecast model (WRF 3.0.1). The details of the model are confidential and only available to Ea.

The supplied data has been extracted from the model grid and only a few points in Denmark are available, which are seen in Fig. 6.7. Because of this, more areas with corresponding wind time series cannot be created from this dataset and is therefore not valid for testing spatial aggregation in energy systems modeling.

6.4 Wind data summary

For simplicity, the most important parameters in terms of modeling of the different datasets are shown in Tab. 6.1.

Wind datasets	CFSR	GWA	Mesoscale
Resolution	0.3°x 0.3°	250 m x 250 m	5 points
Years	1979-2009	1979-2013	2001-2010
Measurement height a.g.l. [m]	10	50, 100, 200	10, 100

Table 6.1: The most important parameters of the different wind datasets inspected.

In conclusion, the resolution of the GWA is the best. The years and heights of the datasets overlap such that a comparison between the datasets can be made. Finally, the mesoscale dataset is unusable for testing spatial aggregation as only five points in Denmark exists.

With the mesoscale data not having enough data points and the GWA data not being a time series, the CFSR dataset has been chosen as the usable dataset. This choice will be validated in the following sections.

CHAPTER 7

Reference year

When modeling future wind generation, it is impossible to know exactly how the wind time series will behave in the future. Therefore, it is necessary to find a wind time series that can be assumed to be consistent with what is believed to be seen in the future. To ease the process, the same wind time series is used for the given area every year. This however, makes the choice of wind time series very important, as this will affect the power production for all years.

EMD International A/S [12] has a database of wind indices, which is calculated on a monthly basis as a percentage of how much wind power is produced compared to a standard month. A standard month is here calculated as the average wind power production of the given month for the last ten years. Wind index data is found for every year since 2001. The CFSR data is made for 1979-2011, meaning that the years where both datasets are available are 2001-2010.

The CFSR data acquired by Ea was only for the years 2001-2010. For the temporal resolution in Balmorel, a programme was created to extract the files to a usable format. The programme was made such that the wind time series started at the Monday closest to the first of January at midnight. Thereby data from the beginning of January 2011 was necessary to create the full 2010 dataset. Data for January 2010 was instead used to fill out the missing data. In order to get a consistent dataset for a single year, 2010 is then discarded as a reference year, limiting the usable years to 2001-2009.

Inspection of the wind index on a monthly basis during these years and comparison of these to the average index for the last 10 years, reveal that few years have an average monthly deviation less than 20 percentage points from the reference year. The years closely related to the average wind index are seen in Fig. 7.1

From the figure it is seen that January 2005 has an wind index above 2. As the wind index in this month is quite high, the year is not chosen, as the huge power production in January is not something seen every year and might therefore distort the results. Both 2004 and 2009 have wind generation close to the average over the last ten years and both of these years seem valid as a reference year. Occurrence of storms is a possibility in Denmark, and these will often result in curtailment of wind turbines as they otherwise might get damaged. These might not directly be shown in the wind index as storms might not last long and will not show in a monthly production average. Fig. 7.2 shows the amount of storms, divided into 5 year bins, in Denmark [9].

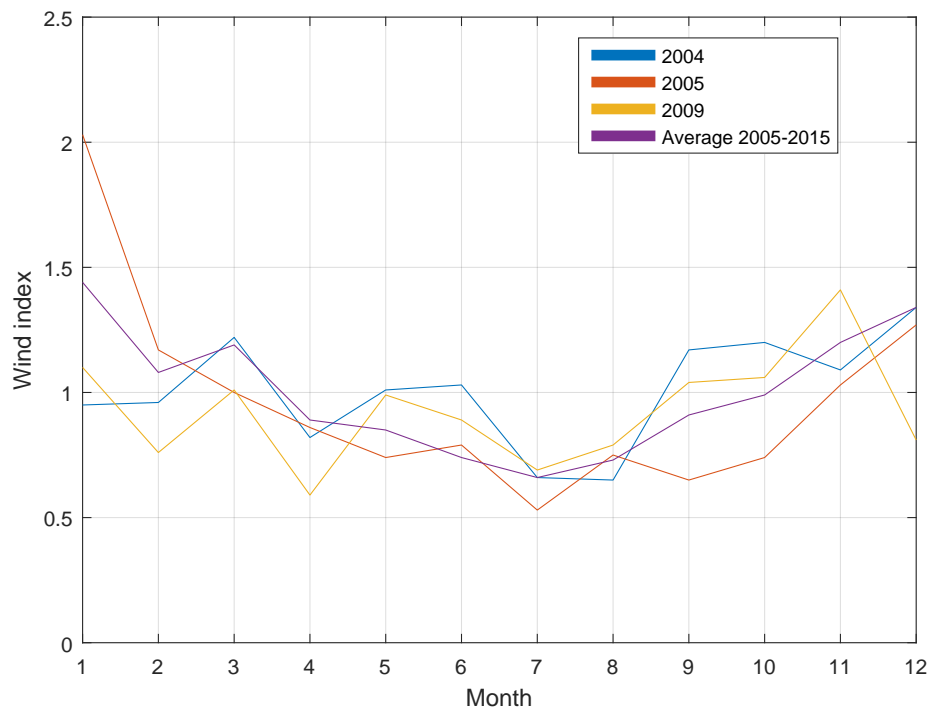


Figure 7.1: Figure showing the wind index for Denmark per month for the years with wind index closest to the ten year average.

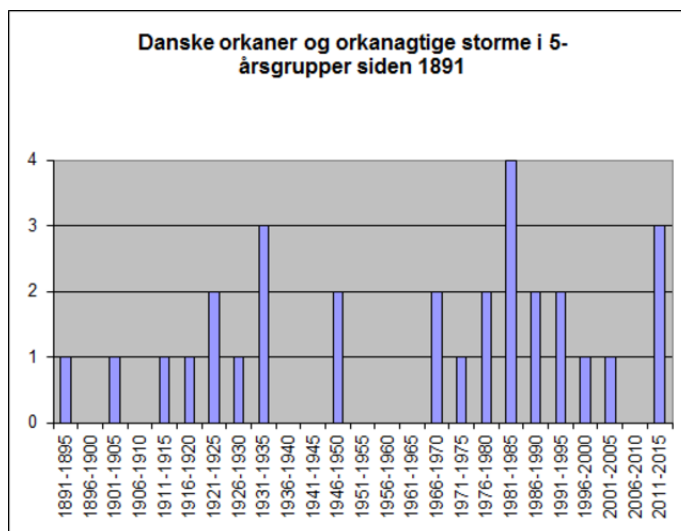


Figure 7.2: Amount of storms during a five year period above level 12 on the Beaufort scale corresponding to mean wind speeds of above 28.5 m/s. Figure from [9].

Inspection of the graph shows that no storms occurred between 2006 and 2010. Therefore, 2009 is chosen as the reference year, to ensure that a storm is not modeled every year for future years. Although further research could go into exactly which years the storms occurred, this is not that important, as the choice of reference year primarily is used to ensure consistency between the input data and the comparison between datasets.

CHAPTER 8

Comparing mesoscale and CFSR data

As previously discussed, changes in spatial aggregation requires more datasets to represent each area. With the limited number of data points from the mesoscale dataset, an investigation is made to investigate the differences between the CFSR and mesoscale datasets. No realized wind data is available for comparison of the different datasets. Therefore the datasets are compared to the mesoscale dataset, currently used by Ea.

Fig. 8.1 shows Probability Density Functions [PDF] for different sites in central Jylland. The wind time series shown are from 2001 at 50 m a.g.l. Vertical extrapolation is done using shear as explained in Chapter 3. The size of the bins are 0.2 m/s.

It is seen that the wind speeds in the mesoscale dataset have a broader distribution as well as a higher mean wind speed. Comparing specifically the Herning area the CFSR dataset is seen to have the highest peak at ≈ 5 m/s with the mesoscale peaking at ≈ 7 m/s. The mesoscale dataset also shows larger distribution for higher wind speeds in particular, which will lead to a higher power production. Therefore, using the mesoscale data would yield a larger power generation than the CFSR data if used for modeling. Another inspection of this effect is done by multiplying the entire wind time series for the year with a reference power curve for a Vestas V42 wind turbine [41]. The reasoning for this choice of reference power curve is that this is the most common type of wind turbine in central Jylland, which is explained further in Chapter 11. Tab. 8.1 shows the accumulated percentage for a year where an area produces at maximum capacity, known as the Capacity Factor (CF), which is calculated using Eq. (8.1).

$$CF = \frac{P_{\text{tot}, y}}{24 \text{ hours/day} \times 365 \text{ days/year} \times P_{\text{cap}}} \quad (8.1)$$

This proves that the CFSR data yields a lower power generation for this type of PC than the mesoscale data. In [24], the measured CF for installed onshore wind in Denmark are seen to have

Area	Mesoscale Herning	CFSR Hobro	CFSR Herning	CFSR Horsens
CF[%]	30.0	6.2	17.2	13.5

Table 8.1: Capacity factor for the given reference power curve.

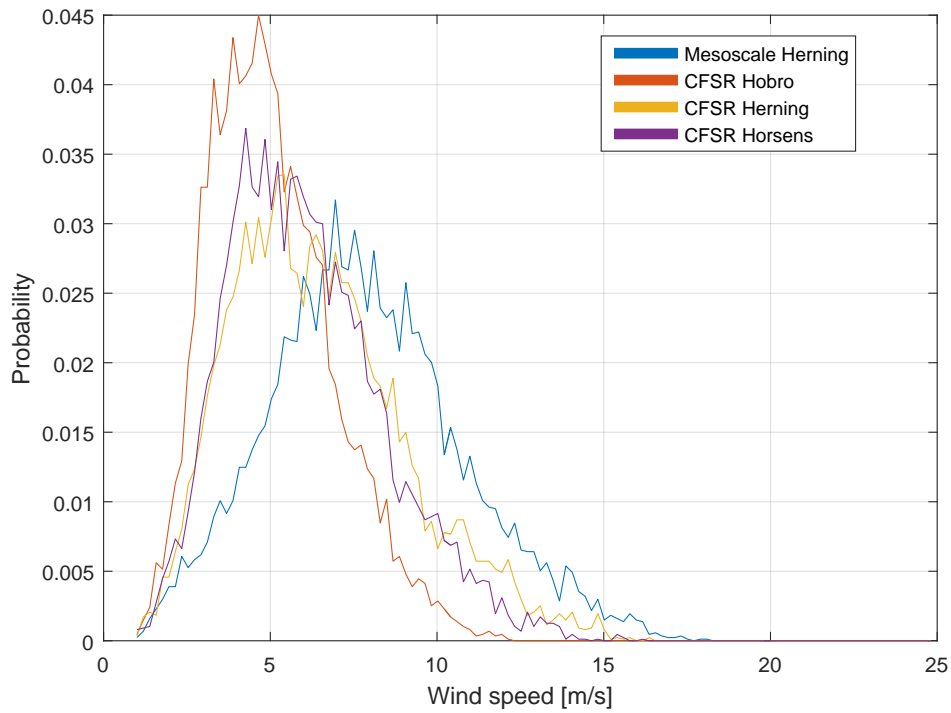


Figure 8.1: Probability density functions comparing mesoscale data with CFSR data for different locations around central Jylland, Denmark. The bin size is 0.2 m/s and the height is adjusted to 50 m a.g.l using shear.

gone from $\approx 22\%$ in 1995 to $\approx 34\%$ in 2014. As the reference turbine was developed around 1999, the actual CF for this site should be around 23%. Using a reference power curve for the calculations, the calculated capacity factor is expected to be higher than the observed data. Comparing the observed CF to the calculated CF in Tab. 8.1 it is seen that the mesoscale shows higher CF whereas the CFSR data shows lower.

The result of course depends on the reference power curve chosen as some power curves will have a lower cut in wind speed and might reach rated power at lower wind speeds. This could have a larger effect on lower wind speeds and therefore the production would look more similar in that case.

CHAPTER 9

Validation of the Global wind atlas

It was previously shown that the CFSR data has lower wind speeds than the mesoscale data and will therefore yield a much lower power production. This chapter will argue for the validity of the GWA dataset. As the GWA does not contain time series, a different validation approach is used, than what was used in the previous chapter.

The Stamdatregister, made by Energistyrelsen, contains information on the Danish wind turbines, with location and annual production [15]. Using the specific site of a turbine, the respective Weibull parameters for the given site, are used to calculate the expected production, using the reference power curve for the model shown in the Stamdatregister. Fig. 9.1 shows a comparison between the calculated and observed capacity factors. The GWA is an average of the years 1973-2013, which, through calculations, yields an average wind index of 1. The wind index for 2015 is used to correct for the higher wind speeds found in 2015 than an average year.

Several problems arise with this comparison. The total production given from the Stamdatregister represents the power delivered to the power grid. This therefore does not show if the turbine has been in operation at all times where wind is present. This means that curtailment, as well as downtime due to maintenance and faults, will decrease the observed CF. Furthermore losses in the electricity from the turbine production to the actual measured electricity production will decrease the observed production even further. The calculated CF has been compensated for the electrical losses by decreasing the CF by 10 % corresponding to the overestimation found in North America for turbines built until 2008 [7].

In order to calculate the wind power production, a reference power curve for the specific wind turbine model is used. These are explained further in Chapter 11. The reference turbine data is given by the manufacturer and will show a generic case. When installed, the reference power curve will change depending on different parameters explained further in Chapter 11. This will therefore result in an overshoot of the production from the GWA. An old wind turbine will not produce as much power due to wear and tear which will also decrease the observed CF [40]. Due to all these effects the points are all expected to be above the line in Fig. 9.1. This is the case for most sites, although some are below the line.

This might be due to GWA data being found for a less windy site than the actual site. Fig. 9.2 shows plots of the Weibull parameters for the points around the chosen site. The turbine site is

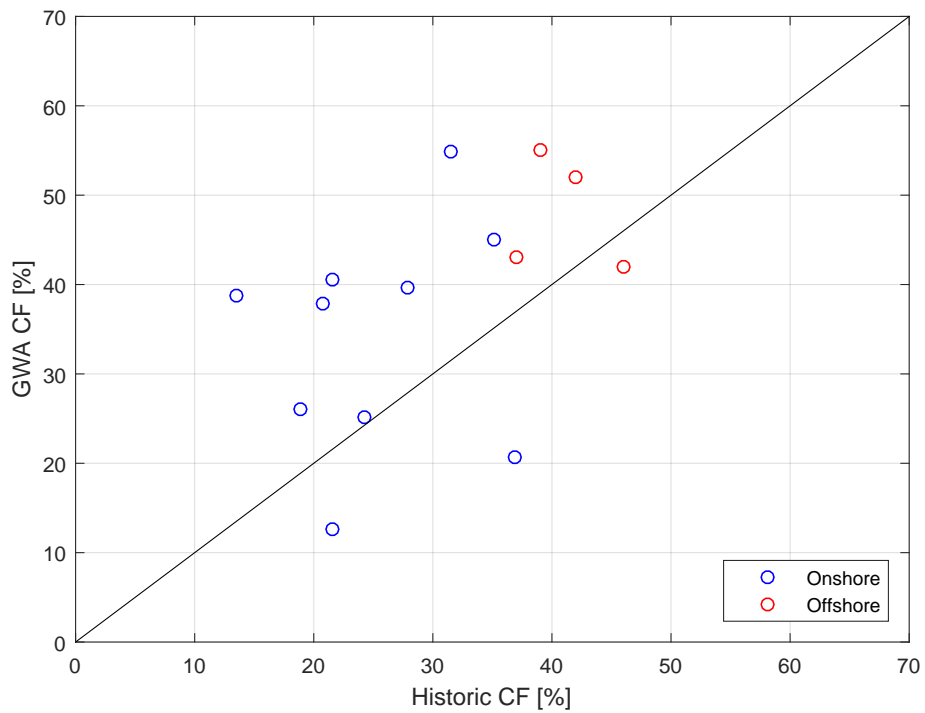


Figure 9.1: Capacity factors calculated from the GWA wind resource compared to the observed production at the site. The line represents the CF being equal. The sites are separated into offshore and onshore. Calculated CF are decreased by 10 % due to electrical losses from the wind turbine to the power grid

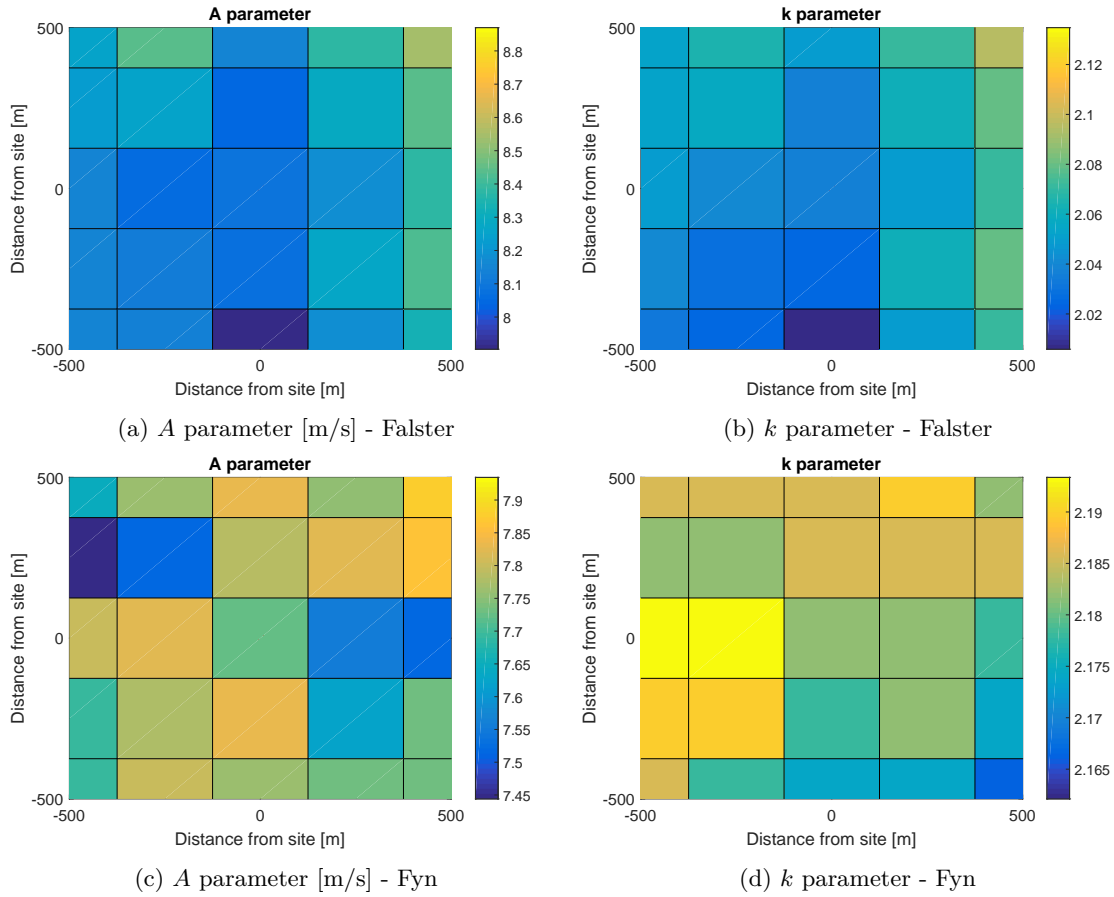


Figure 9.2: Plots of the Weibull parameters from the GWA at two sites on Falster (DK_East) and Fyn (DK_West) respectively.

placed in the middle and the neighbouring Weibull parameters are shown for their representative sites.

It is seen that the Weibull parameters do change around the chosen site. Effects like these can contribute to the CF being higher or lower than expected as the site taken might have been geographically shifted slightly. Another reasoning is that the reanalysis MERRA data, which is used as base for the GWA, does not have a good enough resolution to capture all mesoscale effects of the small islands in Denmark.

In order to completely be able to verify the data sets, many more points would need to be considered. This is however quite time consuming and many of the installed turbines in Denmark do not have reference power curves available to the public. Measured CF for the larger offshore wind farms in Denmark exist [17]. A comparison between these observed CF and the calculated ones are seen in Tab. 9.1.

Once again, the calculated CF are higher than the measured CF. This is again due to the effects explained earlier.

Wind farm	Horns Rev I	Anholt	Rødsand II
Observed CF [%]	42	45	44
GWA CF [%]	55	48	52

Table 9.1: GWA calculated CF compared to observed offshore wind farm values [17]

In conclusion, many losses and assumptions factor into the validation of the GWA data. With the amount of assumptions, the GWA cannot be completely validated for Denmark using this method. Compared to the CFSR dataset capacity factors seen in Tab. 8.1 however, the GWA is still closer to the observed values. Even though the CF are a bit off the observed data, the wind datasets will be corrected further using the aggregated power curve approach. This will be further explained in Chapter 11.

CHAPTER 10

Combining datasets

The GWA dataset fits observed wind power production better than the CFSR data and will therefore yield more accurate results if used in modeling of energy systems. A problem with the GWA data is however, that it is in the form of a Weibull distribution and does not have the hourly fluctuations necessary in the modeling method. Aparicio [1] describes a method for combining different datasets using the Cumulative Density Functions (CDF). Using this approach, it is possible to combine the datasets such that a combined dataset with both the hourly fluctuations from the CFSR dataset, as well as the wind speed distribution from the GWA, can be created. Eq. (10.1) describes the relationship between the Weibull parameters of the two datasets.

$$F_U(U) = 1 - \exp\left(\frac{U_{\text{CFSR}}}{A_{\text{CFSR}}}\right)^{k_{\text{CFSR}}} = 1 - \exp\left(\frac{U_{\text{GWA}}}{A_{\text{GWA}}}\right)^{k_{\text{GWA}}} \quad (10.1)$$

Here U is a wind speed with $F_U(U)$ being the CDF for that wind speed. The CDF refers to the probability that a wind speed is found below the given wind speed from the Weibull distribution. The scale parameter A and the shape parameter k are found for both datasets. Rearranging these terms, Eq. (10.2) is found. The Weibull parameters for the CFSR time series are found by solving the gamma functions from the mean wind speed and variance using Eq. (6.2) and Eq. (6.3) as seen in [5].

$$U_{\text{GWA}} = A_{\text{GWA}} \left(\frac{U_{\text{CFSR}}}{A_{\text{CFSR}}}\right)^{\frac{k_{\text{CFSR}}}{k_{\text{GWA}}}} \quad (10.2)$$

Eq. (10.2) relates the probabilities that a wind speed is below a certain value, found from the Weibull parameters calculated from the datasets. The wind speeds for the combined dataset U_{GWA} is calculated for all hours. From the Weibull parameters, the CDF for the different time series are plotted. This is shown in Fig. 10.1. Tab. 10.1 shows the Weibull parameters for the time series in Jylland 2009. The height of the GWA data used in this thesis is 50 m a.g.l. This is due to the height being closest to the average wind turbine height in Denmark.

Fig. 10.1 shows the CDF for both the CFSR and GWA dataset. It is seen that the CFSR data reaches a probability of 1 at ≈ 10 m/s whereas the CDF from the GWA reaches the same probability

A_{CFSR} [m/s]	k_{CFSR}	A_{GWA} [m/s]	k_{GWA}
4.91	2.24	7.32	2.22

Table 10.1: Weibull parameters for the two time series used to combine the datasets shown in Fig. 10.1.

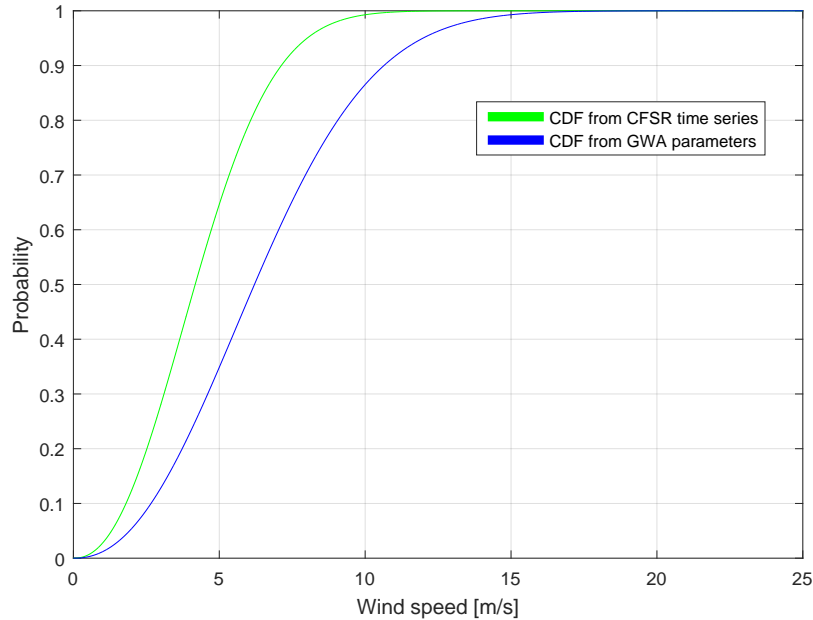


Figure 10.1: Cumulative density functions for the CFSR timeseries and the GWA in Jylland 2009.

closer to ≈ 15 m/s. This means, as previously shown, that the CFSR dataset generally has lower wind speeds than the GWA dataset. With the wind speeds, at all hours, for the new dataset with the GWA Weibull distribution, a section of the first 1000 hours is shown in Fig. 10.2.

The fluctuations are seen to be intact, although the amplitude of the wind has been altered. For most hours the wind speed for the combined dataset is seen to be higher than for the CFSR time series. This new combined dataset therefore has the fluctuations of the CFSR dataset, as well as the Weibull distribution given by the GWA. Matlab script for combining the datasets is seen in Appendix B.

10.1 Sensitivity of GWA Weibull parameters

The method for combining datasets uses the GWA Weibull parameters at the closest location to the site where the CFSR data is found. Even though the spatial resolution is 250 m, a slight misalignment of the coordinates might result in a different parameter set as seen in Fig. 9.2. The effect on the mean wind speed by changing a parameter by a percentage is seen in Fig. 10.3. The sensitivity analysis is made for the site, known as Jylland in Appendix A, with the Weibull parameters of $A_{\text{site}} = 7.32$

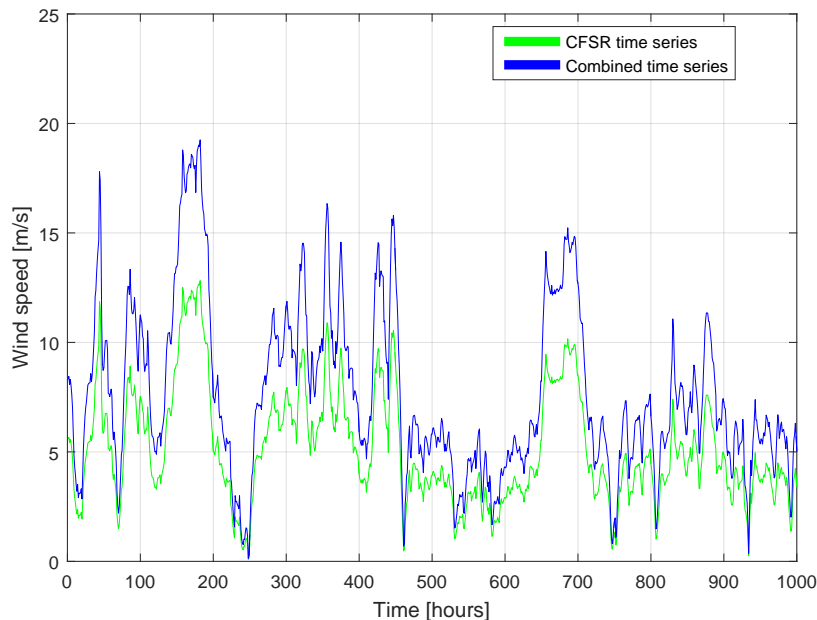


Figure 10.2: Time series from the unaltered CFSR data and the combined dataset created from relating the CDF from Fig. 10.1. Plotted for the first 1000 hours for better visibility.

m/s and $k_{\text{site}} = 2.22$. The mean wind speed of the CFSR time series is 4.4 m/s.

It is seen that the A parameter changes the mean wind speed linearly with the same percentage as the change in the parameter. The k parameter is seen to increase the mean wind speed by as much as 65 % when the k parameter is decreased by 20 %. This also shows that even small alterations in the k parameter will have a large effect on the mean wind speed. Fig. 10.4 shows the first 1000 hours of the wind time series for the extreme cases in the sensitivity analyses.

As seen with the mean wind speeds, the change in the Weibull parameters has a large effect on how the combined time series will look. Therefore it is of great importance to ensure that the GWA parameters are used for the exact site.

10.2 Comparing mesoscale to combined dataset

In the same manner as seen in Chapter 8, the combined dataset is compared to the mesoscale dataset. In this case, the comparison is done for 2001 at a height of 100 m a.g.l. as these datasets are directly comparable without having to do any vertical extrapolation. When choosing a year, it mainly means the fluctuations from 2001, as the GWA Weibull parameters are an average over 34 years. Therefore some changes might occur between the datasets being compared, but the GWA distribution will be more representative for modeling the future.

Fig. 10.5 shows the PDF of the two time series plotted for Herring in 2001, as well as the unaltered

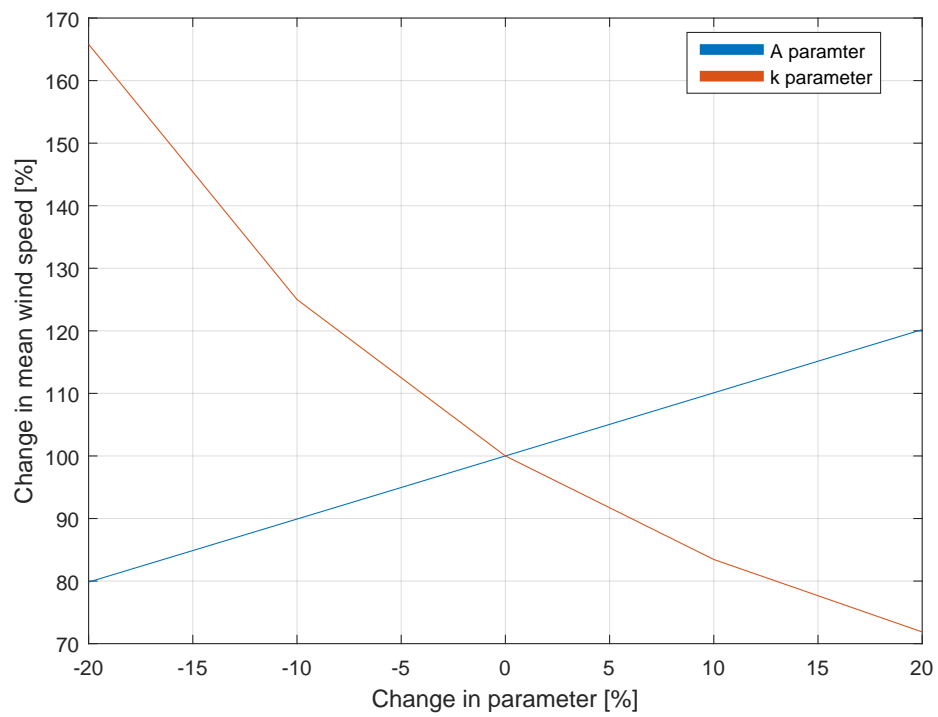


Figure 10.3: Sensitivity analysis for the Weibull parameters used to create the combined GWA and CFSR dataset. In the figure is seen the effect of the mean wind speed for the entire year when changing one of the Weibull parameters by a percentage.

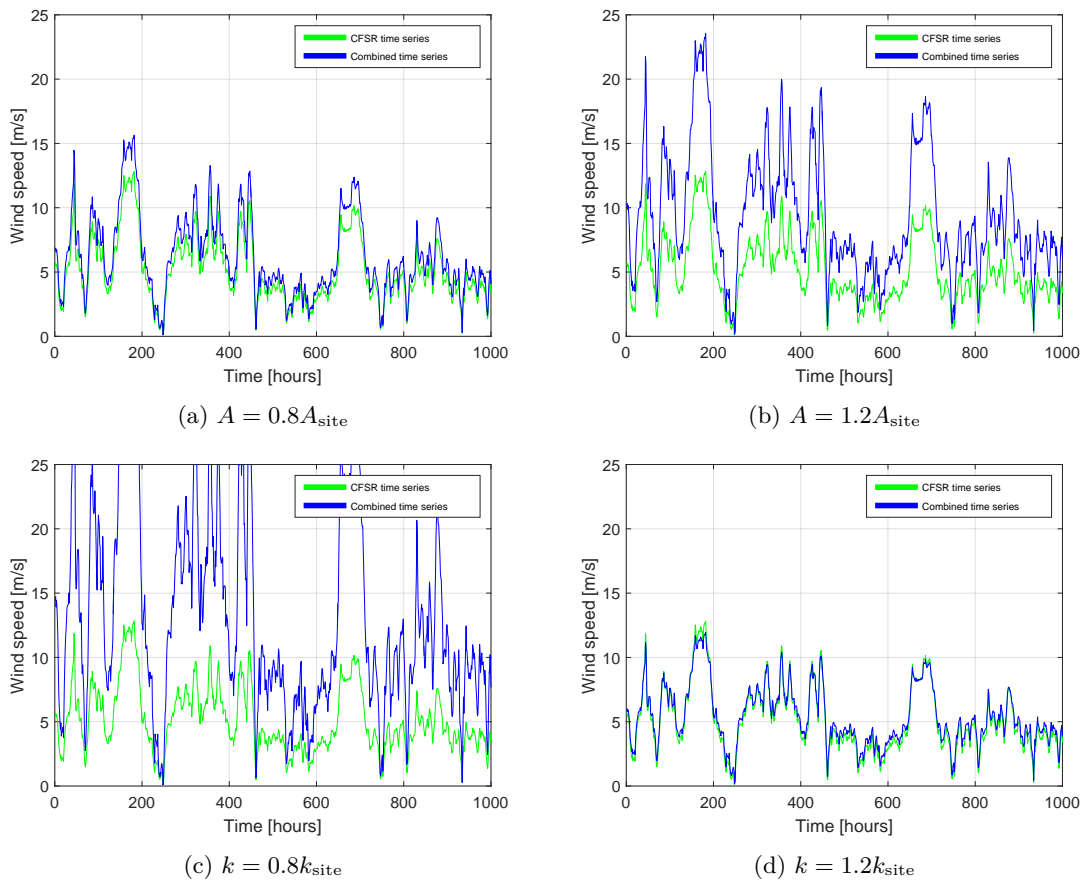


Figure 10.4: Combined CFSR and GWA time series compared to CFSR time series with the extreme changes in the Weibull parameters.

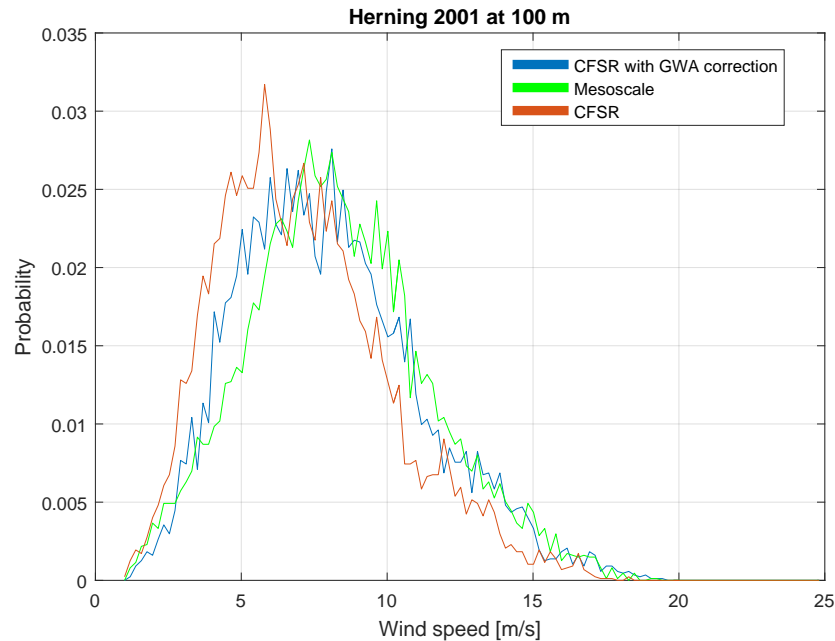


Figure 10.5: PDF-comparison of the mesoscale timeseries and the combined time series from CFSR and GWA data. The time series are extracted at Herring at 100 m a.g.l in 2001.

CFSR data scaled to 100 m using wind shear. It is seen that the GWA generated time series have lower overall wind speeds than the mesoscale time series, with the unaltered CFSR dataset having even lower wind speeds. Using the same approach for calculating the power generation from these time series as seen in Section 8, the capacity factors are calculated and seen in Tab. 10.2. The same reference turbine is used, even though that turbine model would never have a height of 100 m. A taller turbine will see a better wind resource and therefore a larger CF.

Area	Mesoscale	CFSR with GWA	CFSR
CF [%]	35.0	32.0	23.6

Table 10.2: Table showing the CF from the wind time series seen in Fig. 10.5. The scaling of the CFSR data with GWA is seen to be much closer to the mesoscale data compared to what was seen in Tab. 8.1.

The table shows that the combined dataset has a production much closer to the mesoscale data than the CFSR dataset. Compared to Tab. 9.1, the CF for the combined dataset is much closer to the mesoscale CF, although a bit higher than what would be expected. The combined dataset is however closer to observed data and is therefore chosen as the wind dataset used for further modeling. Furthermore a correction of the time series is made in the creation of aggregated power curves explained in the Chapter 11.

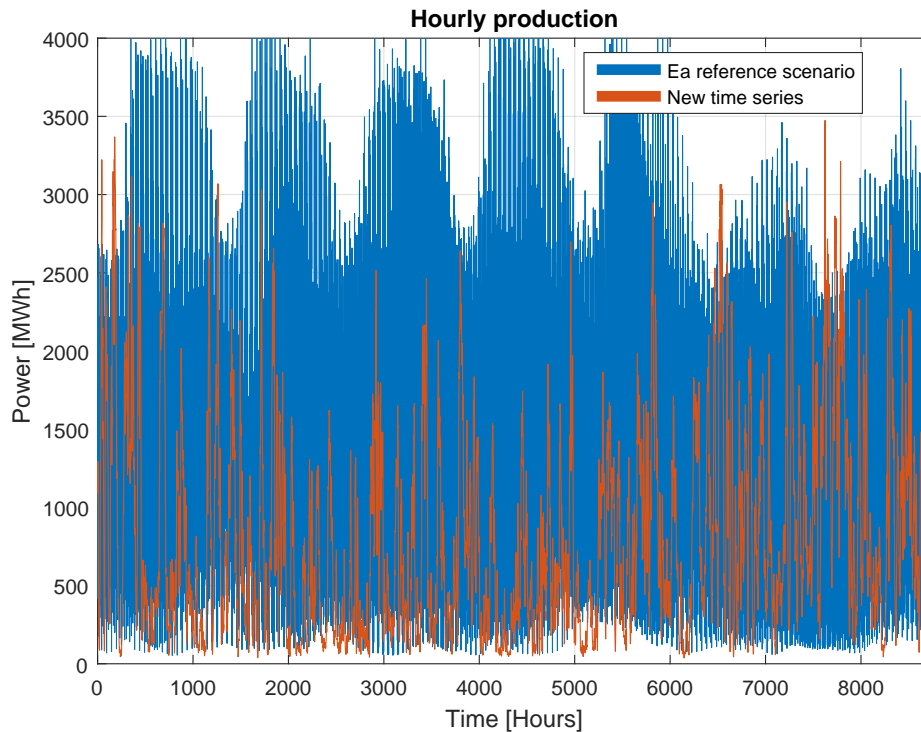


Figure 10.6: Hourly wind power production for the Ea reference case with mesoscale data and CFSR combined with GWA data respectively.

10.3 Using combined time series in Balmorel

With a wind dataset which is usable in modeling, a test is made to see the effect of power curves. This is done by inputting the new wind time series at the same locations into Balmorel and seeing the effect of running the model with the combined dataset. To investigate the effects of the power curves, the combined CFSR and GWA datasets are implemented in the current Ea reference case, such that only the wind time series are altered and the power curves are kept constant. The model was run with hourly resolution for 2015, which, along with Balmorel, will be explained further in Part II. Fig. 10.6 shows the results of the model compared to the Ea reference case with the mesoscale wind time series.

Calculating the total production for both cases seen in Fig. 10.6, the new time series are seen to yield 58 % of the total yearly production. The results on curtailment and the power prices from running the model are seen in Tab. 10.3.

From Tab. 10.3 the curtailment is seen to be much lower with the combined dataset and the power prices being much higher. This is in accordance with the wind power production being much lower for the combined dataset. This effect comes both from the wind speeds being a little lower, but also because the currently modeled power curves are created for the mesoscale dataset.

	Ea reference case	Old PC, new TS
Total Curtailment [GWh]	655	35
Power price DK East [DKK/MWh]	263	377
Power price DK West [DKK/MWh]	242	368

Table 10.3: Results for running Balmorel with hourly resolution for 2015.

CHAPTER 11

Aggregated power curves

The power curves of the wind turbines are an important factor, as these decide how much power is produced for a given wind speed. In the previous sections, the power curves used have all been manufacturer specifications for a single wind turbine. These power curves are however rarely what can be measured, once the wind turbine has been installed. Several factors affect the manufacturer specified power curves such as terrain, electrical losses and wake effects from other turbines if installed close together [21]. Furthermore terrain and wake effects will often change the power curve depending on the direction of the incoming wind.

For Denmark, the different turbines installed can be found from the Stamdataregister [15]. Estimating a power curve for every wind turbine is very time consuming, if all effects are taken into account. For countries without a wind turbine registry it might prove difficult to obtain data for every turbine as well. Therefore, an aggregated power curve valid for a bigger area can be estimated.

Different approaches for creating aggregated power curves exist. Hayes et al. describes a method of estimating the power curves based on measured wind speeds and hourly power production [22]. This method requires huge amounts of data, which will often be unobtainable for the exact wind turbines being considered in the study. Other methods that does not require the exact generation data have been described by Kaiser et al. [23] and Nørgaard et al.[32]. Kaiser et al. describes a method for estimating a power curve for an area using the turbulence intensity. The turbulence intensity for the given site is unfortunately not an easily obtainable parameter, and the method does not take the spatial aggregation of power curves into consideration. Nørgaard et al. describes a method for creating the aggregated power curves using a spatial probability distribution of the wind speeds around the chosen reference power curve at the site. This method is chosen as the basis of the method developed throughout this thesis, and will be further explained in the following sections.

A single representative wind speed for the given area is chosen. Nørgaard et al. proposes a method for creating a rolling average of the wind speeds. As the goal of this thesis is to investigate the effect of spatial aggregation, this effect will be better distinguishable by letting a single wind speed be representative for an area, and then adding more areas instead.

Choosing a reference power curve

The method requires a reference power curve representative for the site. The choice of reference power curve dictates the slope of the aggregated power curve. It is important to choose the reference power curve such that it represents the technology mix in the area. The Stamdatregister provides information on the manufacturer and the turbine model. This registry is unfortunately far from complete, as many turbine manufacturers or models are listed as unknown. By sorting the wind turbines per municipality, the most commonly found wind turbine model in every area can be found. Fig. 11.1 shows a rough separation of the most common turbine models, where data is available, for Denmark.

All of the wind turbine models used as reference turbines are pitch regulated Variable Speed Wind Turbines (VSWT), which is the case for all new model types. Some older technologies still exist in Denmark, which will have a different type of power curve. Tab. 11.1 shows the specifications of the different wind turbine models. Fig. 11.2 shows the power curves in per unit for easier comparison. Generally the Vestas models are seen to have almost the same slope, cut in speed and rated wind speed. The cut in wind speed is the wind speed where the turbine starts producing power and the rated power is the power at which the power curve becomes constant. The Siemens model is seen to have a lower cut in wind speed and rated wind speed, but happens to be a newer model [40].

WT model	Rotor diameter [m]	Hub height [m]	Capacity [kW]
Vestas V27	27	30	225
Vestas V42	42	35	600
Vestas V80	80	67	2000
Siemens SWT2.3	93	80	2300

Table 11.1: Table showing specifications of reference wind turbines used for power curves. The WT models oftentimes exist for different hub height, and the ones listed are corresponding to the hub heights for the given reference power curve. Data from [41].

All of the reference power curves have been assigned a cut out wind speed of 25 m/s.

Creating smoothed power curve

The reference power curve chosen does not take the aggregation of power curves into account. A method for creating the aggregated power curves is based on the approach explained by Nørgaard et al. [32]. First, a smoothed power curve is created. The smoothing comes from taking a spatial distribution of the wind speeds around the reference power curve at the given site. This is done to capture the spatial variations in the wind. In [32], the standard deviation for an area can be found, but requires the turbulence intensity which is unavailable. Furthermore, an offset of the distribution is used. Instead, the standard deviation and offset can be estimated using the production from a reference power curve. The reference power curve is smoothed with the spatial distribution using Eq. (11.1).

$$Pm_j = \sum_i P s_{j+i} \times p s_i \quad (11.1)$$

Here Pm_j is the discrete multi turbine production of the j^{th} power curve element. This is calculated

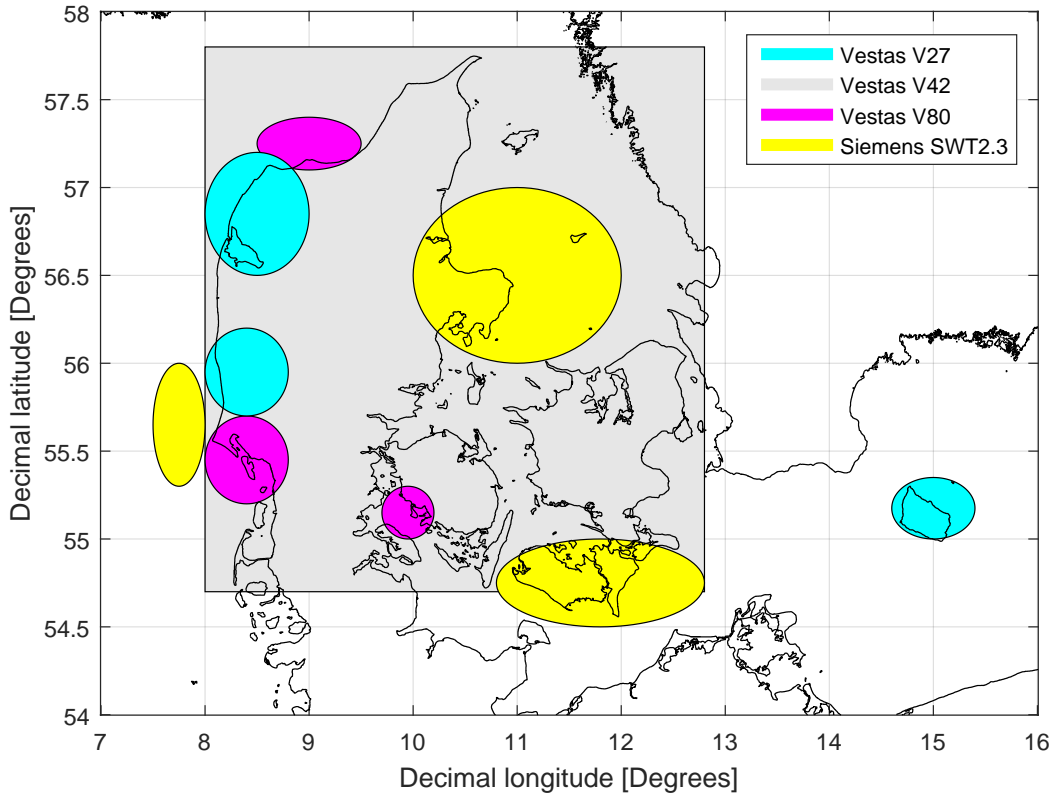


Figure 11.1: Areas where different reference wind turbines are found. Based on data from the Stamdataregister [15].

from the sum product of the probability ps_i of the discrete i^{th} element of the distribution and the production at the chosen site. To avoid using the turbulence intensity, a number of wind time series in the area is used to calculate the production at all sites. An average normalized production for the sites is then found. This is plotted against the representative wind speed for the area. The representative site is chosen as the site where most wind turbines are already found. The reasoning for this, is that this can be assumed to be the site with a good wind resource, but also a site where it is allowed and possible to install wind turbines.

The smoothed power curve is fitted to the power production representative for the area, which takes the spatial distribution into account. This is done by minimizing the absolute difference between the smoothed power curve and the scattered data by altering the standard deviation and the offset of the spatial distribution. The fit is done using the Generalized Reduced Gradient Algorithm (GRG) nonlinear solver in Excel [29]. A figure showing the scattered data, as well as the fitted smoothed power curve, is seen in Fig. 11.3.

From the figure, the effects of the smoothed power curve are compared to the reference power curves shown in Fig. 11.2. It is seen that the sharp decrease at the cut out speed has been smoothed such that the production does not end as abruptly.

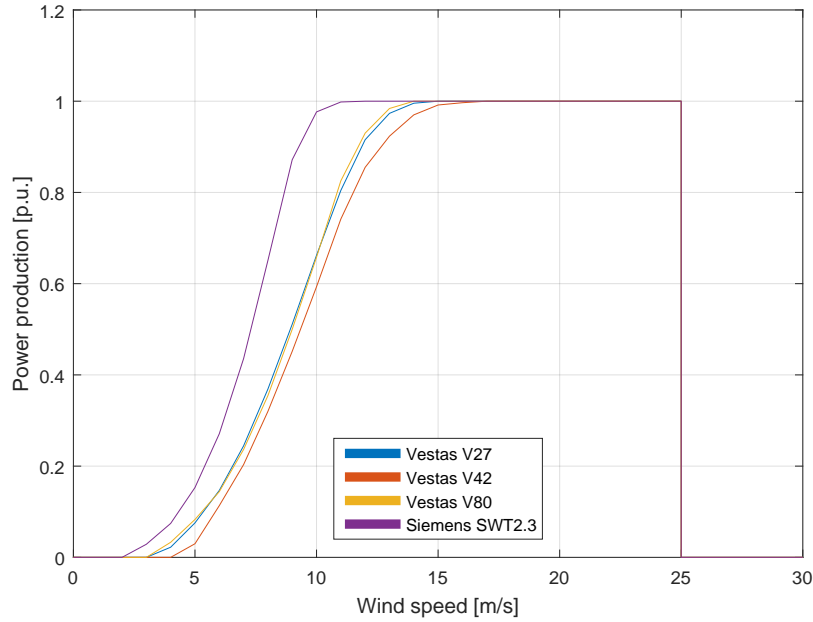


Figure 11.2: Plot showing the different reference power curves used to create aggregated power curves.

Fitting logistic function

The smoothed power curve, found in the previous section, represents the chosen area from a single time series. This smoothed power curve is given as power production value for discrete values of wind speeds. Implementing the smoothed power curve in Balmorel, would in this case have to be done using a look up table. In order to reduce computation times, a function is created such that a value is easily calculated at every wind speed.

Two logistic functions are used to represent the smoothed power curve. Eq. (11.2) shows the logistic functions used for the fit.

$$P = \begin{cases} \frac{1}{1+\exp(-GR_{inc}(U \times HF - MG_{inc}))} & \text{for } U < 25 \text{ m/s} \\ \frac{1}{1+\exp(-GR_{dec}(MG_{dec} - U \times HF))} & \text{for } U \geq 25 \text{ m/s} \end{cases} \quad (11.2)$$

The power production is constrained as seen in Eq. (11.3).

$$0 < P \leq MP \quad (11.3)$$

The first part of Eq. (11.2) represents the incline of the power curve until the cut off wind speed of 25 m/s is reached. The second part represents the decrease to no produced power at wind speeds higher than the cut off wind speed.

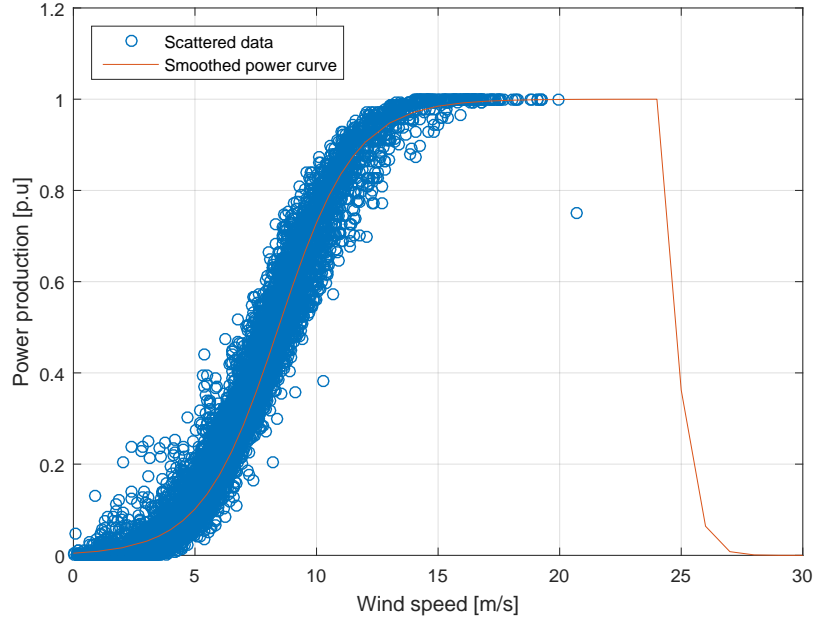


Figure 11.3: Scattered data for central Jylland using one reference time series and three neighbouring wind time series in central Jylland. In the plot also the fitted smoothed power curve.

Symbol	Description	Unit	Constraints
MP	Maximum production	p.u	$0 < MP \leq 1$
GR_{inc}	Growth rate incline		$0.5 < GR_{inc} < 0.9$
MG_{inc}	Max growth incline	m/s	$7 < MG_{inc} < 13$
GR_{dec}	Growth rate decline		$1.5 < GR_{dec} < 10$
MG_{dec}	Max growth decline	m/s	$24 < MG_{dec} < 27$
HF	Height factor		
U	Wind speed	m/s	

Table 11.2: Table showing the different notations, units and constraint for the variables used in the logistic power curve fit.

Several variables are changed in order to get the best fit. These are shown in Tab. 11.2. Eq. (11.3) constrains the power production between 0 and MP . The growth rate GR , both for incline and decline, are variables used to vary the slope of the logistic power curve. The max growth MG is the wind speed, corresponding to the point on the logistic function where the slope is at its maximum. The height factor HF depends on the specific area chosen, calculated from the average wind turbine hub height, time series measurement height and shear factor. This value is calculated to scale the power curve height to the actual wind speed heights found in the given area. The calculation is done using Eq. (11.4) and derived from the wind profile power-law shown in Eq. (3.2). Eq. (11.4) uses the shear factor α at the given site.

$$HF = \left(\frac{z}{z_{mast}} \right)^\alpha \quad (11.4)$$

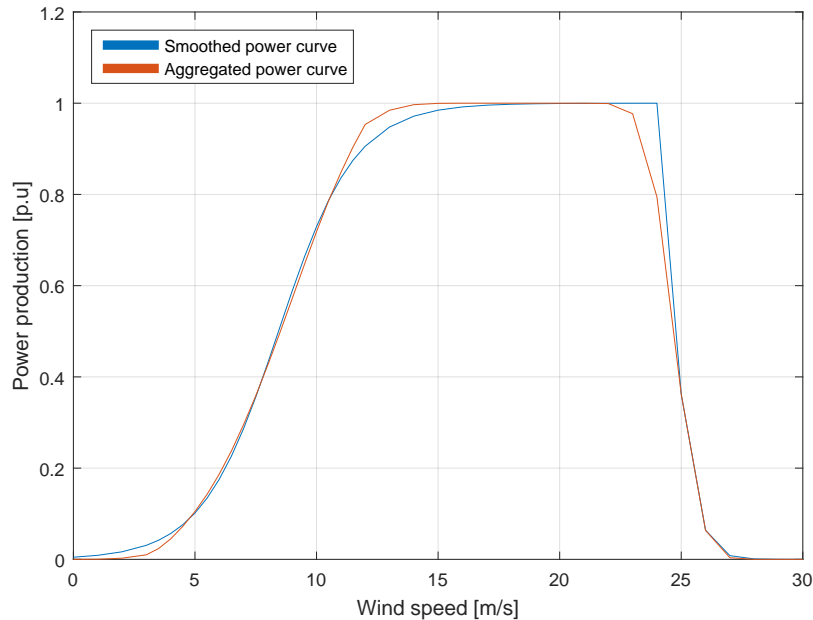


Figure 11.4: Fit of the logistic functions to the smoothed power curve.

Lastly the logistic power curve fit depends on the wind speed U .

The fit to the smoothed power curve is made with the Excel solver tool by varying the growth rates, max growths and maximum production. In order to evaluate the fit, the absolute difference in the power production at every discrete wind speed is calculated and summed which is then minimized by changing the five variables. A plot of the fit is seen in Fig. 11.4.

Differences between the smoothed power curves and the logistic fit is seen in two areas on the incline of the power curve. These does not matter, as the fit to observed data will alter the logistic function further. In the area of 25 m/s, the logistic fit is seen not to fit the smoothed power curve. This is due to the choice of the separation of the which parts of the smoothed power curve the two different logistic function fits to. This has been placed there in order to minimize the number of variables that are altered during the fit. Furthermore this is not a large point of concern as very few hours have average wind speeds in around 24-25 m/s.

Fitting to capacity factor

From the Stamdatregister, the production and installed capacity for every turbine is found. This is used to calculate the capacity factors at every site. The capacity factor is calculated as explained in Eq. (8.1).

As the reference power curve and chosen wind speeds do not correspond to what is actually found, the capacity factors are used in the fit, in order to ensure that the power curve gives the correct production of power. The fit is done by minimizing the absolute value of the difference between

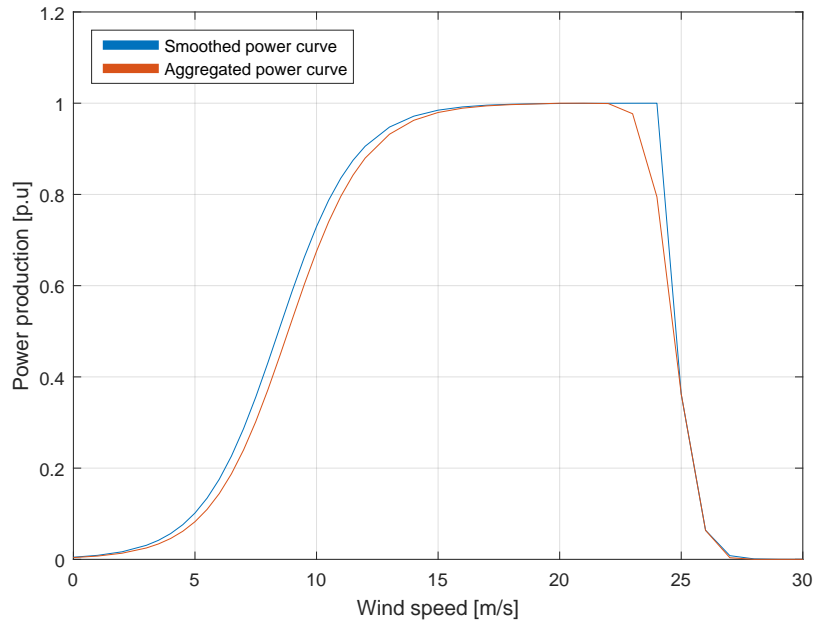


Figure 11.5: Figure showing the smoothed power curve and the aggregated power curve fitted to capacity factors for the given site.

observed and calculated capacity factors. The variables altered for this fit is chosen as the growth rate and maximum growth, only for the incline of the power curve as well as the maximum production.

The reasoning behind this choice, is that most areas will have very few hours where the wind speeds exceeds the cut off wind speed and therefore changing these values will, for most cases, distort the power curves far from the reference power curve. Changing the incline variables will often change the slope of the power curve, which is based on the reference power curve. As the reference power curve rarely corresponds to the technology mix in the area, a small deviation in the slope is of no concern.

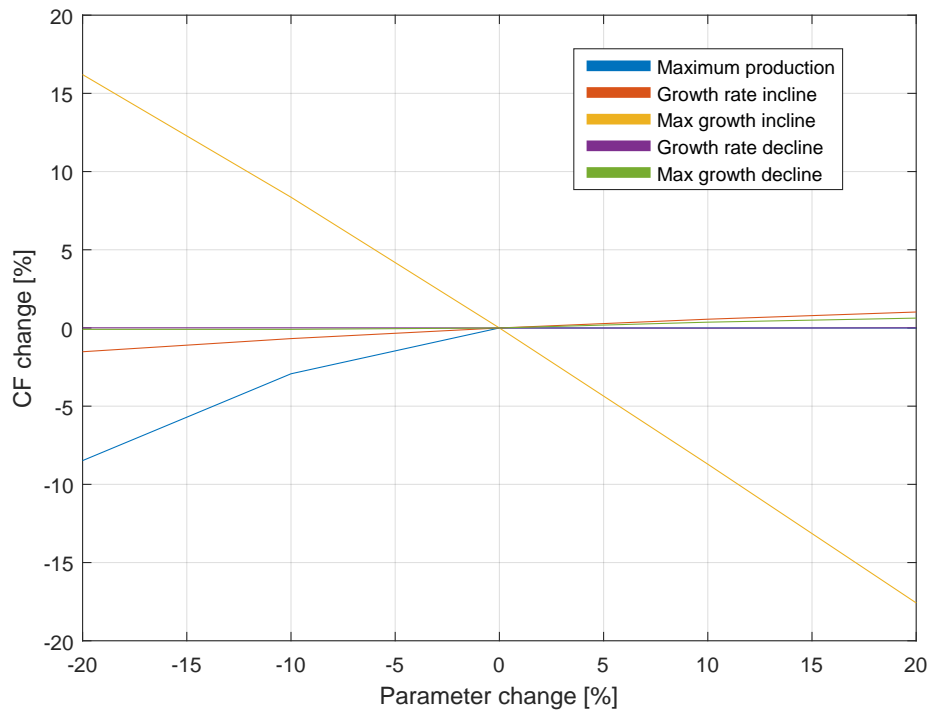


Figure 11.6: Sensitivity of the five parameters used in the logistic fit for power curves. The different parameters are altered $\pm 10\%$ and $\pm 20\%$ one at a time and the effects are shown on the change in capacity factor.

Sensitivity of power curve fitting

Fitting the logistic functions to the smoothed power curve is based on five different parameters, and is as explained earlier a very visual approach. Due to the fact that the fit is based on five parameters, the different parameters might affect the final outcome in different ways. Furthermore some parameters might be prioritized in the Excel solver. These effects are investigated by creating a power curve, with a certain set of parameters, and varying a single parameter a certain percentage, without changing the other parameters. The final effect of the parameter variation is based on the capacity factor that the power curve would yield, as this is the final fit for the logistic functions.

Fig 11.6 shows the effects on the capacity factor by altering the five parameters one at a time for $\pm 10\%$ and $\pm 20\%$ respectively. From the figure it is seen that the different parameters affect the capacity factor in various ways. Maximum production, as seen in Eq. (11.3), only affects the capacity factor when the value of MP is lower than 1. It is however seen to decrease the capacity factor by roughly 10% when the maximum production parameter is decreased by 20%. The inclining growth rate and declining growth rate are seen to only alter the capacity factor a few per cent. The declining maximum growth has barely any effect on the capacity factor.

The parameters with, by far, the most effect on the capacity factor, is the inclining maximum growth. This parameter is seen to change the capacity factor by more than 15% for a change of 20

% on the parameter, meaning that the capacity factor changes almost as much as a change in the inclining maximum growth. Therefore it is important to ensure a correct fit as small alterations, especially for the inclining maximum growth, will alter the power output substantially.

CHAPTER 12

Discussion of wind study

12.1 Discussion of wind datasets

The choice of which dataset to use for modeling is not believed to have a large effect on the power production, due to the aggregated power curves being fitted to observed production data. Therefore, one could be lead to believe that the choice does not matter. This however, might not be the case. When combining the wind power production with the rest of the energy system, the fluctuations might have a huge effect on the power prices. If the demand is high and no wind is present, the power prices will increase because of the other technologies.

The fluctuations from the CFSR dataset, used here, might not be exactly what is experienced by the wind turbines. The wind time series are created at a 10 m height a.g.l, which might not be the same at a wind turbine rotor height, due to the terrain. Therefore, a better dataset might be found if this dataset was proven to have more accurate wind speed fluctuations.

The different wind datasets, that was evaluated, have not been compared to realized wind data. This becomes a concern in cases where the calculated production cannot be corrected to observed power production. This happens in cases where Balmorel is set to invest in new technologies. Therefore, investment runs cannot be validated, without prior validation of the wind data sets used. The same aggregated power curves cannot be used for all years of the investment run, since the technology changes. This is partly due to the shift in technology mix. Wind turbine are becoming bigger, which changes the reference power curves [38]. The aggregated power curves will thereby also change to fit more modern turbine types as the technology mix shifts.

When choosing a wind time series representative for an area, one cannot tell the terrain features at the site. Therefore it is possible to choose a site where the wind speeds are different from the remaining area due to terrain. The site was chosen based on where wind turbines were already found for the site, although the resolution of the CFSR dataset limits the amount of sites that can be chosen.

12.2 Discussion of aggregated power curves

Creation of the aggregated power curves, as defined in this thesis, is in many ways based on visual precision, meaning that some uncertainties occur. Even though the power curves have been calibrated to observed capacity factors, there still is a possibility for the power curves to be a bit off. If minor uncertainties exist in the power curves, this will also affect the production modeled in Balmorel. Therefore a great deal of precision and carefulness is required when creating the aggregated power curves.

The choice of reference power curve will have an effect on the aggregated power curve, although the fit to observed values is made. Air density ρ_{air} will influence the power produced from a wind turbine [28]. The power production is given as seen in Eq. (4.1). Reference wind turbines are calculated at an air density of $\rho_{air} = 1.225 \text{ kg/m}^3$. This air density corresponds to sea level height at 15°C , which is not consistent with all wind turbines in Denmark. The air density changes with temperature as seen in Eq. (12.1).

$$\rho_{air} = \frac{p}{R_{specific}T} \quad (12.1)$$

Here p is the pressure, $R_{specific}$ is the specific gas constant and T is the temperature. From these equations it is seen that the power does change with temperature and pressure across Denmark. Therefore the reference power curves will almost never be the same as experienced in real life. As the reference power curves are rarely close to what is found in real life, the change in the incline parameters in order to fit the power curve to observed capacity factors is justified.

Creation of aggregated power curves is based on many assumptions and therefore many challenges occurs using the method. A problem with the explained method is that it requires a time series for the area chosen. The optimal solution would be to create the aggregated power curves from a purely technology point of view, without having to use the wind speeds. A method for this is however not desired, as this would require much more data on not only all the wind turbines in the given area, but also the location and terrain data. This approach also would be much more time consuming, as every single turbine in the area would need to be used in the aggregation process.

Another challenge arises due to the several fits, which are all based on a visual approach, even though the empirically found constraints seen in Tab. 11.2 will ease the process. Furthermore, human errors can be a factor, especially in the choice of the reference time series. The fit to observed capacity factors does however fix most of the mistakes that might arise in the aggregated power curve creation process.

Part II

Modeling of energy systems

CHAPTER 13

Introduction to modeling of wind power in energy systems

Power generation from wind turbines is easily calculated, once the power curve and wind speeds are known. Other effects might however also factor into the power generation, when connected with the rest of the energy system. As a non-dispatchable source, the generation from wind turbines, and other non-dispatchable renewable technologies such as solar, are prioritized in the system. What is meant by prioritizing, is that all the renewable power is being utilized in the system and the remaining demand, if any, is then covered by more controllable sources like traditional power plants.

The prioritizing does not always make sense though, as sometimes the power generation from renewables will exceed the demand. If this power cannot be stored, it either has to be exported or the power production should be stopped. The viability of exporting power is very much dependent on the neighbouring countries. If the neighbouring country has enough power production to meet its own demand, the power price can actually turn negative in order to get rid of the excess power. For cases like these, it might prove a more feasible option to turn off the wind turbines. This type of curtailment will, along with curtailment due to high wind speeds, also affect the power system.

When using other power producing technologies to generate the remaining power needed to meet the demand, it does take time for these technologies to start and stop. These processes will have an associated cost. Therefore, it might, in some cases, prove economically feasible to not turn off the power plants and curtail some wind turbines instead. Furthermore, some technologies that are supplying heat, will also be able to produce power which will affect the energy system as the heat demand must be met as well.

Using mathematical modeling, it is possible to find the optimal solution to how much and at what times the different technologies should produce power and heat. The mathematical modeling tool Balmorel is used in this thesis and the specifics of the model will be explained in the following chapters.

CHAPTER 14

Balmorel

14.1 Introduction to Balmorel

The Balmorel model is an energy systems optimisation model, developed by Ravn et al, 2001 that focuses on electricity and heat [35] [36]. The model is a bottom-up economic dispatch model that minimizes the overall costs of the energy system. By bottom-up is meant that the model uses the already installed technologies to expand and invest further in, to reach a known goal in terms of production which will always equal the demand.

Balmorel was created to model the energy system of the countries around the Baltic sea, but has also been used in projects in Mauritius, Canada and China to name a few. The model is written using the GAMS modeling language [19]. The Balmorel model is open source and can therefore be altered in many different ways. Because of this, many different add-ons can be created or implemented for different aggregated cases. This means that the model can be altered to a desired system if the modeler has the knowledge to do so.

In Balmorel, different entities are defined in sets. A set can for example be a collection of the areas in a region. This is used for calculations, such that for example the calculations are done for all areas. Parameters are values that are defined by the user. These are often related to known costs of the different aspects of the energy system and will remain constant throughout the model run. Finally, variables are values that are changed in order to minimize the total system costs of the energy system. The different sets, parameters and variables will be further explained in Chapter 14.8. Due to the open-source nature of Balmorel, the setup of the model might have been changed by the user. In this thesis the model described is the one currently used by Ea [10].

14.2 Geography

The model distinguishes between three different geographic entities: countries, regions and areas. Here, regions are specified as a part of a country and areas as a part of a region. Different countries are divided in different ways. For Denmark, the regions used in electricity modeling are separated

into DK_E (Sjælland, Bornholm, Lolland-Falster etc.) and DK_W (Jylland, Fyn etc.) based on the Danish power system as seen in Fig. 1.2. Wind power generation is currently based on areas and is divided into five areas based on the two regions. DK_E is divided into offshore and onshore areas, whereas DK_W is divided into onshore, Horns Rev and Anholt representing the bigger offshore wind farms in western Denmark.

Power balance is calculated on a regional scale, but unlike heat, electricity can be exchanged between regions. The exchange amount is limited by transmission capacity as well as losses and costs. Some factors apply to different geographical entities. Annuity, taxes environmental policies and availabilities of fuels are based on a country level. On a regional level, the electricity demand, consumer price and losses and costs of transmission are modeled. Finally, entities like capacities, investment costs and heat demand is related to the areas.

14.3 Time structure

Much like the geographical structure, time is divided into the entities years, seasons and hours. Here input time and simulation time must be distinguished. Input time ordinarily consists of 168 hours/season and 52 seasons/year meaning that a Balmorel year consists of 8736 hours, which is a bit less than a calendar year. Here, a season corresponds to a week. Simulation time, on the other hand, is chosen to decrease running time of the model. Through this, it is possible to only model some time steps and get the results from there. This could for example be few individual weeks or summer/winter. The number of seasons can be changed by the user, if time aggregation is used. Time aggregation will be explained in Chapter 15.2.

The model can be made to invest in new technologies either in the present or in the future. In investment runs, different entities are either given from data (exogenous) or found using the model (endogenous). This means that the the planned capacities that will be installed in future years are known by the model, but the model will also be able to make investments itself to meet the model goals.

Some parameters, that do not change in the data structure over the years, are entities such as annuity, generation technology characteristics and demand elasticities. Entities like fuel prices and taxes on emissions, change between years, but will not change during the year. Finally entities like generation might change throughout a single year, as the model might invest in new generation technologies. Furthermore demand for heat and power changes depending on the time of year. Different methods for running Balmorel exist, although only the ones used for this thesis will be described. The model can be made to optimize on a yearly basis, which is known as bb1. Another method for reducing run times, is optimizing the model every week and adding up the results. This is known as bb3.

14.4 Generation technologies

The different generation technologies can be divided into five different types. These include extraction plants, back-pressure plants, electric-only generation, heat-only boilers and electric heating. For this thesis, wind turbines are the most important generation technology. These are found in the electric-only category. Each technology has associated values such as fuel type and fixed and

variable costs. The different types of technologies are able to operate in different feasible regions, which are seen in Fig. 14.1. Here the feasible region is marked by blue.

Back-pressure power plants as seen in Fig. 14.1a produces both electricity and heat at a technology specific rate C_b whereas extraction power plants, shown in Fig. 14.1b produces power and can be made to produce heat as well, defined by the technology specific parameters C_b and C_v . Fig. 14.1c shows only electricity generation technologies such as wind turbines, photo voltaic panels and condensing power plants. Fig. 14.1d shows technologies producing only heat and Fig. 14.1e are technologies that produces heat at the cost of electricity with an efficiency of COP . Fig. 14.1f and Fig. 14.1g represent storage technologies of electricity and heat respectively [3].

14.5 Fuel

Different fuel types have associated values as well. These consists of the amount of emissions for each type, along with the taxes associated with the specific type of fuel. Furthermore, the amount of fuel that is usable is dependent on the fuel type, as well as the area, region or country.

This of course, does not affect wind power generation as the fuel here is free and without emission. Wind, which is free, is the resource used by the wind turbines. Therefore the costs pertaining to wind turbines are mainly operation and maintenance costs. Emissions due to manufacturing and transportation are however not considered in the Balmorel model.

14.6 Demand

Demand is based on hourly demand, and must always be met in the model. The demand is on a regional level for power and on an areal level for heat. The demand is based on observed data as well as Energinet.dk's analyseforudsætninger [2], which attempts to predict the evolution of the Danish energy system from 2015-2035.

14.7 Transmission

Transmission connections between regions are illustrated in Fig. 14.2. The transmissions all have different costs and capacities connected to them, and the transmission capacities can be expanded in the modeling if this gives the most feasible solution.

14.8 Objective function and constraints

In this section, the objective function, that minimizes the overall system costs, will be described. As the objective function consists of many parts, only the parts most important to model wind power production in Balmorel, will be described. First, all of the sets, parameters and variables used will be shown.

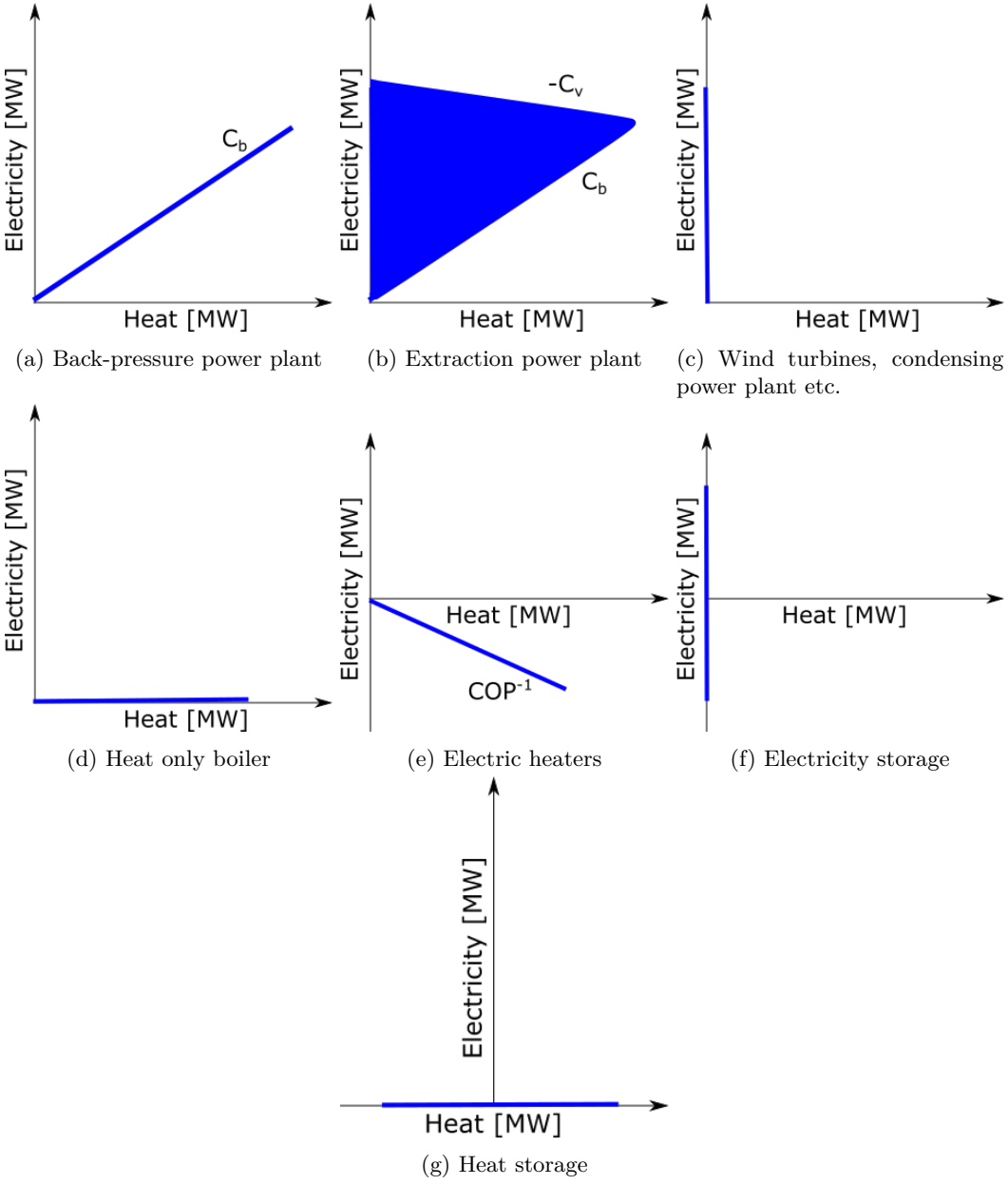


Figure 14.1: Sketch showing the feasible regions for different power and heat producing technologies.



Figure 14.2: Schematic showing the power transmission connections between the regions in northern Europe. Figure made by Niels-Peder Nimb and Rune Brus, Ea Energy Analyses. Figure found in [3].

Sets

a	Area
f	Fuel type
e	Emission type (CO ₂ , SO ₂ and NO _x)
g	Generation technologies
t	Time (Given in either years, seasons or time steps)
r	Region
r_x	Region where power is exported to
c	Country
A_r	Subset of all areas a in a region r
A_c	Subset of all areas a in a country c
\mathbb{R}_x	Subset of all regions r_x where power is exported to

Parameters

$C_{a,f}^{\text{fuel}}$	Fuel costs for fuel type f in area a [DKK/MWh]
$C_{a,g}^{\text{O\&M}}$	Operation and maintenance costs for technology type g in area a [DKK/MWh]
C_{r,r_x}^{trans}	Electricity transmission costs between regions [DKK/MWh]
$C_{c,e}^{\text{emis}}$	Cost of emission e in country c [DKK/kg]
$D_{r,t}^{\text{el}}$	Demand for electricity in a region r at time t [MWh]
$E_{g,e}^{\text{gen.tech}}$	Emission of type e for generation technology g [kg/MWh]
$E_{c,e}^{\text{emis.lim}}$	Limit for emission of type e in country c [kg/GJ]
$\eta_{g,a}$	Efficiency of technology g in area a [-]

Variables

$V_{a,g,t}^{\text{fuel.cons}}$	Fuel consumption for area a and technology type g at time t [MWh]
$V_{a,g,t}^{\text{el.gen}}$	Electricity generation for area a and technology type g at time t [MWh]
$V_{r,r_x,t}^{\text{trans}}$	Transmission of power from one region to another at time t [MWh]

Objective function

$$\text{Minimize } \sum_{a,g,f} \left(C_{a,f}^{\text{fuel}} \sum_t V_{a,g,t}^{\text{fuel.cons}} \right) \quad (14.1a)$$

$$+ \sum_{a,g} \left(C_{a,g}^{\text{O\&M}} \sum_t V_{a,g,t}^{\text{el.gen}} \right) \quad (14.1b)$$

$$+ \sum_{r,r_x} \left(C_{r,r_x}^{\text{trans}} \sum_t V_{r,r_x,t}^{\text{trans}} \right) \quad (14.1c)$$

$$+ \sum_c \sum_{a \in \mathbb{A}_{c,g}} \left(\sum_{t,e} E_{g,e}^{\text{gen.tech}} V_{a,g,t}^{\text{fuel.cons}} C_{c,e}^{\text{emis}} \right) \quad (14.1d)$$

Eq. (14.1) is the most important parts of the objective function for this thesis. The function minimizes the fuel costs for the energy system. Part (14.1a) describes the fuel consumption, part (14.1b) describes the operation and maintenance costs, part (14.1c) describes the cost of transmission between regions and part (14.1d) describes the costs associated with emission taxes. For simplicity, these expressions are all expressed here for existing technologies only.

Balmore constraints

The variables are subject to several constraints. The most important parts, in modeling of wind energy, are shown in Eq. (14.2).

$$\text{s.t. } \sum_{a \in \mathbb{A}_r} \sum_g V_{a,g,t}^{\text{el.gen}} + \sum_{r_x} (V_{r_x,r,t}^{\text{trans}} - V_{r,r_x,t}^{\text{trans}}) = D_{r,t}^{\text{el}}, \quad \forall r, r_x \in \mathbb{R}_x, t \quad (14.2a)$$

$$V_{a,g,t}^{\text{fuel.cons}} = \frac{V_{a,g,t}^{\text{el.gen}}}{\eta_{a,g}}, \quad \forall a, g, t \quad (14.2b)$$

$$\sum_{a \in \mathbb{A}_{c,g}} \sum_t E_{e,g}^{\text{gen.tech}} V_{a,g,t}^{\text{fuel.cons}} \leq E_{c,e}^{\text{emis.lim}}, \quad \forall a \in \mathbb{A}_c, c, e, g, t \quad (14.2c)$$

Eq. (14.2a) ensures that the electricity production and the transmission of power equals the electricity demand at all times. Furthermore the fuel consumption has to equal to the power generation divided by a technology efficiency. This is seen in Eq. (14.2b). Eq. (14.2c) constrains the emissions (CO₂, SO₂, NO_x) to be below a country specific limit.

14.9 Strengths and weaknesses

The Balmorel model can be used for many different problems and energy systems due to the open-source nature. Several add-ons can be utilized or new ones can be created to fit the individual power systems desired for modeling.

The model is however very complex, and strong knowledge of the GAMS programming language is necessary in order to adjust it. Furthermore, the model is divided into many different files, which can make adjustments very hard as one first has to locate the correct file.

Other modeling tools

Many other modeling tools exist. All of these have different strengths and weaknesses. Connolly et al. [8] shows a comprehensive comparison of many different energy system models.

An example of another way to model the energy system is the STREAM model [11]. This model is quick to use and has a user-friendly interface made in Excel and also takes the transport and industry sectors into account. STREAM however only gives a yearly snapshot of the energy system and allows infinite lossless transmission of power and heat inside a country. In the STREAM model differences in scenarios can be found, but it does not optimize to the lowest energy system costs.

CHAPTER 15

Creation of aggregated cases

Several cases are created in order to investigate both spatial and temporal aggregation in the modeling of wind power in the Danish energy system. The creation and reasoning of these cases are explained in this chapter. In order to better evaluate the effects of the aggregation, Balmorel is set to model only Denmark and removing transmission to neighbouring countries effectively modeling Denmark as an island. Furthermore the model is run for 2015 only.

No electricity storage exists in Denmark, meaning that when wind power production exceeds the power demand, curtailment will be seen. Therefore the curtailment seen in these results will be higher than seen in real life. The effects on curtailment can however still be investigated with varying degrees of aggregation.

15.1 Spatial aggregation

Several cases are created in order to test the effect of the spatial aggregation of wind turbines in Denmark. These aggregated cases are created with Denmark being divided into a varying number of areas. The areas are divided based on the installed fleet of wind turbines ultimo 2015 in the Stamdataregister [15]. The installed capacity, yearly production and average turbine height are found for every area and through this, an aggregated power curve is created. This is implemented in Balmorel along with the geographically associated costs and shear factors to model 2015 with the combined CFSR and GWA data with an hourly resolution.

A single wind time series, chosen at a site with the largest capacity of wind turbines, is representative for an area. An aggregated power curve is created for each area and implemented into the model. The operation and maintenance costs for the new areas are all based on the current Ea Balmorel costs shown in Appendix D. Here, the costs only change depending on if the wind turbines are onshore or offshore and is based on observed data. Investigation of the spatial aggregation are all made using the weekly optimization, with hourly resolution known as bb3.

Case 1 - 1 area

To test the spatial aggregation it proves useful to aggregate even further, such that Denmark only is represented by a single area. This is done using the already installed 2015 capacities for DK_W and DK_E. A single time series from central Jylland, assumed representative for the entire country, is then used to aggregate power curves for both areas and fitting these to the observed capacity factors for the different areas. Fig. 15.1 shows the installed turbines marked as stars and Tab. 15.1 shows the values used for the model.

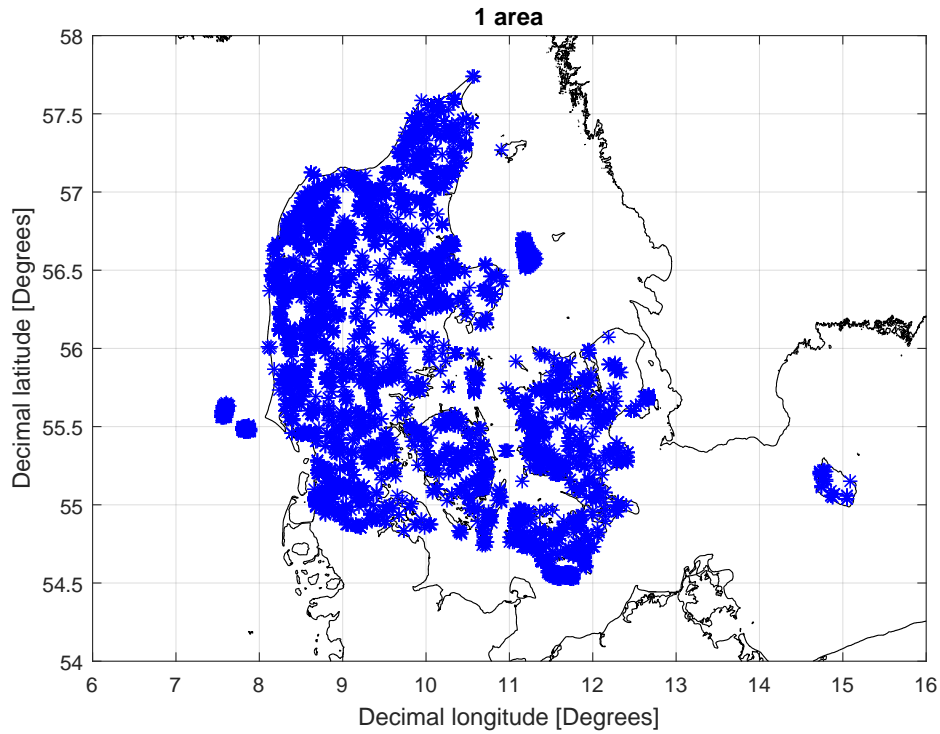


Figure 15.1: Plot of the existing Danish wind turbines in 2015 divided into 1 area.

Region	Timeseries	Color (Fig. 15.1)	Avg hub height [m]	Capacity [MW]	CF [%]
DK West	Jylland	Blue	48.2	3994	31.4
DK East	Jylland	Blue	46.2	1099	32.3

Table 15.1: Table showing the 2 areas (used to model a single area), along with the observed values, used in Case 1.

Case 2 - 2 areas

Another case is created based on the power grid in Denmark, by separating Denmark into DK_W and DK_E. A map showing the separation is seen in Fig. 15.2. This case is very reminiscent of Case 1 as presented in Chapter 15.1. Here the capacity, CF and average wind turbine height have the same values, with only the wind speeds and power curves being changed between the cases.

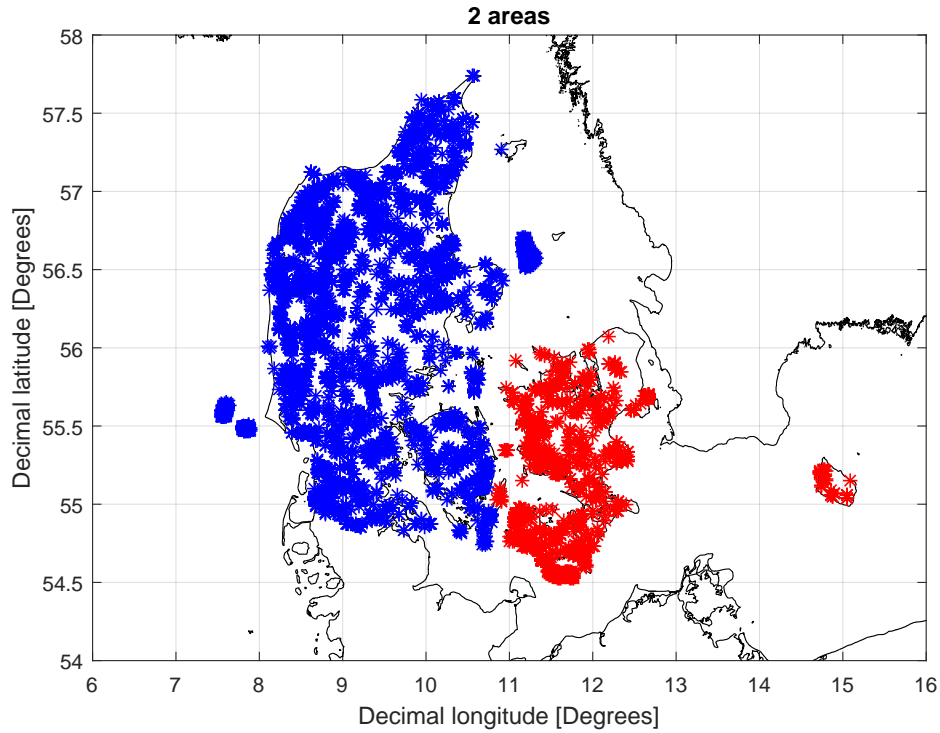


Figure 15.2: Plot of the existing Danish wind turbines in 2015 divided into 2 areas.

Region	Timeseries	Color (Fig. 15.2)	Avg hub height [m]	Capacity [MW]	CF [%]
DK West	Jylland	Blue	48.2	3994	31.4
DK East	Sjælland	Red	46.2	1099	32.3

Table 15.2: Table showing the 2 areas, along with the observed values, used in Case 2.

Case 3 - 5 areas

Currently Ea models Denmark with five areas, separated as seen in Fig. 15.3. More specifically these are divided into East and West onshore as well as eastern offshore, Horns rev and Anholt. The values used are shown in Fig. 15.3

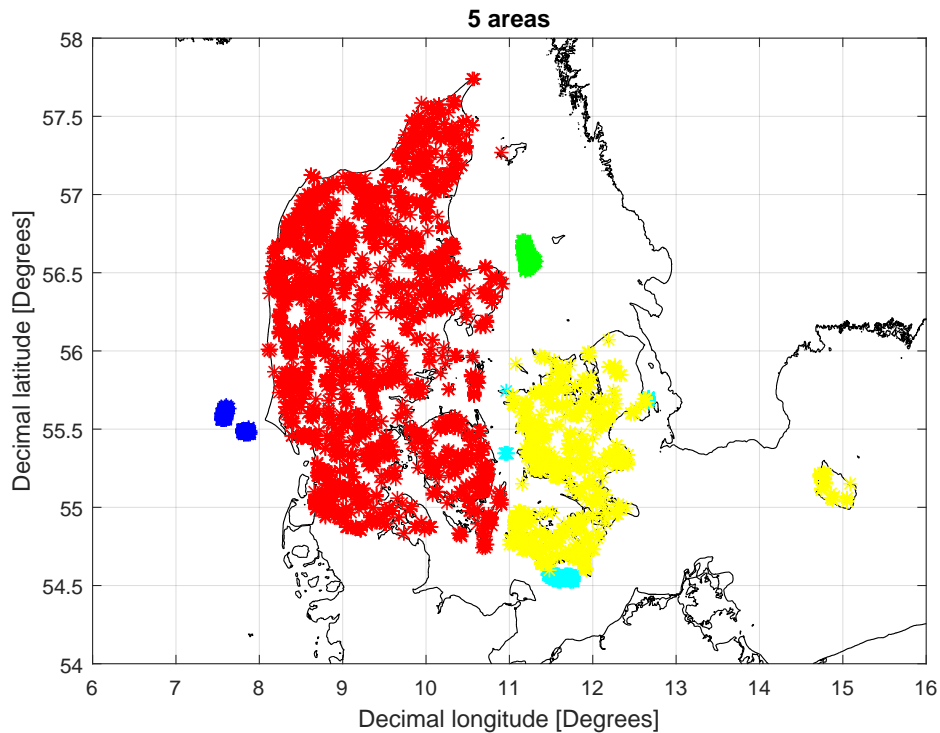


Figure 15.3: Plot of the existing Danish wind turbines in 2015 divided into 5 areas.

Region	Timeseries	Color (Fig. 15.3)	Avg hub height [m]	Capacity [MW]	CF [%]
DK West	Herning	Red	46.5	3240	28.4
DK West	Horns Rev	Blue	62.0	369	42.2
DK West	Anholt	Green	81.6	400	46.6
DK East	Holbæk	Yellow	40.8	651	25.8
DK East	Rødsand	Cyan	73.8	434	42.1

Table 15.3: Table showing the 5 areas, along with the observed values, used in Case 3.

Case 4 - 10 Areas

The fourth case is created by dividing Denmark into ten areas based on the mean wind speeds found through the GWA [16], which is seen in Fig. 15.4.

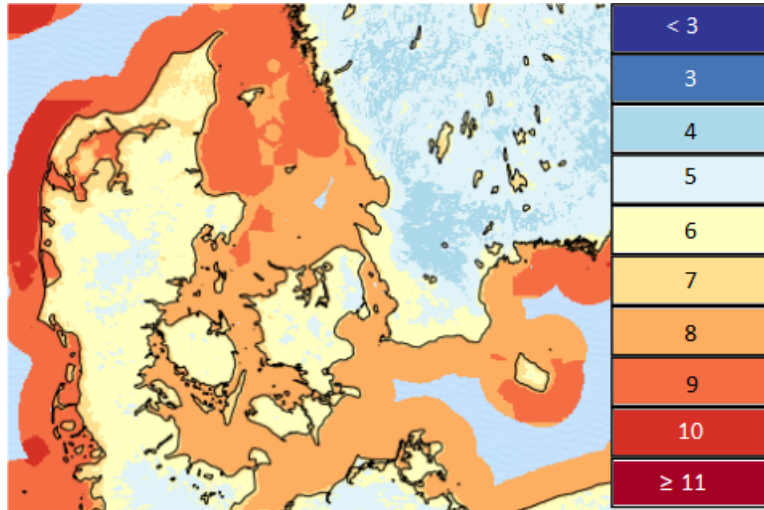


Figure 15.4: Map of Denmark showing the wind speeds in m/s at 50 m a.g.l. [16].

A plot of the turbines in the ten areas is seen in Fig. 15.5.

After separating the different turbines, the average wind turbine height and yearly capacity factors are calculated. These results are seen in Tab. 15.4.

Region	Timeseries	Color (Fig. 15.5)	Avg hub height [m]	Capacity [MW]	CF [%]
DK West	Fyn	Yellow	46.0	170	23.6
DK West	Jylland	Green	47.0	2433	28.0
DK West	Kattegat	Cyan	70.4	440	45.8
DK West	Limfjord	Blue	44.8	532	30.3
DK West	VestkystN	Yellow	39.7	3	31.4
DK West	VestkystS	Red	62.0	369	42.2
DK East	Bornholm	Green	48.4	37	27.7
DK East	Lolland	Green	41.1	266	26.9
DK East	Sjælland	Red	41.2	395	25.4
DK East	Sydhav	Blue	68.1	448	42.2

Table 15.4: Table showing the 10 areas, along with the observed values, used in Case 4.

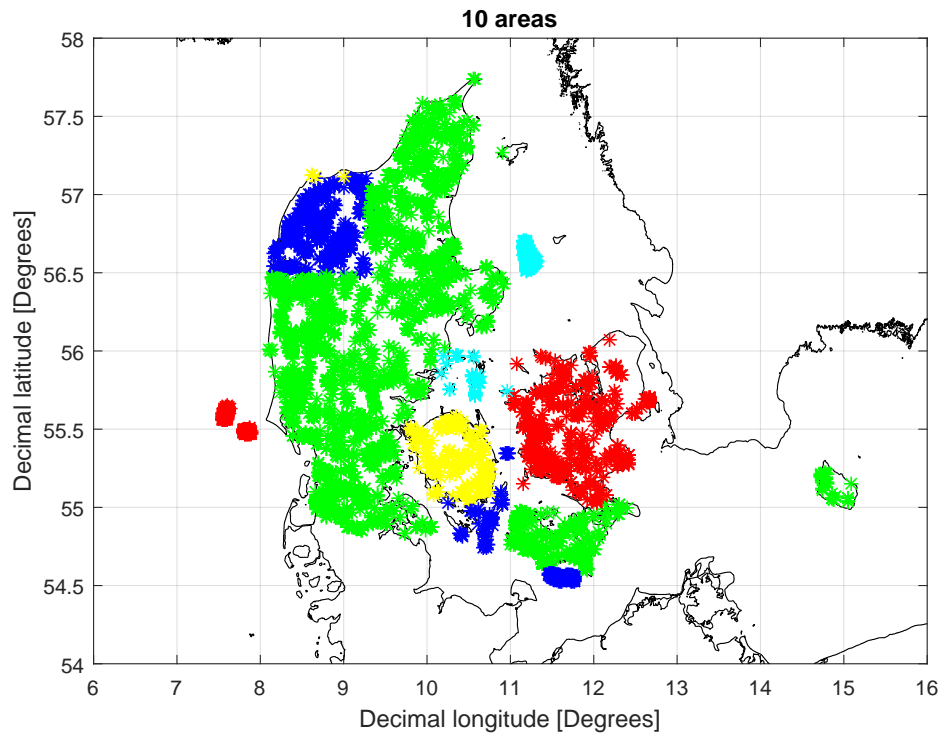


Figure 15.5: Plot of the existing Danish wind turbines in 2015 divided into 10 areas.

Case 5 - 20 areas

An algorithm known as k-mean clustering [27] is used to create more areas. This algorithm uses the coordinates for all installed wind turbines in Denmark, and divides these into a previously specified number of areas. This is done by inserting moving center points and clustering the given coordinates, such that the distance from centers to coordinates are as small as possible with the given amount of areas. A plot of the divided area is seen in Fig. 15.6 with the corresponding observed values seen in Tab. 15.5.

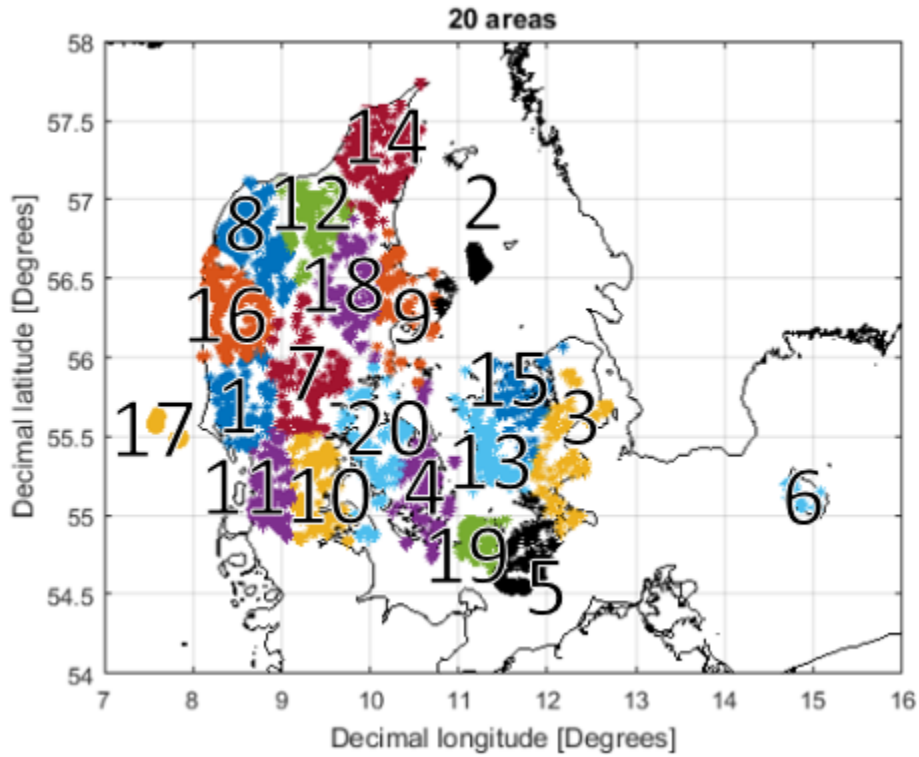


Figure 15.6: Plot of the existing Danish wind turbines in 2015 divided into 20 areas.

Region	Area	Time series	Avg hub height [m]	Capacity [MW]	CF [%]
West	1	Varde	47.5	323	28.0
West	2	Anholt	75.4	411	45.9
East	3	Sjælland	42.3	144	25.4
West	4	Svendborg	49.1	206	39.2
East	5	Rødsand	57.4	455	40.7
East	6	Allinge	48.4	37	27.7
West	7	Jylland	47.7	208	23.1
West	8	Limfjord	43.0	378	31.2
West	9	Djurs	48.9	210	27.4
West	10	Aabenraa	44.8	158	22.5
West	11	Løgumkloster	39.9	201	25.4
West	12	Fjerritslev	50.3	313	29.2
East	13	Fuglebjerg	40.1	159	26.2
West	14	Aalborg	44.7	333	28.3
East	15	Jyderup	41.1	95	24.6
West	16	Ringkøbing	53.4	641	32.5
West	17	Horns Rev	62.0	369	42.2
West	18	Randers	44.1	172	23.8
East	19	Sydhav	42.3	174	26.5
West	20	Brenderup	44.8	105	24.8

Table 15.5: Table showing the 20 areas, along with the observed values, used in Case 5.

15.2 Temporal aggregation

The temporal aggregation is done using the Balmorel add-on *timeaggr*. Using the add-on, simulation time, which is explained in Chapter 14.3, is changed and the effects are observed. The time aggregation takes a normalized total wind speed for all times and uses this to find the ten tallest peaks in the total wind speed per season. These ten points per season are used to decumulate data for the remaining year. Investigation of the temporal resolution is done by dividing 2015 into 12 and 52 seasons, corresponding to weeks and months respectively.

In order to use the time aggregation, the model has to optimize on a yearly level. Therefore the model is run using the *bb1* method. These runs are made for varying degrees of spatial aggregation to investigate how the temporal and spatial dimensions interact.

CHAPTER 16

Results

16.1 Validation of results

Evaluating the difference in cases are based on several factors. Adding more time series to the power systems, odds are that there will be power production in one area, where simultaneously no generation will be seen in another area. For many implemented time series, this effect is expected to smoothen out the power generation compared to very few time series. This effect is investigated by studying the total yearly power production as well as the total curtailment of the system. Power prices for the different regions are other important variables used in the validation.

To verify that the power curves have been created correctly, the capacity factor at the given area is inspected and compared to the capacity factors used to calibrate the power curves. Some differences between observed and simulated power curves are expected due to possible curtailment in the area. Power generation of the system is inspected in order to evaluate the effect of a different spatial aggregation. This is used to see if the wind power is better utilized in a system with another spatial aggregation. As Balmorel is based on always having generation equal to demand, the power production of all other technologies except wind, known as a residual duration curve, is inspected to see the effects coming from the spatial aggregation.

The residual duration curve is made by ordering the production at all hours in descending production. Therefore hours where the residual duration curve has a high value, a low wind power production is experienced. Similarly the hours with a low residual power production corresponds to a high wind power production.

16.2 Spatial aggregation

The results found from running Balmorel, as explained earlier, are seen in Tab. 16.1. These are compared to the results found when running the model, currently used by Ea, without new wind time series and aggregated power curves. From the table, the differences between the cases are seen to be quite small. The total wind production is seen to be close to constant. The curtailment

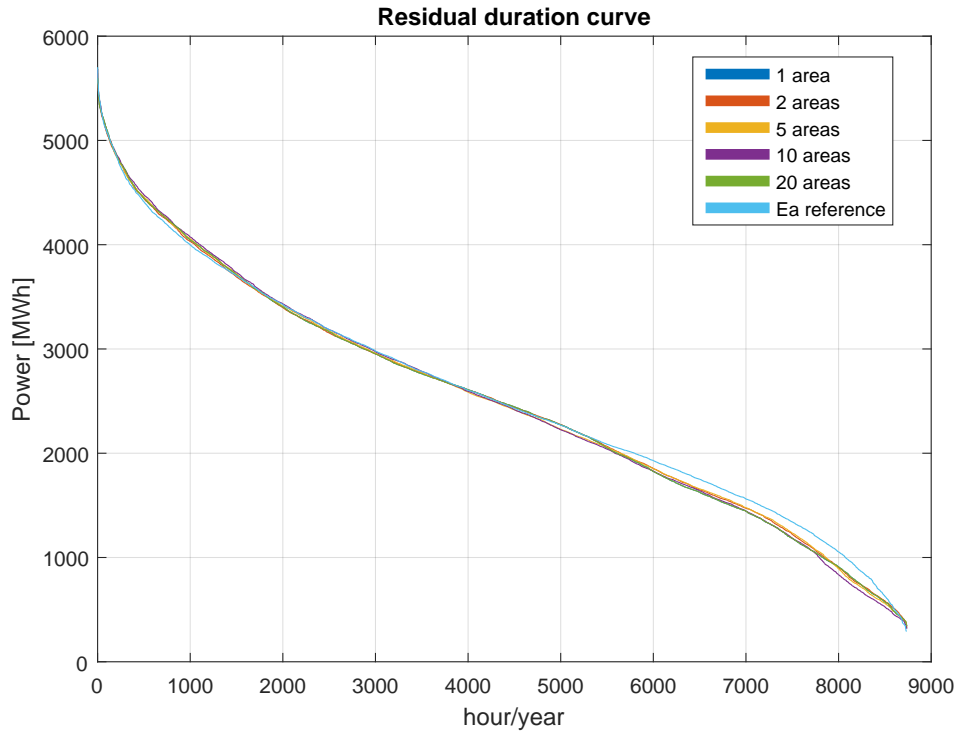


Figure 16.1: Residual duration curve for cases with varying spatial aggregation.

decreases towards five and ten areas, but then increases for twenty areas. The power prices are close to constant for the two regions, although a single area seem to be further from the other results. Finally the power price in DK_W for twenty areas are smaller than the remaining cases.

Number of areas	Ea model	1	2	5	10	20
Total wind production [GWh]	12316	12851	12816	12783	12816	12948
Total wind curtailment [GWh]	656	1510	1515	1420	1415	1567
Power price DK East [DKK/MWh]	263	248	258	260	257	258
Power price DK West [DKK/MWh]	241	228	225	228	228	222

Table 16.1: Results for running Balmorel with a varying degree of spatial aggregation.

The current Ea model is seen to have production in the same order, lower curtailment and higher power prices. This reference case does not use aggregated power curves fitted to observed data and therefore does not yield an accurate result. When running the model with more countries included, this difference seems much smaller as so much else factors in and the precision of modeling wind turbines is therefore not as crucial. Inspection of the residual power curve seen in Fig. 16.1, shows that the amount of areas changes very little on the duration curve.

Initially, the spatial aggregation does not seem to change much in terms of modeling of the energy system in Denmark. It does however seem that the in the case with a single area, the differences are a generally a bit larger in comparison to the remaining cases. These results will be further investigated in Part III. To ensure the implementation in Balmorel is done correctly the capacity

factors calculated with Balmorel are inspected and compared to observed values. These all show to deviate less than $\pm 5\%$ for all areas, which is believed to be due to curtailment effects. Therefore the implementation of new areas and power curves are believed to be correct. For the current Ea model, the CF are seen to be further off compared to the Stamdatregister.

16.3 Temporal aggregation

Few differences were seen in the results, with different degrees of spatial aggregation. Investigation of the temporal aggregation is done by separating the amount of seasons into 12 and 52, mirroring months and weeks, respectively. Tab. 16.2 shows the found results.

12 seasons					
Number of areas	1	2	5	10	20
Total wind production [GWh]	12851	12816	12783	12803	12948
Total wind curtailment [GWh]	1147	1063	1257	1452	1589
Power price DK East [DKK/MWh]	253	312	322	283	292
Power price DK West [DKK/MWh]	244	298	307	268	267
52 seasons					
Number of areas	1	2	5	10	20
Total wind production [GWh]	12428	12897	12321	12472	12334
Total wind curtailment [GWh]	1933	1434	1883	1780	2188
Power price DK East [DKK/MWh]	325	315	327	328	322
Power price DK West [DKK/MWh]	313	279	294	293	290

Table 16.2: Results for running Balmorel with varying degrees of spatial and temporal resolution.

The results show that the modeled wind power production is close to the power production for the cases without temporal aggregation. The curtailment differs, not only from the case without temporal aggregation, but also for varying degrees of spatial aggregation. The power prices are far from the power prices found without temporal aggregation. Fig. 16.2 shows zooms on a duration curve of the power prices in DK_E for the case without temporal aggregation along with temporal aggregation on 12 and 52 seasons. Here the amount of areas are five corresponding to Case 3 and the current Ea model. In cases with temporal aggregation the power prices are decumulated using Balmorel to get power prices for all hours in the year. This decumulation method is responsible for the steps seen on the curve.

A zoom of the hours with the highest power prices, seen in Fig. 16.2a, reveal that very high power prices are found more often with spatial aggregation. For the remaining power curve, seen in Fig 16.2b, the power prices are almost constantly higher with time aggregation, although not as pronounced. For DK_W the same trend is observed. Due to this, the average yearly power prices are much higher as seen in Tab. 16.2. The reasoning for this must be that the Balmorel time aggregation does not capture the wind power production completely. This is also seen in the large differences in curtailment between the different cases. Generally this difference is much smaller when not modeling Denmark as an island and implementing neighbouring countries. As the time aggregation is crucial when investigating Balmorel investment runs, this method will need to be investigated further before the investment runs will make sense.

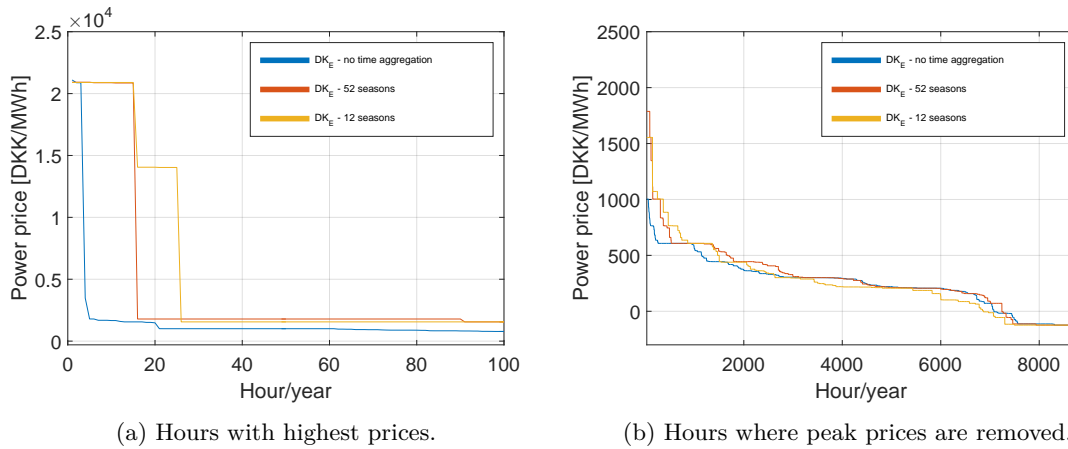


Figure 16.2: Zoom of the duration curve for the power prices in DK_E with different degrees of temporal aggregation.

16.4 Model run times

Run time of the model is crucial in how beneficial a model is. If a very small increase in the accuracy of the model, increases the run time significantly, the accuracy might be lowered to decrease run times. As wind power production is prioritized in the system, the production at all hours are calculated initially. This means that extra run time, compared to the reference case, comes from curtailment calculations. Running the model however shows no significant change (<60 s) in run time. Therefore, more areas can be implemented without increasing model run times. The implementation time of creating the new areas however, does take longer time especially in the creation of aggregated power curves.

16.5 Choice of reference year

In Chapter 7, the reference year was chosen to be 2009. The observed data for the installed wind turbines along with the wind fluctuations found from the CFSR data were therefore used to create the aggregated power curves used for the cases.

With the power curves being fitted to a certain year, with a known wind time series, a case is created where everything except wind speeds is kept constant. With 2004 being close to the average yearly production, data from these time series were created using the CFSR data combined with the GWA.

The results from running the model with 20 areas is seen in Tab. 16.3 and the residual duration curve is seen in Fig. 16.3.

Year	2004	2009
Total wind power production [GWh]	12521	12948
Total curtailment [GWh]	1267	1567
Power price DK East [DKK/MWh]	267	258
Power price DK West [DKK/MWh]	242	222

Table 16.3: Table showing different values from running Balmorel (bb3 for 2015) for wind speeds from 2004 using aggregated power curves made with 2009 data. Results are shown for Case 5 with 20 areas.

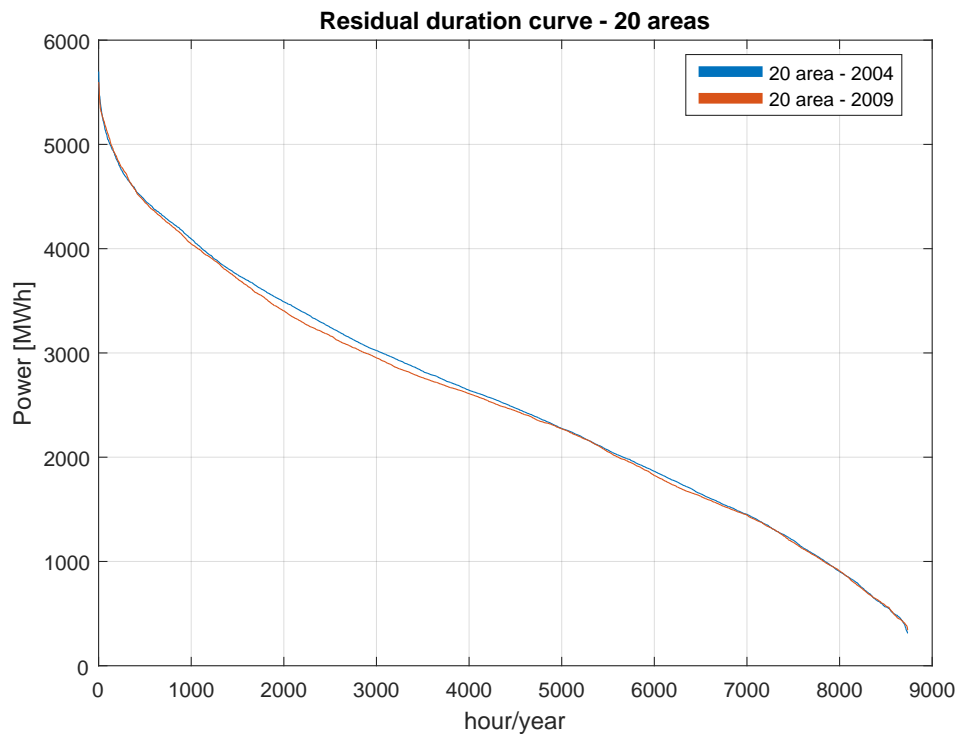


Figure 16.3: Residual duration curve from the power generation modeled in Balmorel (bb3 for 2015) for wind speeds from 2004 using aggregated power curves made with 2009 data.

Some differences in curtailment and power prices are seen in between the different reference years, however the residual duration curves looks close to identical. When considering the many other assumptions going into Balmorel, the differences in power prices does not change that much. Generally it seems possible to model the energy system with wind time series that the aggregated power curves were created for. If few areas are used, it is recommended to create new aggregated power curves each time the wind time series are altered, as this will increase the accuracy.

Running Balmorel with 2004 wind time series for other degrees of spatial aggregation give similar results.

16.6 Power curve swapping

Creation of power curves requires precise area data, in order to get a proper fit to observed data. With less aggregation, more power curves are needed. This however increases the risk of human mistakes when implementing the power curves into Balmorel. A test of human error was made, using five areas representing current Balmorel modeling as explained in Chapter 15.1, by swapping the power curves for the onshore regions Sjælland and Jylland. Results from running the model is seen in Tab. 16.4 and the residual duration curve is seen in Fig. 16.4.

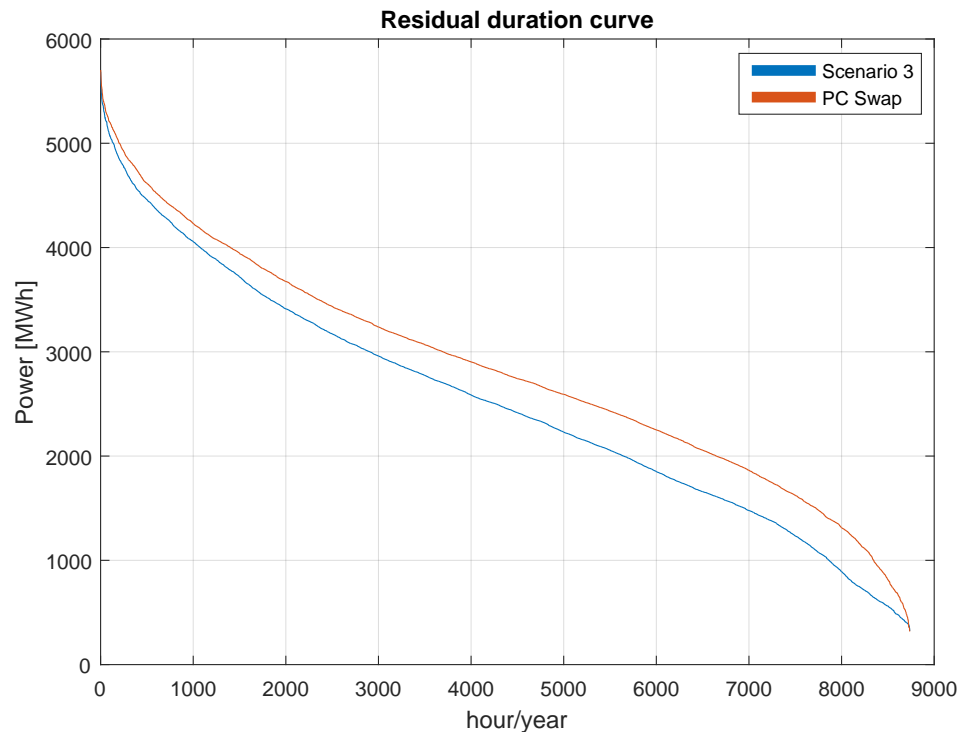


Figure 16.4: Residual duration curve for Case 3 (5 areas) and Case 3 where the power curves for Jylland and Sjælland have been swapped.

It is seen that much less wind power production is found when swapping the power curves. This

	Case 3	PC swap
Total wind power production [GWh]	12783	9614
Total curtailment [GWh]	1420	436
Power price DK East [DKK/MWh]	260	323
Power price DK West [DKK/MWh]	228	319

Table 16.4: Result for running Balmorel (bb3, 2015) for the case explained in Chapter 15.1 where the power curves have been swapped for the onshore regions of Jylland and Sjælland.

effect decreases curtailment and increase power prices. This shows the importance of implementing the power curves correctly.

CHAPTER 17

Discussion on energy systems modeling

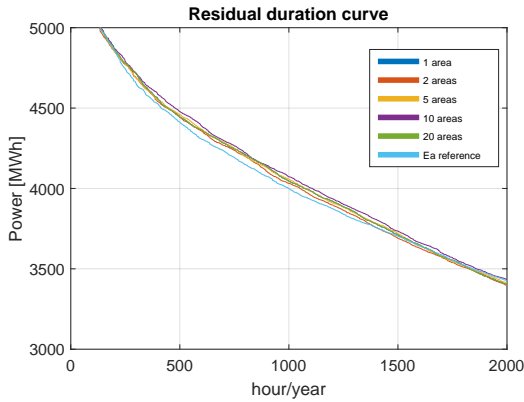
The Balmorel model has many assumptions in its implementation. For this study, only the wind power modeling was investigated and therefore the remaining assumptions have not been investigated. Ea continuously improves and evaluates their model and therefore only minor deviations from real values are expected from other technologies. Creation of the spatial aggregation cases, were all done for a single year with Denmark being modeled as an island. This is almost never done, when modeling the energy system, and minor assumptions will be much more pronounced in a smaller system.

Separating the country into smaller areas is based on different approaches, but one could argue that the capacity installed in the areas, might be more important than the distance from the representative wind speed site chosen. This is because an area will have no effect on the overall energy system if no wind turbines are installed there. Inspection of the results of the spatial aggregation show differences in the total production and curtailment. As the power demand is the same for all the cases, the difference must come from either the implementation of the aggregated power curves or from the different fluctuations in the wind. As the CF are all seen to be very close to the observed values, the wind speed fluctuations are believed to have an effect of the energy system.

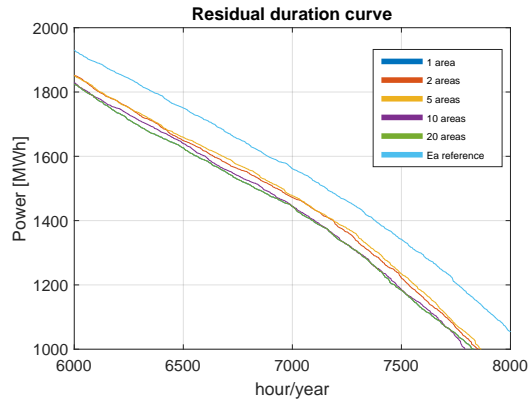
Very few changes were seen by altering the spatial aggregation in wind time series for the existing technologies in Chapter 16.2. The expectation for the spatial aggregation was that for more areas, the power production would be flatter throughout the year compared to more extreme power production for few areas. Inspection of the residual duration curve in Fig. 16.1 shows some traces of this effect. A zoom at the high and low production hours respectively are seen in Fig. 17.1.

A zoom of the high residual production hours, seen in Fig. 17.1a shows that the residual production, with more areas, is higher. From this it follows that the wind power production for these hours is lower with more areas. In the same manner, the lower residual production hours are shown in Fig. 17.1b. Here the opposite effect occurs with the wind power production being higher for more areas. This shows that the wind power production will have more averaged values with more areas implemented into Balmorel. This effect is however so small that the extra time needed, for implementation of more areas, does not seem necessary in order to get a more accurate result.

As discussed, investments runs requires a better understanding of the time aggregation used in the



(a) Zoom in on high production hours



(b) Zoom in on low production hours

Figure 17.1: Zoom of low and high production hours on the residual duration curve shown in Fig. 16.1.

model. When doing investment runs in Balmorel, it is necessary to limit the capacity that can be installed in the different wind areas. Otherwise Balmorel would invest only in the windiest area, meaning that this would be filled with wind turbines. In reality, this would not be seen, as areas might not be able to fit all wind turbines. Furthermore the amount of turbines is limited by the amount of sites with good wind resources as well as public dislike towards a huge amount of wind turbines. The limiting factor could be modeled as an increasing cost with the number of turbines in the area, thus distributing the investments more evenly between the areas. The costs should then reflect the change in wind resource, when all the best sites have been taken, as well as the public opinion towards more wind turbines.

Part III

Correlations in wind power production

CHAPTER 18

Correlations in wind time series

The spatial aggregation does not seem to have a large effect on the outcome of the model. Is this due to Denmark simply being too small for any spatial differences in the wind? This part will focus on the correlations between the wind speeds in Denmark, to better understand the spatial and temporal uniformity. Investigations into spatial aggregation in energy systems modeling is based on the theory that wind speeds will have a spatial variation. This theory can be investigated by finding the temporal correlation coefficients, known as the Pearson's correlation coefficients [18], between the time series for the different datasets, calculated as seen in Eq. (18.1).

$$CC(V1, V2) = \frac{1}{N-1} \sum_{i=1}^N \left(\frac{V1_i - \mu_{V1}}{\sigma_{V1}} \right) \left(\frac{V2_i - \mu_{V2}}{\sigma_{V2}} \right) \quad (18.1)$$

The correlation coefficient CC is calculated from two vectors $V1$ and $V2$ with length N . i denotes an element in the vectors, μ is the mean value and σ is the standard deviation for the different vectors. The correlation coefficients describe a percentage of how many, of all time steps, the trend in the fluctuations are the same. Meaning that two time series will have a larger correlation if both time series experience a simultaneous increase and a lower correlation if the time series does not show the same alteration in wind speed. This method does have some flaws in that it just explains the trends and not the amplitudes of the increases and decreases. In this chapter, the correlation coefficients between the different datasets are evaluated.

18.1 Mesoscale data

First, the currently used mesoscale data set is inspected to find the temporal correlation coefficients between the areas. Fig. 18.1 shows a plot of the first 1000 hours of the five points included in the mesoscale dataset. A purely visual inspection of the time series show that, even though the time series are distributed across Denmark, the larger scale fluctuations in wind speed are generally happening simultaneously. In order to give a better idea of the time series, the correlation coefficients are calculated and are seen in Tab. 18.1.

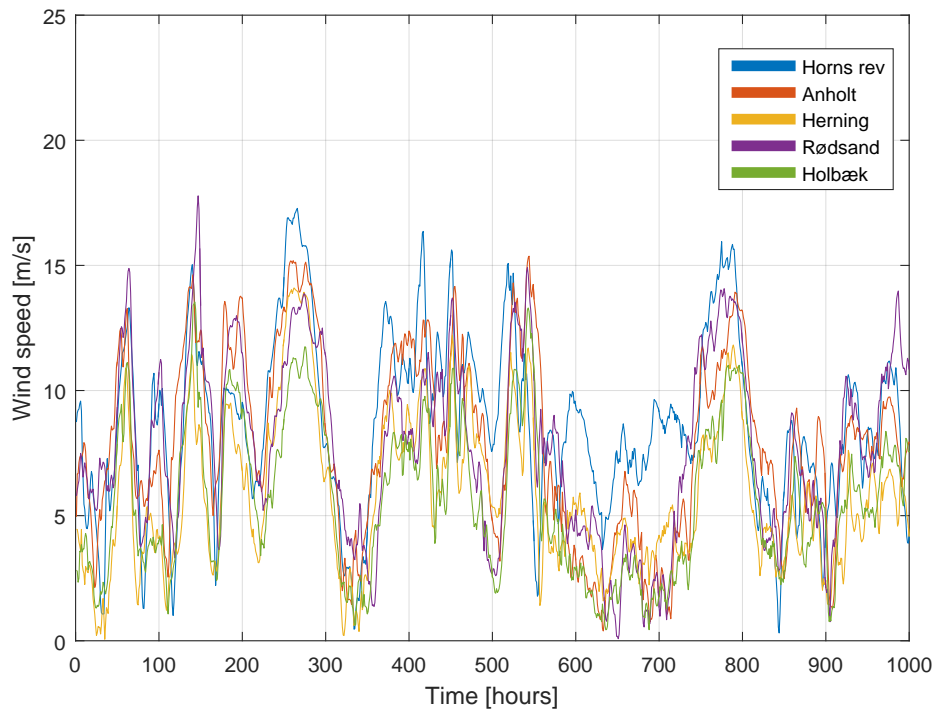


Figure 18.1: Plot of the different time series for the first 1000 hours of 2009 for the mesoscale dataset.

Correlation coefficient [%]	Horns Rev	Herning	Anholt	Holbæk	Rødsand
Horns Rev	-	-	-	-	-
Herning	75	-	-	-	-
Anholt	62	68	-	-	-
Holbæk	58	79	79	-	-
Rødsand	60	55	65	73	-

Table 18.1: Correlation coefficients between wind time series from the mesoscale dataset.

It is seen that the correlation coefficients between the time series are in the order of 55-80 %, meaning that at the least correlated areas, the fluctuations are roughly the same half the time. These differences seem, from a purely visual inspection, to be the smaller scale fluctuations.

18.2 CFSR combined with GWA data

For the combined dataset, four different locations are chosen at four different corners points in Denmark. The hourly wind speeds for the first 1000 hours are seen in Fig. 18.2. The corresponding temporal correlation coefficients are seen in Tab. 18.2. For this dataset as well, it is seen that the correlation coefficients are roughly in the same order as seen in Tab. 18.1. Even though the distances between the points are not completely the same, the correlation coefficients of the temporal

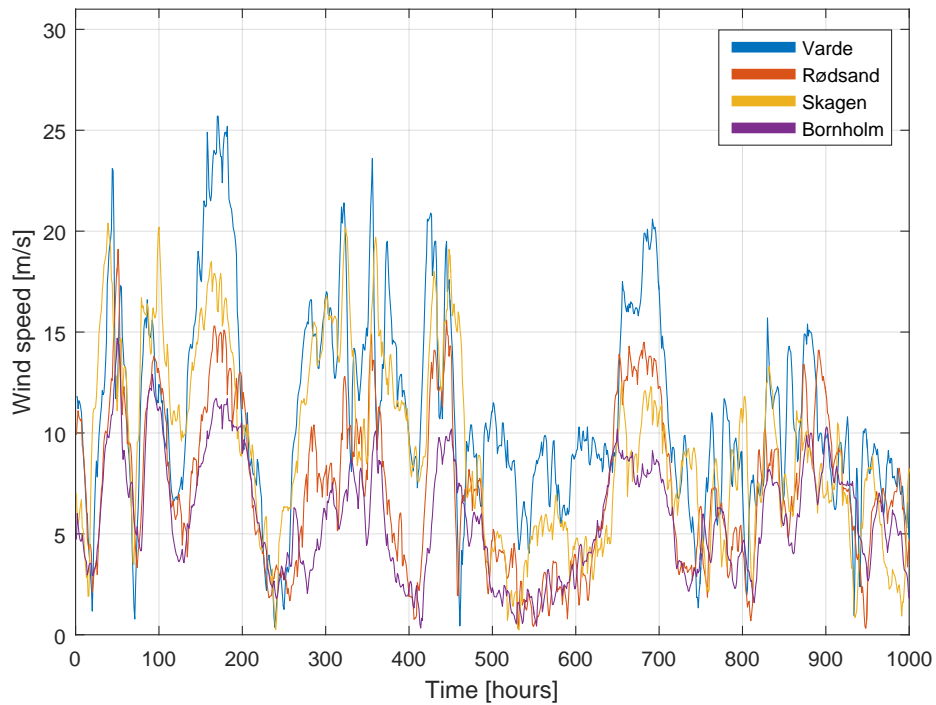


Figure 18.2: Plot of different time series in the corners of Denmark for the first 1000 hours of 2009 for the combined CFSR and GWA dataset.

fluctuations are in the same order for both datasets.

Correlation Coefficient [%]	Varde	Skagen	Rødsand	Bornholm
Varde	-	-	-	-
Skagen	63	-	-	-
Rødsand	65	49	-	-
Bornholm	49	51	73	-

Table 18.2: Correlation coefficients between wind data sets from the combined CFSR and GWA data set.

18.3 Hourly wind speeds

The correlation coefficients does not completely capture all spatial and temporal variations in the wind speeds. Another method for studying the wind speed fluctuations are by looking at the hourly changes in the wind for the different areas used in the cases. This is done for the combined GWA and CFSR dataset.

Every day is divided into 24 hours and the median wind speed of each hour-span is calculated.

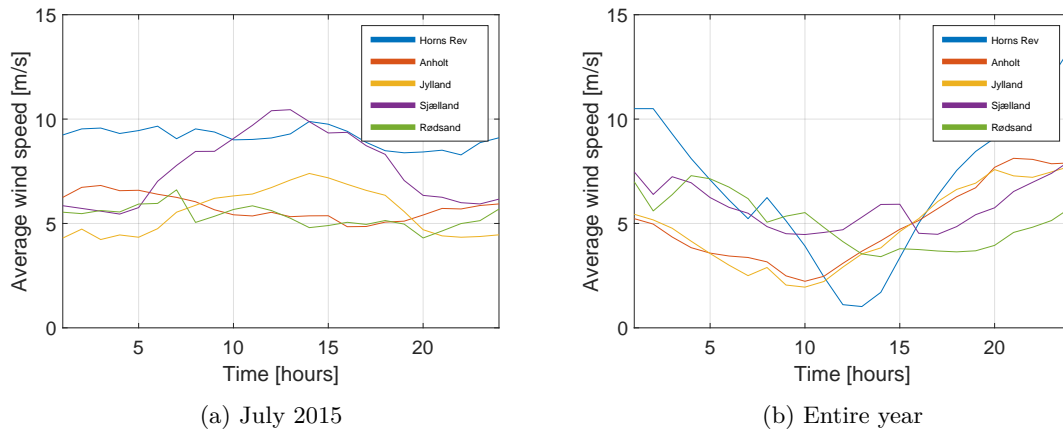


Figure 18.3: Hourly median wind speeds for July 2015 and the entire year 2015. Figure shown for 5 areas.

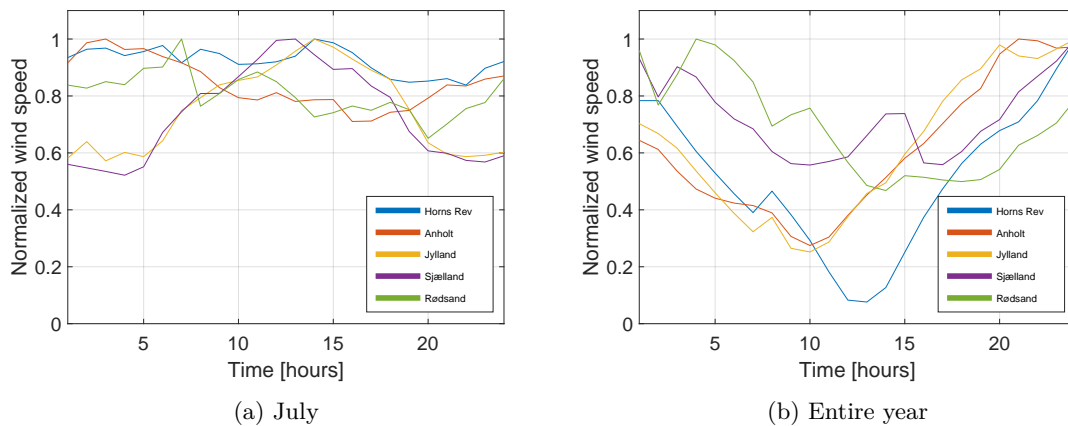


Figure 18.4: Normalized hourly median wind speeds for July 2015 and entire 2015.

These hourly medians are then inspected on a monthly and yearly scale. Fig. 18.3 shows the hourly median of the wind speed for July 2015 as well as the yearly median of the hourly wind speeds.

Fig. 18.3a shows that offshore wind speeds are almost constant throughout an average day. Onshore wind speeds are seen to increase during the day (hours 8-20). July, being a summer month, sees these changes in wind speeds due to the heating of the land. For the hourly median wind speeds, seen in Fig. 18.3b, the trend is seen to be lower wind speeds during the daytime hours. To get a better understanding of the tendency of the wind speeds the plots have been normalized as is seen in Fig. 18.4.

For July, seen in Fig.18.4a, the non-constant sites are seen to peak two hours apart. This shows that daily changes in the wind speeds happens at roughly the same times for the entire country. For the yearly wind speed medians, seen in Fig. 18.4b, show a similar trend in that increases and decreases happens roughly at the same hours. This investigation, along with the calculated correlation coefficients, both show that only minor differences in wind speed fluctuations occurs for

Denmark.

18.4 Weighted wind speeds

Previously, the wind speeds of the different sites have all been expected as being equally important, but this is not the case in reality. Different capacities are installed at the sites, and a site with very low capacity will barely influence the overall energy system even if the fluctuations are completely different from the remaining sites.

In order to investigate the temporal correlation coefficients for varying amount of spatial aggregation, a weighted wind speed for the entire country is made. This weighted wind speed can be seen as a representative wind speed for the entire country. This is done by multiplying the hourly wind speeds at all areas, with the installed capacity in the area. The values are then summed for each hour and divided with the total installed capacity. The resulting weighted wind speeds are shown in Fig. 18.5.

From Fig. 18.5 it is seen that for varying spatial aggregation, the representative wind speed for the entire country does not differ much. A larger difference is however seen for the case with a single wind speed. The single wind speed case is seen to have lower wind speeds and in the following sections the effects of this on the overall wind power production will be investigated. Tab. 18.3 shows the temporal correlation coefficients between the weighted wind speeds with varying spatial aggregation. These are all seen to be very closely related, with some minor differences especially between few and many areas.

Correlation coefficient [%]	1 area	2 areas	5 areas	10 areas	20 areas
1 area	-	-	-	-	-
2 areas	98	-	-	-	-
5 areas	98	99	-	-	-
10 areas	96	98	100	-	-
20 areas	94	97	99	99	-

Table 18.3: Correlation coefficients for weighted wind speeds with varying degrees of spatial aggregation.

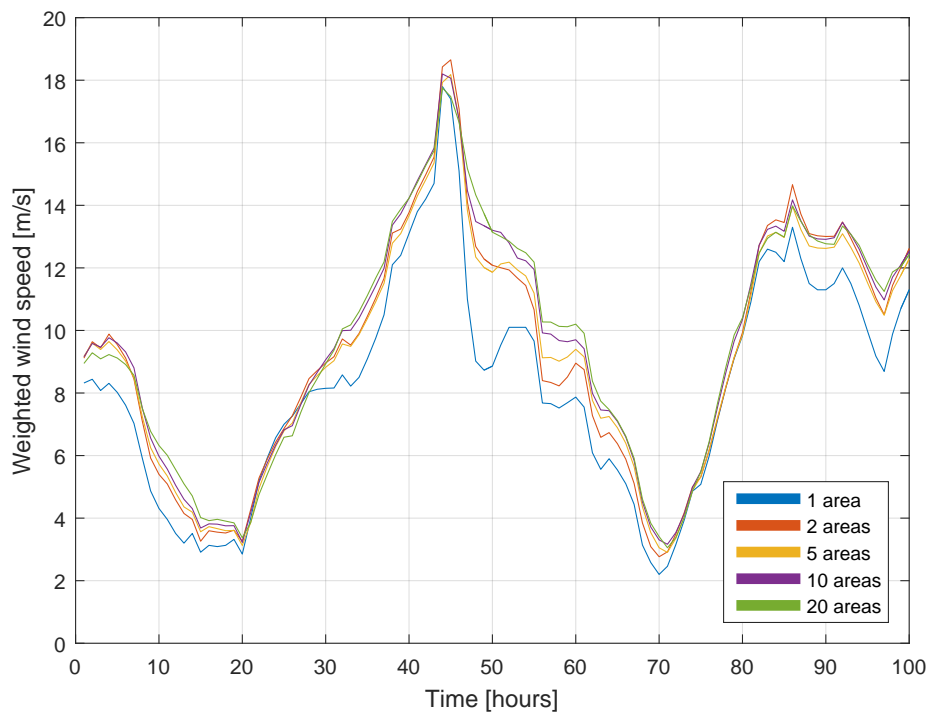


Figure 18.5: Weighted wind speeds representative for the energy system with varying degrees of spatial aggregation.

CHAPTER 19

Correlations in power production

An effect of power curves is a smoothing of the produced power. Low wind speeds (< 3 m/s) will all show roughly the same production, as well as higher wind speeds will all produce at rated power until the cut off wind speed is reached. The hourly power production for the entire year of 2015 is calculated using the combined datasets, as well as the aggregated power curves made for the different cases, explained in Chapter 15. The calculated power production is seen in Fig. 19.1.

The hourly wind power production from the different cases are seen to fluctuate at almost the same times. The smoothing through the power curves is experienced here as the weighted wind speeds, seen in Fig. 18.5, differed more for especially the single area case. Tab. 19.1 shows the correlations between the power productions for the entire year.

The total yearly wind power production for the cases are calculated and seen in Tab. 19.2. These are all seen to be higher than their corresponding values for Balmorel seen in Tab. 16.1. This is as expected, since curtailment is not included here.

From these correlation coefficients, it is clearly seen that the fluctuations in power production, for different number of areas, are happening almost simultaneously. A greater difference in correlation coefficients are seen when the difference in the amount of areas becomes higher. These correlation coefficients are all very close to the correlation coefficients found for the weighted wind speeds in Tab. 19.1. It is again seen that the difference between few and many areas increases with difference in areas.

Correlation coefficient [%]	1 area	2 areas	5 areas	10 areas	20 areas
1 area	-	-	-	-	-
2 areas	99	-	-	-	-
5 areas	97	99	-	-	-
10 areas	96	98	100	-	-
20 areas	93	96	99	99	-

Table 19.1: Correlation coefficients for the entire 2015 power production calculated without taking the remaining energy system into account.

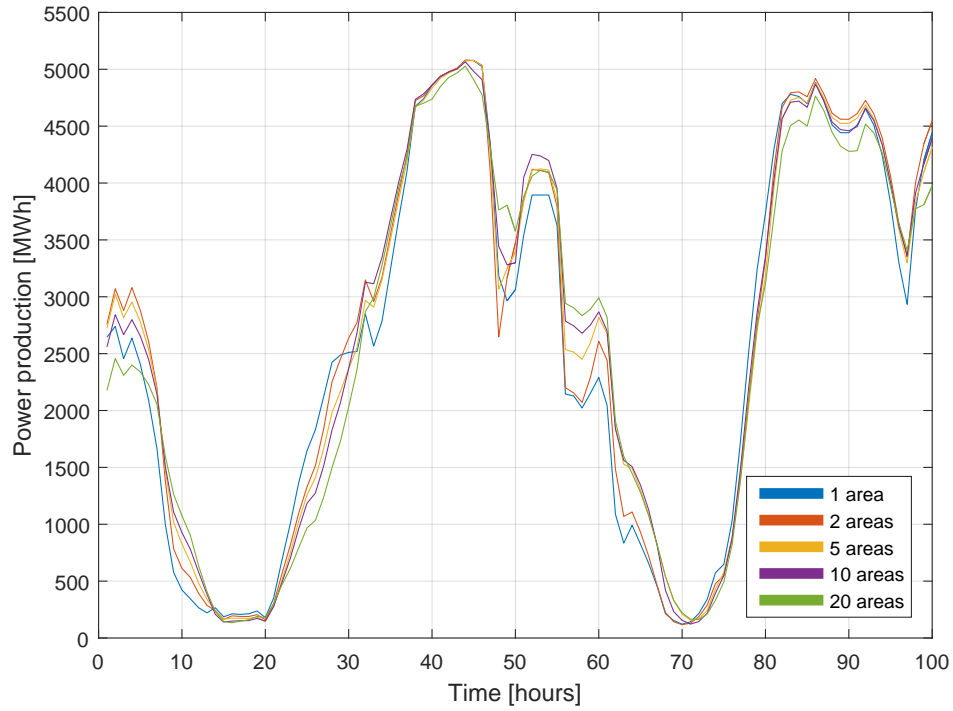


Figure 19.1: Power production calculated for the five cases using the same reference wind speeds and aggregated power curves. Plot has been limited to the first 100 hours of the year.

Number of areas	1	2	5	10	20
Total wind production [GWh]	14335	14323	14195	14226	14180

Table 19.2: Total wind power production before Balmorel implementation.

CHAPTER 20

Correlations in power production after Balmorel implementation

The fluctuations in the power production, without taking the remaining energy system into account, was seen to not differ much with a varying degree of spatial aggregation. These correlation coefficients were however calculated without the use of Balmorel to implement the remaining energy system. Using the model, demand for power, as well as curtailment, now affect the wind power production. Fig. 20.1 shows the first 100 hours of the power production after the cases have been implemented in Balmorel.

From the figure it is still seen that the production is not affected much by the varying spatial aggregation. The correlation coefficients between the time series are seen in Tab. 20.1. These are again seen to have a larger difference in the correlation coefficients between many and few areas.

For most times, the power production from wind seems not to differ depending on the spatial aggregation. It is however seen that some differences do arise from spatial aggregation. A zoom of Fig. 20.1 is seen in Fig. 20.2.

Here it can be seen that the wind power production differs by almost 900 MWh for few hours around the 58th hour. Interestingly, the power production at these few hours are seen to increase with the number of areas. This is believed to be due to the temporal difference in fluctuations, which is investigated further in Chapter 22. Furthermore, hours where few areas produce more power also exists. These hours do not happen as often, and the differences in production are not as large.

Correlation coefficient [%]	1 area	2 areas	5 areas	10 areas	20 areas
1 area	-	-	-	-	-
2 areas	98	-	-	-	-
5 areas	96	98	-	-	-
10 areas	95	97	100	-	-
20 areas	93	95	99	99	-

Table 20.1: Correlation coefficients for the entire 2015 power production modeled in Balmorel.

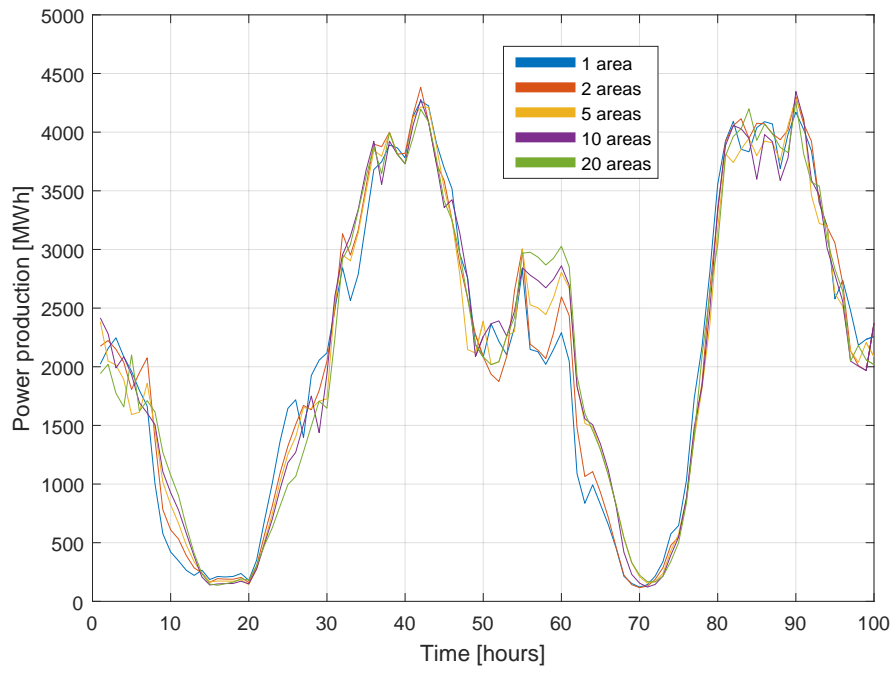


Figure 20.1: Hourly power production for the first 100 hours in 2015. Modeled using Balmorel.

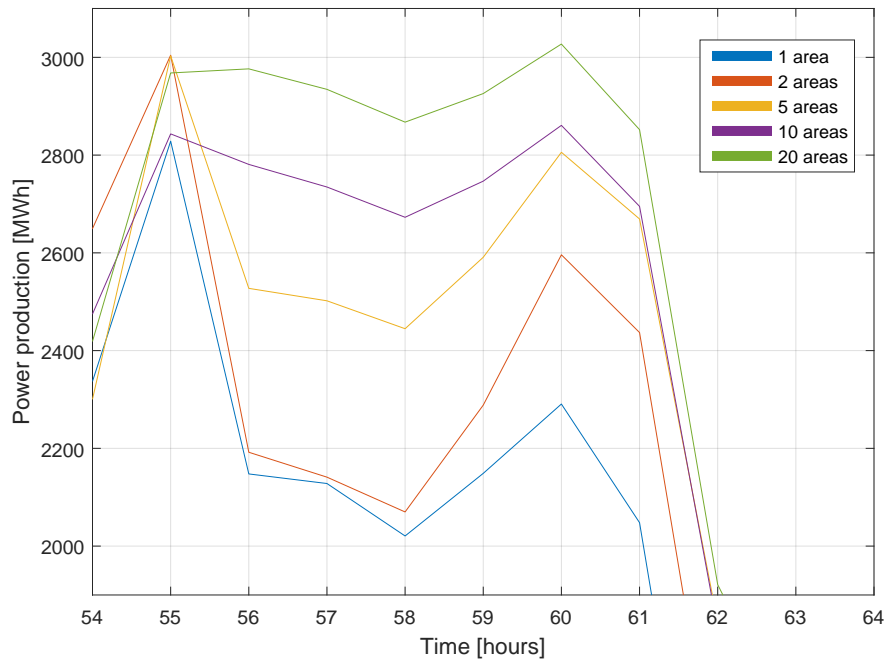


Figure 20.2: Fig. 20.1 zoomed in on the power production between 54 and 64 hours.

20.1 Comparison of power production before and after Balmorel implementation

It is seen that there is a difference between the power production before and after the remaining energy system has been modeled. But how big is this difference actually? Fig. 20.3 shows the first 100 hours of power production before and after the remaining energy system has been implemented in Balmorel for the different cases.

Here, the effects of Balmorel modeling are clearly seen. The wind power production in Balmorel follows the calculated power production exactly, until times with high wind penetration. Here the calculated power production is higher. This is due to the effect of applying a demand of power, and the difference between the two productions are all due to curtailment. The curtailment is seen to be fairly consistent for the first 100 hours of 2015 for the different cases. The correlation coefficients between the calculated power production and the modeled power production were all very close to 96 %, meaning that the effects of Balmorel are close to constant for the varying degrees of spatial aggregation.

20.2 Wind areas in Denmark

The model results when investigating spatial aggregation, shown in Tab. 16.1, shows that the total wind power production and curtailment is a bit higher in the case with twenty areas. This indicates that more areas capture the spatial fluctuations in the wind better, however the differences are so small that adding more areas barely adds anything to the precision of the model. Inspection of the power prices, shown in Tab. 16.1 and correlation coefficients seen in Tab. 18.3, 19.1 and 20.1 indicate that the improvement of adding more wind areas in Denmark than two, is so small that for most model runs it becomes redundant.

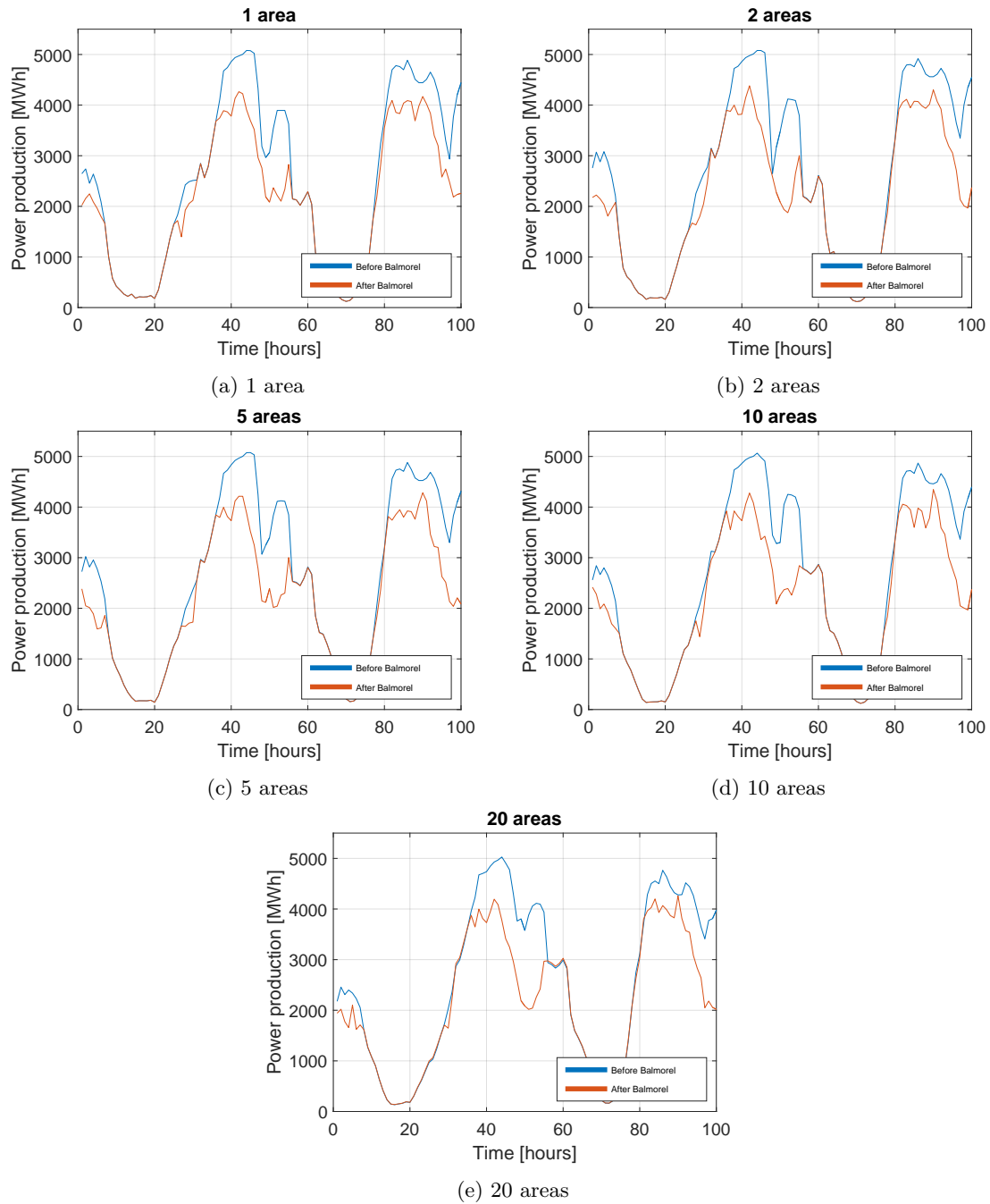


Figure 20.3: First 100 hours of the power production before and after implementation of the remaining power system in Balmore for different levels of spatial aggregation.

CHAPTER 21

Correlations in wind speeds for longer distances

Only small differences in the effects of spatial aggregation were seen for Denmark. Denmark, being a small country, might not be big enough to see a bigger change on an hourly level between the data points. The correlation coefficients between the time series are expected to decrease as the distance between datapoints increases. A study was conducted to see the effects of the temporal correlation coefficients for larger distances in Europe.

The terrain at the given site will affect the wind speeds found. Therefore the correlation coefficients between time series might be distorted by terrain rather than actual wind patterns. In northern Europe the wind speeds will primarily be coming from the south west. To ensure a somewhat consistent terrain, the datasets used are chosen from the western coast of Europe, such that the sites generally will see the ocean to the west. These are compared to correlation coefficients between time series taken in a line directly south. Here the terrain will become more complex due primarily to the Alps. The locations where CFSR time series were taken for both cases are shown in Fig. 21.1.

Fig. 21.2 shows the temporal correlation coefficients between the different sites plotted against the aerial distance between all the sites. The correlation coefficients are calculated between each location in the two different cases.

For the case of the European west coast, a trend is seen in correlation coefficients when going to larger distances. For the case with sites straight south however, the correlation coefficients do not seem possible to relate directly to the distance between points. This is believed to be caused by the complex terrain primarily due to the Alps. From this study it seems that the correlation coefficients decrease with distance as long as the terrain remains roughly the same. Furthermore it is found that correlation coefficients between 50-80 % is found in the 100-400 km distance range. When deciding on wind area modeling size, this results can be used to find the expected correlation coefficient between sites.

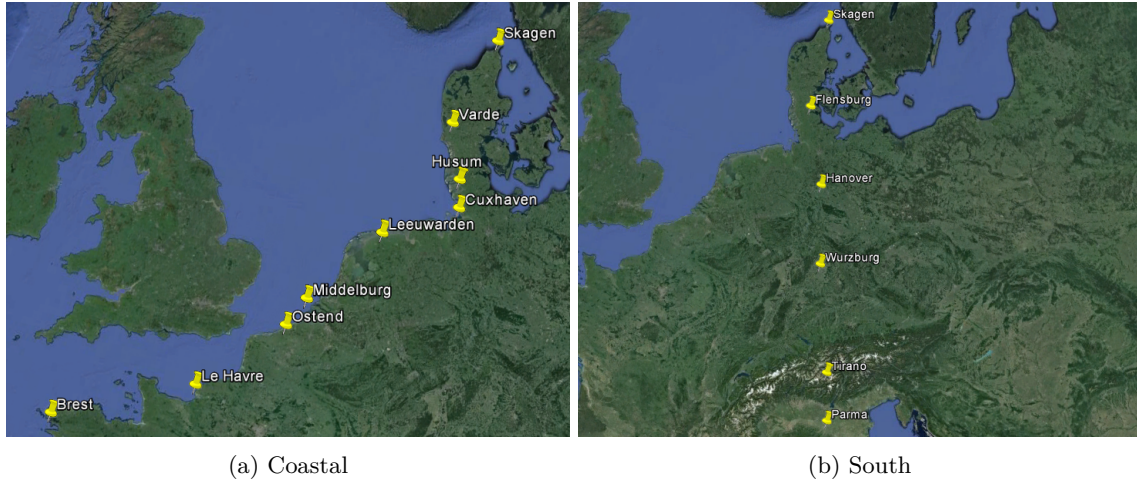


Figure 21.1: Locations in Europe where correlation coefficients between wind time series are calculated. Figure made in Google Earth [20].

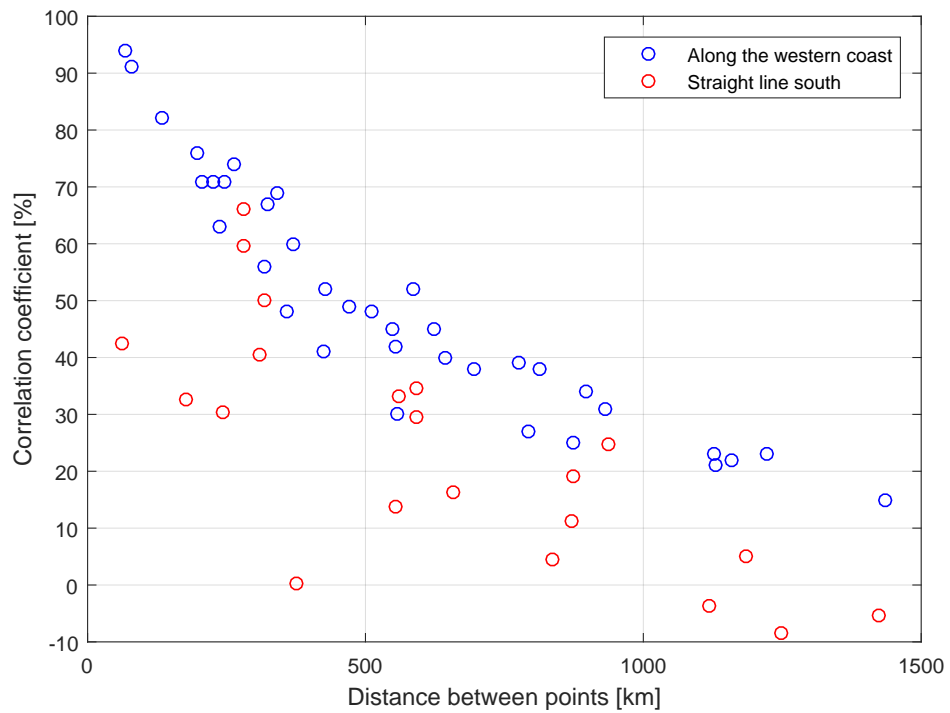


Figure 21.2: Scatter data for the correlation coefficients and distances between the points shown in Fig. 21.1

CHAPTER 22

Area size

Implementation of more wind areas when modeling the Danish wind power production seems to matter very little when modeling more than a single area. In this section the before-mentioned results will be used to suggest a maximum area dimension when modeling wind power production.

As it was seen that two areas are enough to capture almost all effects of the spatial fluctuations, Case 2 is used as the reference. For this investigation, it is imagined that the total capacity of DK_W and DK_E are placed at a corner point shown in Tab. 18.2 respectively. Here Skagen and Varde represents DK_W and Rødsand and Bornholm represents DK_E. Aggregated power curves are created such that a single site represents the region and the power production, without the response of the remaining energy system, is calculated.

	Correlation coefficient [%]	Distance [km]	Power production [%]
Case 2	78	178	100
Skagen/Bornholm	51	388	35
Skagen/Rødsand	49	357	52
Varde/Bornholm	49	409	83
Varde/Rødsand	65	244	100

Table 22.1: Correlation coefficients, distances and total power production compared to Case 2. The combined CFSR and GWA dataset is used.

Tab. 22.1 shows the correlation coefficients, distance and power production compared to Case 2 for cases where sites at corner points have been used as the representative time series. It is seen that for cases, where the correlation coefficient is $\approx 50\%$, the difference in total power produced compared to Case 2 is large. For smaller distances, which are seen between Varde and Rødsand it is however seen that the correlation coefficient is 65 %, which leads to the same total power production as Case 2.

From this it can be concluded that a new area should be implemented before reaching a correlation coefficient of 50 %. The maximum distance between sites can from the distances in the Tab. 22.1 be seen to be between ≈ 250 -350 km. In order to ensure that the wind speed is representative for the area, the distance from the wind site should be no longer than 250 km. This corresponds with Fig. 21.2.

To ensure the accuracy of the model, the maximum distance from the chosen site where the wind time series is still representative, should be no longer than 250 km. The dimensions in Denmark are roughly 500 km x 350 km, which is in accordance with Denmark being able to model realistically with 2-3 areas. The model does become more precise with more implemented areas, although the difference in results compared to the increased implementation time does not seem necessary. This might however still be worth it as wind areas only have to be created once and can then be used to many subsequent model runs.

Part IV

Discussion and conclusion

CHAPTER 23

Discussion

Two wind areas was found to be enough to model the Danish energy system. This result was found using the combined CFSR and GWA dataset. When calculating the power production from the wind dataset, the total yearly power production was ensured through the method of creating aggregated power curves. This however did not take the fluctuations of the wind speeds into account. Tab. 22.1 showed that even though the correlation coefficients are almost the same, the power production differs much more. The use of the CFSR dataset might therefore not prove to be the best dataset used for modeling until the fluctuations in the winds have been validated at heights corresponding to the wind turbine hub heights.

The method for creating aggregated power curves is visually based and does take some time to use. This could potentially be improved by better constraints on the parameters as well as decreasing the number of parameters. Furthermore, it is possible to increase the accuracy by fitting for the cut out wind speed as well instead of fixing this to 25 m/s. Choice of the representative wind time series should be done carefully, with an investigation going into the exact site chosen to evaluate the terrain. The representative site could then be chosen such that it avoid site in valleys or forests.

The spatial aggregation modeling results did not show much difference between the cases. It could however be seen that the fluctuations of the wind speeds will have an effect especially on curtailment. This should be considered for future modeling, as even though the power production is the same for different wind time series, the curtailment might still differ substantially. Investigations into temporal aggregation showed that the time aggregation of Balmorel will result in higher electricity prices when modeling Denmark as an island. These effects should be investigated further before attempting investment runs in Balmorel, even though the differences will be minor when modeling the neighbouring countries as well. Furthermore, with the amount of assumptions going into prediction future energy systems, this effect might not prove the biggest cause for concern.

It was found in Chapter 22, that two areas are enough to model the wind power production in Denmark. It was also concluded that areas should not have dimensions of above 250 km in radius in order to get realistic results. This area size is however influenced by the capacity installed in the area as well as the terrain of the area. From Fig. 21.1 it is seen that the correlation coefficients are not well correlated to the distance between sites, when the terrain becomes more complex. Modeling of areas with complex terrain requires smaller areas to ensure a wind speed, that is representative for the entire area. The area size however, also depends on the capacity installed in the area. A

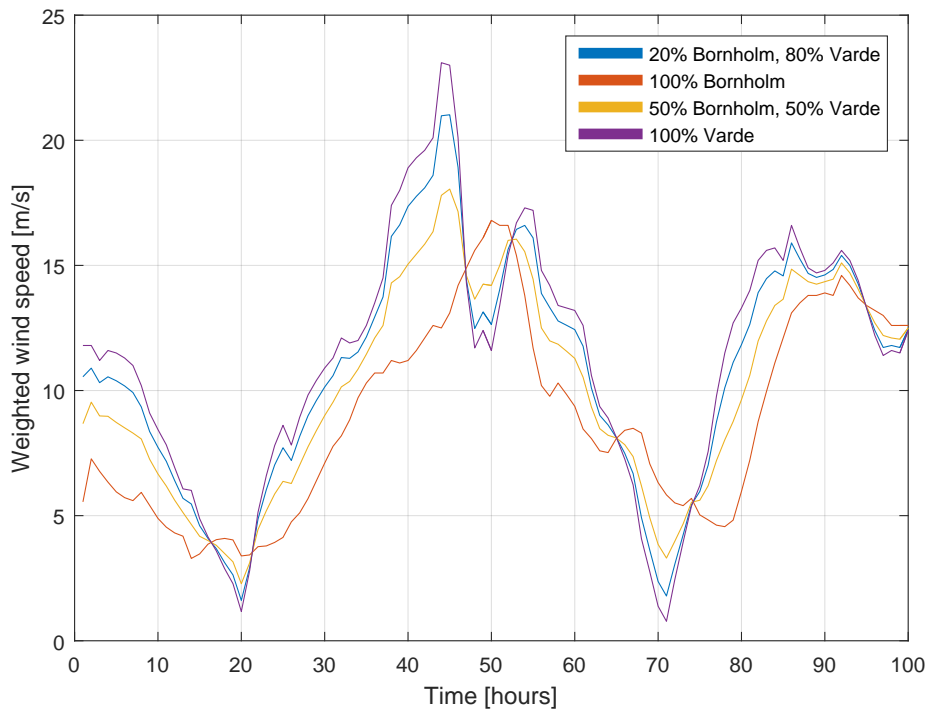


Figure 23.1: Weighted representative wind speed for Denmark with a varying capacity at the two sites.

complex terrain area does not necessarily have to be separated into many small areas, if no wind turbines are installed in the area. Referring to the imaginary case where DK_W is represented by a wind speed from Varde and DK_E is represented by Bornholm, shown in Chapter 22, the effects of changing the capacity weighting is investigated. Fig. 23.1 shows the representative wind speeds for the first 100 hours of 2015 in the case with two wind areas with varying capacity weight.

In Denmark, the weighting of capacity is $\approx 80\%$ in DK_W and 20% in DK_E. Comparing this to cases where all of the capacity is imagined to be installed in DK_W and DK_E respectively as well as evenly distributed, it is seen that the representative wind speed changes substantially. A change in the wind speeds will change the wind power production and thereby the entire energy system. When modeling a country, it is therefore necessary to research where wind turbines are already installed and focus particularly on these sites. A modeled area can easily be larger than the 250 km radius previously suggested, if the capacities installed outside the 250 km radius, is much lower than the capacity inside the radius. This is because a small installed capacity of wind turbines will barely affect the overall energy system even if the wind speeds are not representative for the area. Furthermore, wind patterns for a region might differ much more than for Denmark and should therefore also be taking into account when modeling wind areas using Balmorel.

CHAPTER 24

Conclusion

In this thesis, the influence of spatial aggregation when modeling wind areas were investigated. It was hypothesized that the implementation of more wind areas would better be able to capture the fluctuations in the wind speeds. In order to test this hypothesis, a wind dataset for Denmark was necessary. In this thesis, different wind datasets were described and compared. The wind datasets investigated was the CFSR dataset, the GWA dataset and a mesoscale dataset made specifically for the use in modeling. It was found that the CFSR dataset resulted in low capacity factors compared to GWA and mesoscale datasets. The mesoscale dataset only had few sites where wind data is available, which made testing of spatial aggregation impossible. The GWA was seen to yield capacity factors much closer to observed values. Therefore, the GWA dataset was deemed suitable for energy systems modeling. A method was implemented for combining fluctuations of one wind time series with a distribution from another wind dataset. This was done using the Weibull distribution of the wind time series to equate the CDF. The combined wind time series was found to retain the fluctuations from the CFSR datasets and have the wind distribution from the GWA dataset.

A method for creating aggregated power curves valid for a larger wind areas in Denmark was developed and discussed. Implementation of more areas in the Balmorel model was done using a representative wind time series for the area as well as an aggregated power curve specific to the area. The aggregated power curves were created using one or more representative wind time series for the area. Furthermore, a reference power curve representative of the given site, as well as observed wind turbine data is necessary. The aggregated power curves was fitted to observed capacity factors in order to ensure the correct power production when implemented in the Balmorel model.

Alterations in the degree of spatial aggregation of the wind areas in Denmark, showed only minor differences after implementing the cases in Balmorel and running the model. It was found that a single wind area representative for Denmark is too few areas to fit the wind speeds for the entire country. Two areas was seen to be the minimum amount of areas required to accurately model the wind power production in Denmark as adding more areas barely has an effect on the final results.

Inspection of temporal aggregation showed that the time aggregation cannot completely capture all effects on the energy system that hourly resolution can. This was seen in that hours, with very high electricity prices, were found more often than it was in cases with hourly resolution. Even though the difference in power prices were found to be higher than expected, when including the

neighbouring countries in the energy system, the time aggregation limits investigations into future investment modeling scenarios.

A trend between correlation coefficients and distances between sites were seen for cases where the terrain was close to uniform. These results were used to estimate the largest spatial dimensions when modeling wind areas in Balmorel. A distance of 250 km seems to be the maximum distance from the reference site to where the wind speeds are representative for the area. This distance however, was found to depend both on the terrain as well as the installed capacity in the area and the wind patterns.

The maximum wind area size can be used to improve how modeling is done especially for other countries. Few areas are necessary for Denmark, but for a country like China, the division into wind areas requires a much bigger effort. Therefore, the maximum distance where wind speeds are still representative will ease this process substantially.

CHAPTER 25

Future work

25.1 Capacity weighting

The capacity weighting of the different areas was seen to have an effect on how the areas are created. Investments into exactly how large the difference in capacity between areas, could be used to better clarify the maximum wind area site used for modeling.

25.2 Transmission to neighbouring countries

An investigation into connecting the Danish energy system to neighbouring countries would enable the power prices and curtailment to reach more realistic values. This will require a larger study into creating power curves for the countries as well as attempting to divide the countries into more areas, whilst also getting more knowledge of the terrain effects in the different countries.

25.3 Time aggregation

Further study into exactly how the time aggregation affects wind power production would make it possible to improve the time aggregation such that all the effects of the wind were taken into account. This would enable a larger study into the effects of temporal aggregation.

25.4 Investment runs

With neighbouring countries as well as the correct time aggregation in place, it would be possible to investigate how the effects of spatial aggregation will look for investment runs. This requires knowledge of capacity planned to be installed in the future, as well as assumptions into how the new technology mix will affect the aggregated power curves. Furthermore, this would require a limit on how many wind turbines can be installed in a certain area, such that a small windy area will not get completely filled with new wind turbines.

Bibliography

- [1] Blanca Naudin Aparicio. Aggregated power curve for multiple wind turbines in power system area. (August), 2013.
- [2] Maria C Arildsen. Energinet.dk's analyseforudsætninger 2015-2035. pages 1–25, 2012.
- [3] Bjarne Bach, Brian Elmegaard, Marie Münster, Jesper Werling, and Torben Schmidt Ommen. Integration of Heat Pumps in Greater Copenhagen. 2014.
- [4] Jake Badger, Merete Badger, Mark Kelly, and Xiaoli Guo Larsén. Global Wind Atlas Methodology. <http://globalwindatlas.com/methods.html>, DOA: 2016-06-07.
- [5] Jacob Berg, Jakob Mann, Mark Kelly, and Morten Nielsen. Introduction to Micrometeorology for Wind Energy - Course notes. pages 1–61, 2015.
- [6] S Besio, A Mazzino, and C F Ratto. Local log-law-of-the-wall in neutrally-stratified boundary-layer flows. *Boundary-Layer Meteorology*, 107(1):115–142, 2003.
- [7] Michael C. Brower. *Wind Resource Assessment*. John Wiley & Sons, Inc., Hoboken, NJ, USA, jun 2012.
- [8] D Connolly, H Lund, B V Mathiesen, and M Leahy. A review of computer tools for analysing the integration of renewable energy into various energy systems. *Applied Energy*, 87:1059–1082, 2009.
- [9] DMI. Vind i Danmark. <http://www.dmi.dk/klima/klimaet-frem-til-i-dag/danmark/vind/>, DOA: 2016-05-21.
- [10] Ea Energianalyse. Vindintegration i Danmark - Vindens værdi - og tiltag for at sikre den. 2014.
- [11] Ea Energy Analyses and Risø National Laboratory for Sustainable Energy. STREAM - an energy scenario modelling tool. www.streammodel.org, DOA: 2016-06-19.
- [12] EMD International A/S. Wind index. <http://www.vindstat.dk/Hovedtabel.php>, DOA: 2016-01-26.
- [13] Energinet.dk. Dansk vindstrøm slår igen rekord. <http://energinet.dk/DA/E1/Nyheder/Sider/Dansk-vindstroem-slaar-igen-rekord-42-procent.aspx>, DOA: 2016-06-07.
- [14] Energistyrelsen. Eksisterende parker og aktuelle projekter. <http://www.ens.dk/undergrund-forsyning/vedvarende-energi/vindkraft-vindmoller/havvindmoller/idriftsatte-parker-nye>, DOA: 2016-06-23.

-
- [15] Energistyrelsen. Stamdataregister for vindkraftanlæg. <http://www.ens.dk/info/tal-kort/statistik-noegletal/oversigt-energisektoren/stamdataregister-vindmoller>, DOA: 2016-01-26.
- [16] DTU Wind Energy. Global Wind Atlas. <http://globalwindatlas.com/>, DOA: 2016-05-21.
- [17] Energy Numbers. Capacity factors at Danish offshore wind farms. <http://energynumbers.info/capacity-factors-at-danish-offshore-wind-farms>, DOA: 2016-06-07.
- [18] R.A. Fisher. *Statistical Methods for research Workers*. Oliver and Boyd, 1944.
- [19] GAMS. GAMS documentation. <https://www.gams.com/>, DOA: 2016-05-22.
- [20] Google. Google Earth. <https://www.google.com/earth/>, DOA: 2016-06-07.
- [21] Sam Hawkins. A High Resolution Reanalysis of Wind Speeds over the British Isles for Wind Energy Integration. 2012.
- [22] B. P. Hayes, I. Ilie, a. Porpodas, S. Z. Djokic, and G. Chicco. Equivalent power curve model of a wind farm based on field measurement data. *2011 IEEE Trondheim PowerTech*, pages 1–7, 2011.
- [23] K Kaiser, W Langreder, H Hohlen, and J Højstrup. Turbulence Correction for Power Curves. *Wind Energy Proceedings of Euromech Colloquium*, pages 159–162, 2007.
- [24] Erik Kjaer. -Quality Wind - Performance of Danish Onshore Wind Portfolio -a study prepared for selected Chinese wind farm owners. 2015.
- [25] M. L. Kubik, P. J. Coker, J. F. Barlow, and C. Hunt. A study into the accuracy of using meteorological wind data to estimate turbine generation output. *Renewable Energy*, 51:153–158, 2013.
- [26] C. D. Lai, D. N P Murthy, and M. Xie. Weibull distributions. *Wiley Interdisciplinary Reviews: Computational Statistics*, 3(3):282–287, 2011.
- [27] Stuart P. Lloyd. Least Squares Quantization in PCM. *IEEE Transactions on Information Theory*, 28(2):129–137, 1982.
- [28] J.F. Manwell, J.G. McGowan, and A.L. Rogers. *Wind Energy Explained*. 2002.
- [29] Microsoft. Solver Uses Generalized Reduced Gradient Algorithm. <https://support.microsoft.com/en-us/kb/82890>, DOA: 2016-06-07.
- [30] Global Modeling and Assimilation Office. MERRA-2: File specification . *Earth*, 9(9):0–1, 2007.
- [31] NCEP. NCEP Climate Forecast System Reanalysis (CFSR) 6-hourly Products, January 1979 to December 2010. <http://rda.ucar.edu/datasets/ds093.0/>, DOA: 2016-05-29.
- [32] P Norgaard and H Holttinen. A Multi-Turbine Power Curve Approach. *Nordic Wind Power Conference*, (March):1–2, 2004.
- [33] NSIDC. Special Sensor Microwave Imager (SSM/I). <https://nsidc.org/data/docs/daac/ssmi{ }instrument.gd.html>, DOA: 2016-06-07.
- [34] University of Hawaii. GSHHG A Global Self-consistent, Hierarchical, High-resolution Geography Database.

- [35] Hans Ravn. Balmorel: A Model for Analyses of the Electricity and CHP Markets in the Baltic Sea Region. 2001.
- [36] Hans F Ravn. The Balmorel Model: Theoretical Background. 2001.
- [37] Suranjana Saha. The NCEP climate forecast system reanalysis. *Bulletin of the American Meteorological Society*, 91(8):1015–1057, 2010.
- [38] Javier Serrano-González and Roberto Lacal-Aránegui. Technological evolution of onshore wind turbines—a market-based analysis. *Wind Energy*, 2016.
- [39] Ed Sharp, Paul Dodds, Mark Barrett, and Catalina Spataru. Evaluating the accuracy of CFSR reanalysis hourly wind speed forecasts for the UK, using in situ measurements and geographical information. *Renewable Energy*, 77:527–538, 2015.
- [40] Iain Staffell and Richard Green. How does wind farm performance decline with age? *Renewable Energy*, 66:775–786, 2014.
- [41] Stefan Kopp. Windenergie im Binnenland - The truth about windpower. <http://www.windenergie-im-binnenland.de/powercurve.html>, DOA: 2016-06-16.
- [42] I. Troen and E. Lundtang Petersen. *European wind atlas*. 1989.

APPENDIX A

Coordinates of extracted CFSR data

The points where CFSR data is extracted for Denmark is seen in Table A.1 and Figure A.1.

Site	Longitude	Latitude	Site	Longitude	Latitude
Bornholm	15	55.11	Brenderup	10	55.421
Lollandfalster	11.25	54.796	Farsø	9.375	56.67
Sjælland	11.875	55.421	Fjerritslev	9.375	56.982
Sydhav	10.937	54.796	Grenå	10.937	56.357
Fyn	10.312	55.421	Haarby	10.312	55.108
Jylland	9.375	56.045	Holstebro	8.437	56.357
Kattegat	11.25	56.67	Horsens	9.687	55.733
Limfjord	8.75	56.67	Læsø	11.25	57.294
Vestkystnord	8.75	57.294	Løgumkloster	9.062	55.108
Vestkystsyd	8.125	55.733	Nyborg	10.625	55.421
Ærø	10.312	54.796	Randers	10	56.357
Allinge	14.687	55.108	Samsø	10.937	55.733
Fuglebjerg	11.562	55.421	Struer	8.437	56.357
Gedser	11.875	54.484	Svendborg	10.625	55.108
Hillerød	12.5	55.733	Thisted	8.75	56.982
Jyderup	11.562	55.733	Varde	8.437	55.733
Klippinge	11.875	55.421	Vendsyssel	10.312	57.294
Lillebælt	10	55.108	Viborg	9.375	56.357
Nakskov	11.25	54.796	Ringkøbing	8.75	56.045
Nexø	15	55.108	Rødding	9.062	55.421
Rødsand	11.562	54.484	Billund	9.062	55.733
Rønne	14.687	55.108	Aalborg	10	56.982
Sakskøbing	11.562	54.796	Skanderborg	10	56.045
Småland	11.562	55.108	Skagen	10.312	57.606
Stubbekøbing	11.875	54.796	Djurs	10.525	56.357
Svaneke	15	55.108	Aabenraa	9.375	55.108
Anholt	11.25	56.67	Horns rev	8.125	55.421

Table A.1: Coordinates of extracted CFSR data, shown in Fig. A.1.

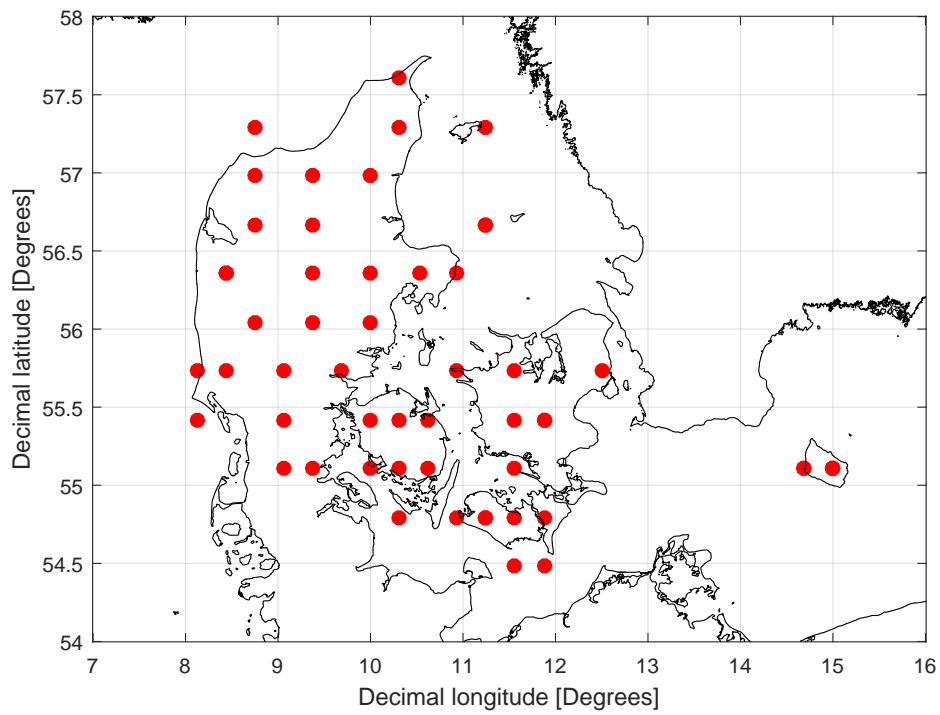


Figure A.1: Map showing the extracted CFSR coordinates.

APPENDIX B

Matlab script to combine CFSR and GWA data

```
clear all; close all; clc;

% Load in GWA geotiff files
%%%%%%%%%%%%%%%%%%%%%%%%%%%%%%%%%%%%%%%%%%%%%%%%%%%%%%%%%%%%%%%%%%%%%%%%% Specify file with correct mast height
%%%%%%%%%%%%%%%%%%%%%%%%%%%%%%%%%%%%%%%%%%%%%%%%%%%%%%%%%%%%%%%%%%%%%%%%%
[A_all,R_A] = geotiffread('50m_omni-A');
[K_all,R_K] = geotiffread('50m_omni-K');
%%%%%%%%%%%%%%%%%%%%%%%%%%%%%%%%%%%%%%%%%%%%%%%%%%%%%%%%%%%%%%%%%%%%%%%%%

%%%%%%%%%%%%%%%%%%%%%%%%%%%%%%%%%%%%%%%%%%%%%%%%%%%%%%%%%%%%%%%%%%%%%%%%% Specify time series
%%%%%%%%%%%%%%%%%%%%%%%%%%%%%%%%%%%%%%%%%%%%%%%%%%%%%%%%%%%%%%%%%%%%%%%%%
filename = 'DK_W_Jylland.inc';
%%%%%%%%%%%%%%%%%%%%%%%%%%%%%%%%%%%%%%%%%%%%%%%%%%%%%%%%%%%%%%%%%%%%%%%%%

%%
% Load data and create time series
data = importdata(filename, ' ', 6);
TS = data.data;

str = char(data.textdata(1,1));
Longitude = strsplit(str, ':');
Longitude = cell2mat(Longitude(1,2));
Longitude = str2num(Longitude);

str = char(data.textdata(2,1));
Latitude = strsplit(str, ':');
Latitude = cell2mat(Latitude(1,2));
Latitude = str2num(Latitude);
%%
% Decimal degrees for extracted time series
%%%%%%%%%%%%%%%%%%%%%%%%%%%%%%%%%%%%%%%%%%%%%%%%%%%%%%%%%%%%%%%%%%%%%%%%% Decimal degree for extracted time series
%%%%%%%%%%%%%%%%%%%%%%%%%%%%%%%%%%%%%%%%%%%%%%%%%%%%%%%%%%%%%%%%%%%%%%%%%
```

```

X = Longitude;
Y = Latitude;
%
%
%%%%%%%%%%%%%%%%%%%%%%%%%%%%%%%%%%%%%%%%%%%%%%%%%%%%%%%%%%%%%%%%%%%%%%%%

%% Coordinate reference

xdeg = load('xcordGWA.txt');
ydeg = load('ycordGWA.txt');

%%
xmin = abs(xdeg-Longitude);
ymin = abs(ydeg-Latitude);

diffmin = xmin+ymin;

[value , index] = min(reshape(diffmin , numel(diffmin) , 1));
[Y_element ,X_element] = ind2sub(size(diffmin) , index);

A = A_all(Y_element ,X_element);
K = K_all(Y_element ,X_element);

%% plot test af koordinat
% figure(5)
% plot(X_element ,Y_element ,'k. ')
% hold on
% axis([1 3052 1 1912])

%% Weibul parameters

mean = mean(TS);
sigma2 = var(TS);

syms A_c k_c

[A_c_sol , k_c_sol] = solve([mean == A_c*gamma(1+1/k_c) , sigma2 == A_c^2*(
    gamma(1+2/k_c)-gamma(1+1/k_c)^2) ] , [A_c , k_c] );

A_T = double(A_c_sol);
k_T = double(k_c_sol);

A_GWA = A;
k_GWA = K;

%% CDF weibull

u = [0:25/8735:25];
CDF_Wbl = 1-exp(-(u./A_GWA).^k_GWA);

```

```

%CDF_Wbl_ML = wblcdf(u,A_GWA,k_GWA);

%% CDF timeseries

figure(1)
hold on
%CDF_T_plot = cdfplot(DK_W_Onshore)
CDF_T = cdf('Weibull',u,A_T,k_T);
plot(u,CDF_T,'g')
plot(u,CDF_Wbl,'b')
[legh,objh,outh,outm] = legend('CDF from CFSR time series','CDF from GWA
    parameters','location','best');
set(objh,'linewidth',5);
xlabel('Wind speed [m/s]')
ylabel('Probability')
grid on
box on

%% Compare CDF

CDF_Factor = CDF_Wbl./CDF_T;

TS_GWA = abs(A_GWA*(TS./A_T).^(k_T./k_GWA));

figure(2)
plot(TS,'g')
hold on
plot(TS_GWA,'b')
[legh,objh,outh,outm] = legend('CFSR time series','Combined time series
    ','location','best');
set(objh,'linewidth',5);
xlabel('Time [hours]')
ylabel('Wind speed [m/s]')
grid on
box on
axis([0 2000 0 25])

%% Write .inc file
test = (data.textdata(7:end,1:5));

Matr = cell(length(TS_GWA),6);
Matr(:,1) = test(:,1);
Matr(:,2) = test(:,2);
Matr(:,3) = test(:,3);
Matr(:,4) = test(:,4);
Matr(:,5) = test(:,5);
Matr(:,6) = num2cell(TS_GWA);

fid=fopen(filename,'wt');
[rows,cols]=size(Matr);

```

```
for i=1:rows
    fprintf(fid, ' % s ', Matr{i,1});
    fprintf(fid, ' % s ', Matr{i,2});
    fprintf(fid, ' % s ', Matr{i,3});
    fprintf(fid, ' % s ', Matr{i,4});
    fprintf(fid, ' % s ', Matr{i,5});
    fprintf(fid, ' % s\n', Matr{i,end});
end
fclose(fid);
```

APPENDIX C

Power curve implementation in Balmorel

```
* WindToPower.inc

* PARAMETER WND_SPEED_POWER_T contains the description of seasonal and
  daily variation
* of the windturbine power generation.
* Units: % of full capacity.

SET windset /'FLH','FLH teo','FLH act','up s1t1','Growth_rate','Profile
  '/
  windcat /'Ext','New var','New speed'/
;

PARAMETER
  WND_SPEED_POWER_T(AAA,GGG,SSS,TTT)      'Wind power based on wind
  speed variation and power curve parameters'
  WND_HEIGHT_FACTOR(AAA,GGG)              'Technology hight factor
  adjustment of area wind speed'
  windTest(AAA,GGG,windcat,windset)
  WND_FLH(AAA,GGG)
;

* Ajust wind speed acoording to shear factor and hight
* Note, both hights and shear factor must be given otherwise the
  resulting default factor becomes 1
WND_HEIGHT_FACTOR(IA,IGWND)$ (GWNDATA(IGWND,'height') and WNDATA(IA,'
  height') and (SUM(Y,GKFX(Y,IA,IGWND)) OR AGKN(IA,IGWND)
  $ifi %ADDINVEST%=yes OR SUM(Y,GKVACCDECOM(Y,IA,IGWND))
  ))
  = log (GWNDATA(IGWND,'height') /WNDATA(IA,'height')) ;

WND_HEIGHT_FACTOR(IA,IGWND)$ ((SUM(Y,GKFX(Y,IA,IGWND)) OR AGKN(IA,IGWND)
  $ifi %ADDINVEST%=yes OR SUM(Y,GKVACCDECOM(Y,IA,IGWND))
  ))
```

```

= exp( WNDATA(IA, 'Shear_factor') * WND_HEIGHT_FACTOR(IA, IGWND) );

* Convert wind speed to power output based on GWNDATA
* 1. For wind speeds less than 25 m/s
WND_SPEED_POWER_T(IA, IGWND, SSS, TTT) $ (GWNDATA(IGWND, 'Growth_rate_inc')
AND WND_SPEED_T(IA, SSS, TTT) <= 25 AND (SUM(Y, GKFX(Y, IA, IGWND)) OR AGKN
(IA, IGWND)
$ifi %ADDINVEST%=yes OR SUM(Y, GKVACCDECOM(Y, IA, IGWND))
))=
GWNDATA(IGWND, 'Start_production') + (1 - GWNDATA(IGWND, '
Start_production')) / (1 + exp(-GWNDATA(IGWND, 'Growth_rate_inc') * (
WND_SPEED_T(IA, SSS, TTT) * WND_HEIGHT_FACTOR(IA, IGWND) - GWNDATA(
IGWND, 'Max_growth_inc'))));

* 2. For wind speeds more than 25 m/s
WND_SPEED_POWER_T(IA, IGWND, SSS, TTT) $ (GWNDATA(IGWND, 'Growth_rate_inc')
AND WND_SPEED_T(IA, SSS, TTT) > 25 AND (SUM(Y, GKFX(Y, IA, IGWND)) OR AGKN(
IA, IGWND)
$ifi %ADDINVEST%=yes OR SUM(Y, GKVACCDECOM(Y, IA, IGWND))
))=
1 / (1 + exp(-GWNDATA(IGWND, 'Growth_rate_dec') * (WND_SPEED_T(IA, SSS, TTT)
* WND_HEIGHT_FACTOR(IA, IGWND) - GWNDATA(IGWND, 'Max_growth_dec'))))
;

* 3. Constrain Power Curve between 0 and Max_production
WND_SPEED_POWER_T(IA, IGWND, SSS, TTT) $ (GWNDATA(IGWND, 'Growth_rate_inc')
AND (SUM(Y, GKFX(Y, IA, IGWND)) OR AGKN(IA, IGWND)
$ifi %ADDINVEST%=yes OR SUM(Y, GKVACCDECOM(Y, IA, IGWND))
))=
MAX(MIN(WND_SPEED_POWER_T(IA, IGWND, SSS, TTT), GWNDATA(IGWND, '
Max_production')), 0);

WND_FLH(IA, IGWND) $ (GWNDATA(IGWND, 'Growth_rate_inc') AND (SUM(Y, GKFX(Y,
IA, IGWND)) OR AGKN(IA, IGWND)
$ifi %ADDINVEST%=yes OR SUM(Y, GKVACCDECOM(Y, IA, IGWND))
))=
SUM((SSS, TTT), WND_SPEED_POWER_T(IA, IGWND, SSS, TTT));

```

APPENDIX D

Wind turbine costs from Ea

Rounded off values of the costs are shown in Tab. D.1.

	Investment cost [DKK/MW]	Variable O&M cost [DKK/MWh]	Yearly O&M cost [DKK/MWh]
Onshore	0.9×10^6	19	2×10^3
Offshore	2×10^6	35	3×10^3

Table D.1: Approximate default costs for wind turbines.



DTU Wind Energy is a department of the Technical University of Denmark with a unique integration of research, education, innovation and public/private sector consulting in the field of wind energy. Our activities develop new opportunities and technology for the global and Danish exploitation of wind energy. Research focuses on key technical-scientific fields, which are central for the development, innovation and use of wind energy and provides the basis for advanced education at the education.

We have more than 240 staff members of which approximately 60 are PhD students. Research is conducted within nine research programmes organized into three main topics: Wind energy systems, Wind turbine technology and Basics for wind energy.

Technical University of Denmark

Department of Wind Energy
Frederiksborgvej 399
4000 Roskilde
Denmark
Telephone 46 77 50 85

info@vindenergi.dtu.dk
www.vindenergi.dtu.dk